

Valence-specific Enhancements in Visual Processing Regions Support Negative Memories:

Author: Sarah Marie Kark

Persistent link: <http://hdl.handle.net/2345/bc-ir:108471>

This work is posted on [eScholarship@BC](#),
Boston College University Libraries.

Boston College Electronic Thesis or Dissertation, 2019

Copyright is held by the author, with all rights reserved, unless otherwise noted.

VALENCE-SPECIFIC ENHANCEMENTS IN VISUAL PROCESSING REGIONS SUPPORT NEGATIVE MEMORIES

Sarah Marie Kark

A dissertation
submitted to the Faculty of
the department of Psychology
in partial fulfillment
of the requirements for the degree of
Doctor of Philosophy

Boston College
Morrissey College of Arts and Sciences
Graduate School

May 2019

VALENCE-SPECIFIC ENHANCEMENTS IN VISUAL PROCESSING REGIONS SUPPORT NEGATIVE MEMORIES

Sarah Marie Kark

Advisor: Elizabeth A., Kensinger, Ph.D.

Abstract

Research in four parts examines the effects of valence on the neural processes that support emotional memory formation and retrieval. Results show a consistent valence-specific enhancement of visuocortical engagement along the ventral visual stream and occipital cortex that supports negative memories to a greater extent than positive memories.

Part I investigated the effects of valence on the interactions between trial-level physiological responses to emotional stimuli (i.e., heart rate deceleration) during encoding and subsequent memory vividness. Results showed that negative memory vividness, but not positive or neutral memory vividness, is tied to arousal-related enhancements of amygdala coupling with early visual cortex during encoding. These results suggest that co-occurring parasympathetic arousal responses and amygdala connectivity with early visual cortex during encoding influence subsequent memory vividness for negative stimuli, perhaps reflecting enhanced memory-relevant perceptual enhancements during encoding of negative stimuli.

Part II examined links between individual differences in post-encoding increases in amygdala functional connectivity at rest and the degree and direction of emotional memory biases at retrieval. Results demonstrated that post-encoding increases in

amygdala resting state functional connectivity with visuocortical and frontal regions predicted the degree of negative memory bias (i.e., better memory for unpleasant compared to pleasant stimuli) and positive memory bias, respectively. Further, the effect of amygdala-visuocortical post-encoding coupling on behavioral negative memory bias was completely mediated by greater retrieval-related activity for negative stimuli in visuocortical areas. These findings suggest that those individuals with a negative memory bias tend to engage visual processing regions across multiple phases of memory more than individuals with a positive memory bias.

While **Parts I-II** examined encoding-related memory processes, **Part III** examined the effects of valence on true and false subjective memory vividness at the time of retrieval. The findings showed valence-specific enhancements in regions of the ventral visual stream (e.g., inferior temporal gyrus and parahippocampal cortex) support negative memory vividness to a greater extent than positive memory vividness. However, activation of the parahippocampal cortex also drove a false sense of negative memory vividness. Together, these findings suggest spatial overlap in regions that support negative true and false memory vividness.

Lastly, **Part IV** utilized inhibitory repetitive transcranial magnetic stimulation (rTMS) to test if a portion of occipito-temporal cortex that showed consistent valence-specific effects of negative memory in Parts I-III was *necessary* for negative memory retrieval. Although some participants showed the hypothesized effect, there was no group-level evidence of a neuromodulatory effect of occipito-temporal cortex rTMS on negative memory retrieval.

Together, the results of the current dissertation work highlight the importance of valence-based models of emotional memory and consistently implicated enhanced visuosensory engagement across multiple phases of memory. By identifying valence-specific effects of trial-level physiological arousal during encoding, post-encoding amygdala coupling during early consolidation, and similarities and differences between true and false negative memories, the present set of work has important implications for how negative and positive memories are created and remembered differently.

TABLE OF CONTENTS

LIST OF TABLES	II
LIST OF FIGURES	IV
ACKNOWLEDGEMENTS	VI
NOTE	X
GENERAL INTRODUCTION.....	1
1.0 PHYSIOLOGICAL AROUSAL AND AMYGDALA-VISUOCORTICAL CONNECTIVITY PREDICT SUBSEQUENT VIVIDNESS OF NEGATIVE MEMORIES	8
1.1 ABSTRACT	9
1.2 INTRODUCTION	10
1.3 METHODS.....	12
1.4 RESULTS	17
1.5 DISCUSSION.....	30
1.6 REFERENCES	33
2.0 POST-ENCODING AMYGDALA-VISUOSENSORY COUPLING IS ASSOCIATED WITH NEGATIVE MEMORY BIAS IN HEALTHY YOUNG ADULTS.....	37
2.1 ABSTRACT	38
2.2 INTRODUCTION	39
2.3 METHODS.....	41
2.4 RESULTS	57
2.5 DISCUSSION.....	77
2.6 REFERENCES	85
3.0 EFFECTS OF EMOTIONAL VALENCE ON TRUE AND FALSE MEMORY VIVIDNESS 93	
3.1 ABSTRACT	94
3.2 INTRODUCTION	96
3.3 METHODS.....	104
3.4 RESULTS	116
3.5 DISCUSSION.....	138
3.6 REFERENCES	148
4.0 EMOTIONAL VALENCE AND SUBJECTIVE RE-EXPERIENCING: AN RTMS STUDY 159	
4.1 ABSTRACT	160
4.2 INTRODUCTION	161
4.3 METHODS: STUDY 1	164
4.4 RESULTS: STUDY 1	166
4.5 METHODS: STUDY 2	171
4.6 RESULTS: STUDY 2	179
4.7 DISCUSSION.....	187
4.8 REFERENCES	193
GENERAL DISCUSSION	198
REFERENCES FOR GENERAL INTRODUCTION AND DISCUSSION	212

List of Tables

Part I

- *Table 1.* Main effects of subsequent vividness for neutral and positive memories.
- *Table 2.* Main effects of heart rate deceleration for negative stimuli.
- *Table 3.* Main effects of heart rate deceleration for positive stimuli.
- *Table 4.* Main effects of heart rate deceleration for neutral stimuli.
- *Table 5.* Valence-specific psycho-autonomic interaction (PAI) effects.

Part II

- *Table 1.* Group pre-to-post encoding increases in amygdala resting state functional connectivity.
- *Table 2.* Across-subject correlations between post-encoding increases in right amygdala resting state functional connectivity and emotional memory performance.

Part III

- *Table 1.* Regions that showed a significant positive parametric relation of true memory vividness across all valences.
- *Table 2.* Valence-specific effects of true memory vividness.
- *Table 3.* Regions that showed a greater positive parametric effect for true memory vividness than false memory vividness by valence.

- *Table 4.* Regions that showed a positive parametric effect of vividness for true and false memories by valence.
- *Table 5.* Parametric functional connectivity of the right parahippocampal cortex for negative true memory vividness.

Part IV

- *Table 1.* Descriptive statistics of memory measures and reaction times for Study 1 and Study 2.

List of Figures

Part I

- *Figure 1.* Statistical maps of amygdala parametric functional connectivity with subsequent vividness, heart rate deceleration, and their interactions.

Part II

- *Figure 1.* Scanning procedures and task structure.
- *Figure 2.* Memory task-based fMRI results.
- *Figure 3.* Group-level amygdala resting state functional connectivity results.
- *Figure 4.* Post-encoding enhancement of right amygdala connectivity and valence-specific emotional memory biases.
- *Figure 5.* Exploratory moderated mediation analysis.

Part III

- *Figure 1.* Sample stimuli and recognition memory vividness responses.
- *Figure 2.* Valence-invariant effects of memory vividness.
- *Figure 3.* Effects of valence on true memory vividness.
- *Figure 4.* Effects of valence on true and false memory vividness.
- *Figure 5.* Exploratory functional connectivity analysis of the right parahippocampal cortex for true and false memories.

Part IV

- *Figure 1.* Study 1 visual and internal re-experiencing ratings for hits by valence and response type for the full sample.
- *Figure 2.* Study 1 visual and internal re-experiencing ratings for false alarms by valence and response type for a subset of participants.
- *Figure 3.* Visualization of the LOTC ROI in MNI space (left column) and in native space of a sample participant (right column), shown in red.
- *Figure 4.* Perceptual matching control task.
- *Figure 5.* Average d-prime memory performance values by valence and rTMS stimulation site.
- *Figure 6.* Average re-experiencing ratings by valence, re-experiencing type, and stimulation site.
- *Figure 7.* Study 2 average and individual re-experiencing ratings by valence and rating collapsed across stimulation site.

Acknowledgements

I first thank my advisor, Dr. Elizabeth Kensinger, for the immeasurable impact she has had on my life. Six years later and an untold number of hours of training in cognitive science, late-night and early morning email exchanges, discussion, and devoted mentorship have culminated in this dissertation. But her impact on my training transcends this document: After years of her devoted advising and mentorship, I feel like a scientist that can hold her own. It has been life-changing to learn by example from a such a rigorous and passionate scientist as Elizabeth. There is a truly unique feeling of elation and joy that Elizabeth exudes on the road to scientific discovery, and sharing in that process has not only been a tremendous source of reward but also a wellspring from which to draw perseverance in the face of the great challenges that graduate school presents. There is truly no proper way to articulate my gratitude for the expertise, time, and thoughtfulness Elizabeth has invested in me over the past six years, so I can only hope to pay it forward. I am already looking forward to future collaborations and bringing our laboratories together at conferences. Thank you for taking me on six years ago, for your guidance and support, and for always helping me to see the forest for the trees.

I thank the members of my dissertation committee, who each have mentored and guided my training in their own unique ways. I thank Drs. Scott Slotnick and Alexa Veenema for their support and feedback during my time at Boston College. The challenging writing assignments and constructive feedback from Scott in his

“Controversies in Cognitive Neuroscience” course brought me up to speed with writing early in graduate school, which made publishing with Scott all the more fun and insightful. In her “Neurobiology of Mental Illness” course, my master’s thesis, and in this dissertation work, Alexa has always challenged me to think deeply about the role of the amygdala in the emotional memory network as well as the important links with mental health disorders. I thank my external committee member and future post-doctoral advisor, Dr. Michael Yassa, for his mentorship and encouragement over the past several years. I am excited to see what we will discover together.

None of the neuroimaging or brain stimulation work would have been possible without the help of Tammy Moran, Ross Mair, Stephanie McMains, and Caroline West of the Harvard Center for Brain Science. I am especially grateful for the support I have received from Stephanie McMains and her tireless efforts to help me with implementing concurrent psychophysiological recording with fMRI. I thank neurologist Dr. Mark Eldaief and again Stephanie McMains for their hands-on support as I learned how to administer rTMS.

Further, I would like to thank the past and present members of the Cognitive and Affective Neuroscience Laboratory of Boston College. The insightful discussions and feedback in laboratory meetings have taught me so much about other intriguing aspects of memory and have challenged me to reflect and constantly seek to improve my own work. I thank Ryan Daley for the hundreds of hours (yes, hundreds) we spent together collecting the fMRI data that makes up Parts I-III of this dissertation and for being such a great office-mate and friend. I thank Dr. Jaclyn Ford for her support throughout the years

both in and out of the laboratory, as well as teaching me so many things about functional connectivity analysis. I especially want to thank my colleague and dear friend, Dr. Holly Bowen. From theorizing about recapitulation processes and writing articles together, to Sunday dinners and spin classes, Holly has been immensely supportive. I thank her for flying out from Dallas, TX to attend my dissertation defense. I am so thankful for the assistance of a stellar undergraduate research assistant, Kevin Fredericks, who assisted with both fMRI and rTMS data collection. And it is not a hyperbole to say that the rTMS project would not have been possible without the help of Sandry Garcia.

I am grateful for the support from Mike Ring and Barbara O'Brien, who make the behind-the-scenes aspects of the science in our department run so smoothly.

I want to thank the various funding sources over the past six years that made the time and resources required for this work possible: The National Science Foundation (Graduate Research Fellowship [DGE1258923] to SMK and BCS Award [1539361] to EAK), The National Institutes of Mental Health (Ruth L. Kirschstein National Research Service Award [5F31MH113304-02] to SMK; R01MH080833 awarded to E.A.K), American Psychological Association (Dissertation Research Award to SMK), Sigma Xi (Grant-in-Aid to SMK), National Institutes of Health (Shared instrumentation grant [S10OD02003 to Harvard Center for Brain Science]), and the various sources of travel funding at Boston College (GSAS, Provost, GSA).

Last, but certainly not least, I thank my family. My parents, Ken and Cindy Kark, and my brother, Chris Kark, for their boundless love and support since the very beginning. They have made their encouragement felt all the way from the West Coast,

which has been paramount to me completing the massive endeavor that is graduate school. I would be remiss to not acknowledge my cats, Nala and Bowtie, for the countless hours they spent warming my lap. Finally, the daily support and love I have received from my wife, Laurie, as I have pursued my doctoral degree is truly ineffable. Thank you for your patience, your hippocampus jokes, for quite literally picking me up when I felt discouraged, and for being there to celebrate the milestones together.

Note

The contents of Parts I-III have been submitted to peer-reviewed journals for publication or are already published. The tables and figures are in the submission format for those journals.

GENERAL INTRODUCTION

The ability to re-experience our past influences everything from how we behave in the present moment to how we imagine our future (Wheeler et al., 1997). Over the course of a life time, memorial experiences of both triumph and tribulation give rise to a sense of personal identity and a persistent sense of self (Klein and Nichols, 2012). The very ability to re-experience the who, what, when and where of an experience in itself implies our very existence at the time of the remembered event (Reid, 1785). This sense of ‘mental time travel’ is a hallmark feature of episodic memory (Tulving, 2002; Tulving and Thomson, 1973). Yet, not all memories can be re-accessed with a rich sense of vividness or endure over long periods of time. How do the images of the World Trade Center engulfed in flames beneath a bright blue September sky seem forever seared into our minds? How do those memory traces differ from the intensely pleasant memories of walking across the stage at our graduation or down the aisle on our wedding day? And importantly, how do some individuals remember more of life’s unpleasant moments than the pleasant ones?

There are now hundreds of psychological and neuroscience studies that demonstrate the enhancing effects of emotional arousal on memory. Neuroimaging and patient studies have demonstrated the importance of the amygdala—and its interactions with the hippocampus—in emotionally enhanced memory (Buchanan, 2007; Phelps, 2004). However, one key factor that is known to influence the sense of re-experiencing different aspects of a prior event is emotional valence (Phelps and Sharot, 2008)—the

degree of negative or positive emotion associated with an event. For instance, memory re-experiencing tends to be stronger for negative stimuli, compared to positive stimuli, in that negative stimuli are endorsed as strongly recollected or with strong visual details, while positive memories tend to be endorsed as more familiar, semantic, or gist-based (Comblain et al., 2004; Johansson et al., 2004; Kensinger and Choi, 2009). Accordingly, there is evidence that arousal enhances memory formation in valence-specific ways, with more sensory engagement for negative stimuli and more frontal engagement for positive stimuli (Balconi and Ferrari, 2013; Markowitsch et al., 2003; Mickley and Kensinger, 2008; Mickley Steinmetz et. al., 2010). That is, while amygdala engagement and arousal enhance emotional memory, there is evidence that negative and positive memories have diverging phenomenology and neural underpinnings. The present set of dissertation research examines how negative and positive memories are differentially instantiated in the brain across multiple phases of memory.

Functional magnetic resonance imaging (fMRI) work over the past decade has additionally suggested a valence-specific enhancement of memory-related activation in the ventral visual stream for negative memories compared to neutral and positive memories, perhaps explaining the enhanced sense of visual re-experiencing. In a fMRI meta-analysis of twenty emotional memory encoding studies, Murty and colleagues (2011) not only found the expected enhancement of amygdala and hippocampal activation related to successful emotional memory formation, but also enhanced engagement of the ventral visual stream, a “pattern of findings [that seemed] to be borne out within the literature” (pg. 701). In a 2015 fMRI study of emotional encoding and

retrieval processes observed over a 20-minute study-test delay, I showed valence-specific enhancement of retrieval-related reactivation (or ‘recapitulation’) of encoding processes in the ventral visual stream—providing evidence of enhanced encoding-to-retrieval overlap in the ventral visual stream for negative memories (Kark and Kensinger, 2015), consistent with Tulving’s notion of ‘mental time travel’. That evidence—along with work from Bowen and Kensinger (2017a, b)—lead to the development of the Negative Valence Enhances Recapitulation (‘NEVER’) valence-based model of emotional memory (Bowen et al., 2018), which purports that negative valence enhances 1) sensory-focused encoding, 2) selective consolidation of sensory information, 3) recapitulation of sensory information during retrieval, and 4) subjective memory vividness. While prior available theories of emotional memory have accounted for the enhancing effects of arousal on memory, the NEVER model provides a valence-based account of emotionally enhanced memory.

Methods and Logic

In a series of four studies, the present dissertation research directly tests multiple predictions of the valence-based NEVER model of emotional memory by examining the effect of valence on memory-related enhancements in the ventral visual stream across three phases: Encoding, post-encoding rest (early consolidation), and retrieval. **Parts I and II** focus on encoding and peri-encoding memory processes while **Parts III and IV** focus on retrieval processes. Based on prior work, a secondary hypothesis throughout **Parts I-III** is that positive valence enhances memory-related frontal activation and

amygdala-frontal functional connectivity. The present work highlights not only group effects, but the importance of examining individual differences in emotional memory bias.

Part I tests the sensory-focused encoding tenant of the NEVER model by examining valence-specific effects of trial-level physiological arousal and amygdala coupling on subsequent memory vividness. While heightened physiological arousal (i.e., heart rate deceleration) was associated with enhanced amygdala coupling throughout the cortex—perhaps reflective of enhanced attentional processes—amygdala coupling with the ventral visual stream increased as a function of arousal to a greater extent for negative stimuli, compared to neutral and positive stimuli. Critically, enhanced negative subsequent memory vividness was predicted by amygdala coupling with early visual cortex in the presence of heightened physiological arousal responses. Hence, Part I demonstrates that amygdala functional connectivity patterns depend on not only the magnitude of physiological arousal, but also on valence. The findings also demonstrate that arousal-related amygdala modulation of early visual cortex specifically influences negative memory vividness.

Part II addresses tenants 1-3 of the NEVER model by examining group and individual differences in memory as a function of valence across the encoding, post-encoding, and retrieval phases of memory. First, the original negative memory recapitulation findings from a 20-minute study-test delay (Kark and Kensinger, 2015) were replicated and extended to a 24-hour delay, providing evidence that negative memory recapitulation of encoding processes persist in long-term memory. **Part II** also

provides novel evidence that the degree of negative memory bias (i.e., better memory for the bad than the good) and positive memory bias across individuals is linked with post-encoding increases in amygdala resting state coupling with visuocortical and frontal areas, respectively. Further, post-encoding amygdala coupling predicted negative memory bias by influencing the degree of visuocortical retrieval-success activity during retrieval of negative memories. Thus, enhanced visual processing activity is not only related to group-level effects of negative memory formation and retrieval, but also explains a substantial amount of individual variability in negative memory biases.

In **Part III**, retrieval-related reactivation in ventral visual regions showed valence-specific enhancements of negative memory vividness, compared to positive memory vividness. While emotion can enhance a sense of vividness for events that truly occurred, emotion can also increase the likelihood and vividness of false memories (Porter et al., 2003), making them behaviorally indistinguishable from true memories. For instance, famed psychologist Jean Piaget has described a highly emotional childhood false memory of someone trying to kidnap him from his nanny. Piaget later learned that the nanny had fabricated this story and that his emotional memory was false, and yet he could still strongly re-imagine watching the nanny fight off the kidnapper, the gashes on her face, and the cloak and white baton of the police officer who intervened. Piaget wrote "I therefore must have heard, as a child the account of this story...and projected it into the past in the form of a visual memory, which was a memory of a memory, but false." To that end, Part III also examined the effect of valence on false memory vividness and demonstrated spatial overlap in the ventral visual regions that support vividness for true

and false negative memories, implying that negative true and false memories activate similar brain regions.

While Parts I-III provided consistent correlational evidence for negative memory enhancements of ventral visual regions using fMRI, **Part IV** utilized inhibitory repetitive transcranial magnetic stimulation (rTMS) to decipher if activity in one portion of occipito-temporal cortex (posterior inferior temporal gyrus) is causally related to the ability to retrieval and re-experience negative memories. While there was no specific effect of negative valence on subjective visual re-experiencing or group effect of stimulation site (posterior inferior temporal gyrus compared to a vertex control region) on negative memory retrieval, future work is needed to understand the wide-range of individual differences observed in Part IV.

Implications

Together, the findings of these studies suggest that negative valence not only influences visual memory processes in the ventral visual stream at the moment of encoding (Part I) and shortly thereafter (Part II), but that negative valence tightens the links across multiple memory phases, increasing the amount of retrieval-related recapitulation (Part II) and vividness (Part III) at the moment of retrieval. However, while activation in these areas support the likelihood of remembering, compared to forgetting (Part II), signals emanating from these areas can also drive an inaccurate sense of vividness for false negative memories (Part III). Moreover, while these regions are clearly and consistently enhanced in negative memory, they may or may not be *necessary*

for successful retrieval or enhanced subjective re-experiencing (Part IV) and might rather play a more circumscribed role within the broader amygdala-centered emotional memory network. Future work is needed to understand the content of negative visual memoranda and its contribution to memory success and vividness. Nevertheless, a basic science understanding of visual negative memory processes and biases is crucial to understanding aberrant visual memories that are prominent in a range psychopathologic conditions (Brewin et al., 2010).

**1.0 PHYSIOLOGICAL AROUSAL AND AMYGDALA-VISUOCORTICAL
CONNECTIVITY PREDICT SUBSEQUENT VIVIDNESS OF NEGATIVE
MEMORIES**

Submitted Manuscript:

Kark, S. M., Kensinger, E. A., submitted. Physiological arousal and amygdala-
visuocortical connectivity predict subsequent vividness of negative memories.

1.1 ABSTRACT

Relative to neutral memories, negative and positive memories both exhibit an increase in memory longevity, subjective memory re-experiencing, and amygdala activation. These memory enhancements are often attributed to shared influences of arousal on memory. Yet prior work suggests the intriguing possibility that arousal affects memory networks in valence-specific ways. In particular, amygdala-visuocortical functional connectivity (AVFC) increases with arousal for negative memories while amygdala-frontal functional connectivity is associated with positive arousal. Psychophysics work has separately shown that arousal-related heart rate deceleration (HRD) responses are related to enhanced AVFC and visual perception of negative stimuli. However, in the memory realm, it is not known if the effect of AVFC influences subsequent negative memory outcomes as a function of the magnitude of physiological arousal (i.e., HRD) during encoding. Using psycho-autonomic interaction (PAI) analyses and trial-level measures of HRD as an objective measure of arousal during encoding of emotional and neutral stimuli, the current findings suggest the magnitude of HRD responses modulates the effect of AVFC on subsequent negative memory vividness. Specifically, AVFC effects in early visual cortex predicted negative memory vividness—and not neutral or positive vividness—but only in the presence of heightened physiological arousal. This novel PAI approach was grounded in a replication of prior work showing enhanced HRD effects in the insula for negative stimuli regardless of memory. These findings provide further evidence for a valence-based account of emotional memory by demonstrating the effect of arousal on amygdala-centered emotional memory networks depends on valence.

1.2 INTRODUCTION

William James made a prescient observation when he wrote; “An impression may be so exciting emotionally as almost to leave a scar on the cerebral tissues” (James, 1890, pg. 670). Negative memories can differ from positive and neutral memories both in brain and in behavior (Bowen et al., 2018), with functional magnetic resonance imaging (fMRI) studies linking negative valence with enhanced visual processing during successful encoding (Mickley Steinmetz and Kensinger, 2009), post-encoding rest (Kark and Kensinger, in press), and retrieval (Bowen et al., 2018; Kark and Kensinger, 2015, in press) of vivid memories (Kark et al., submitted; Mickley and Kensinger, 2008). Almost all levels of the ventral visual system receive feedback projections from the amygdala, including V1 (Amaral et al., 2003), yet the impact of amygdala-related arousal on memory may depend on valence: Arousal enhances amygdala-visuocortical functional connectivity (AVFC) during encoding of negative memories but amygdala-prefrontal cortex (PFC) connectivity for positive memories (Mickley Steinmetz et al., 2010).

The present study directly examined the effects of physiological arousal on encoding-related amygdala connectivity by using an objective, trial-level metric of arousal: Heart rate deceleration (HRD). HRD is a common metric of arousal corresponding to a phasic parasympathetic response associated with stimulus attention and orienting, with an exaggerated decelerative response to negative stimuli (Lang et al., 1993). In fearful situations, HRD is associated with noradrenergic release in the amygdala and a defensive mode of attentive immobility (i.e., freezing), which are thought to facilitate an organism’s sensory processing of its surroundings to assess threats (Lacey

and Lacey, 1970). Memory research has provided evidence that HRD responses can predict subsequent memory for negative stimuli (Cunningham et al., 2014), however, the neural mechanisms of this memory-enhancing effect have not been formally tested. Recent psychophysics work has shown concurrent HRD responses and increased AVFC enhance *visual sensitivity* (Lojowska et al., 2018), raising the intriguing possibility that arousal enhances perceptual encoding of negative stimuli during memory formation. Previous work has shown that HRD magnitudes correlate with activation in regions linked to emotional memory enhancement: the medial temporal-lobe, including the amygdala (Inman et al., in press), and in the insula and visual processing regions (Critchley et al., 2005; Hermans et al., 2014; Hermans et al., 2013). If negative valence is associated with perceptual enhancements related to HRD-related increases in arousal during the initial experience of a negative stimulus (Lojowska et al., 2018), this could lead to long-term consequences on memory vividness specifically for negative—but not positive—stimuli, consistent with our recent valence-based emotional memory model proposing a disproportionate link between perceptual recapitulation and negative memory (Bowen et al., 2018). Alternatively, HRD responses could relate to AVFC and memory vividness for all arousing stimuli (positive and negative) or even for neutral stimuli (consistent with an attention-based account of HRD).

In the current fMRI study, we asked: Does the magnitude of physiological arousal during encoding facilitate the “searing” of negative experiences into long-term memory? We examined the effect of valence on AVFC profiles associated with an interaction between trial-level HRD responses and subsequent memory vividness by conducting

psycho-autonomic interaction (PAI) analyses (Farrow et al., 2012). We utilized a dataset from an emotional recognition memory fMRI study with a 24-hour delay that demonstrated valence-specific memory enhancements for negative stimuli in visuocortical regions (Kark and Kensinger, in press; Kark et al., submitted). We predicted that heightened HRD response magnitudes and greater AVFC would specifically predict vividness for negative, but not positive, memories, with effects for neutral falling intermediately.

1.3 METHODS

All procedures were approved by the Boston College Institutional Review Board and written informed consent was obtained from all participants. Full explanations of the study stimuli and procedures, including fMRI acquisition parameters, pre-preprocessing, and thresholding have been previously reported (Kark and Kensinger, in press; Kark et al., submitted). We outline the key methods for the current analyses.

Participants.

Thirty-three participants were recruited as a part of a larger study examining the effects of stress and sleep on emotional memory. The participants included in the present analysis did not undergo the stress condition prior to encoding. Data from six participants were excluded from present analyses: One due to a structural anomaly (female, 23), one due to chance-level memory performance (a d' value below zero; male, 25), one from a

technical error resulting in psychophysiology data loss (male, 24), and three participants due to poor HR signal recordings for unknown reasons (2 females). The final analyzed sample included twenty-seven participants ages 18-29 years ($M = 22.2$, $SD = 2.8$, 12 females). Behavioral performance on this task has been reported previously (Kark and Kensinger, in press; Kark et al., submitted).

Recognition Memory Task.

In brief, participants incidentally encoded 150 images of negative, neutral, and positive scenes (50 of each valence) while undergoing concurrent fMRI and psychophysiological recording. Each image was presented for 3s and was preceded by a 1.5s presentation of a line-drawing sketch of the scene. A jittered fixation was presented between trials (6-12s), which allowed the physiological response to return to baseline. The next day, participants completed a surprise recognition task in which all of the old line-drawings from the prior day and an equal number of new line-drawings they had not seen before were presented for a memory judgement. For each line-drawing, participants used a 0-4 scale to make a one-step Old-New memory and vividness rating (0="New", 1="Old, Not Vivid", 2="Old, Somewhat Vivid, 3="Old, Vivid", 4="Old, Extremely Vivid"). Participants were instructed that vividness ratings could be based on any combination of their memory for the visual details or any thoughts, feelings, or reactions of the full colorful photo seen on the prior day.

Heart rate data acquisition, pre-processing, and event analysis.

HR data were acquired at a 1000 Hz sampling frequency during the encoding phase using an MRI-compatible fiber-optic oximetry sensor (Model 7500FO Fiber-Optic Pulse Oximeter, Nonin Medical, Inc) attached to the left index finger in conjunction with the BIOPAC System MP150 module and *AcqKnowledge* software (BIOPAC Systems Inc., Goleta, CA). For each MRI run, the beginning of the HRD data recording through *AcqKnowledge* was time-locked to onset of the MRI scanner and the onset of individual trials were marked in an events channel. Participants were also fitted with a respiration belt and two skin conductance electrodes were attached to their left palm.

The raw HR data (in beats-per-minute) and event markers for each encoding run were analyzed using custom scripts implemented in MATLAB R2017a. Before applying preprocessing steps to the raw HR data, the HR data were first adjusted for a ~4s time delay between the stimulus presentation and the change in HR (Shermohammed et al., 2017). To reduce high-frequency fMRI noise, the HR timeseries for each encoding run was smoothed (moving median window = 1.5s) and then linearly detrended, z-scored, and averaged in 0.5s time-bins.

For each encoding event, a 1s pre-line-drawing baseline was calculated by averaging the normalized HR values in the two, 0.5s time bins immediately preceding the onset of the line-drawing. For each trial, the pre-stimulus baseline was subtracted from the trial analysis segment that covered the line-drawing, IAPS image, and 4s of fixation. Since the line-drawings were relatively devoid of emotion, HRD was calculated by identifying the minimum baseline-corrected HR value that occurred within 1-7s after the

onset of the IAPS image. For easier interpretation, the sign of the HRD values were inverted such that a more positive value corresponded to a stronger deceleration response. All of the event-related HRD traces were inspected for artifacts (0-2% of trials across participants), which were removed from the remaining analyses.

As our neural hypotheses were specifically about HRDs, only trials with a deceleration response (i.e., positive HRD value) were included as effects of interest in the fMRI analyses. Trials associated with an acceleration response (i.e., negative HRD value; ~20% of trials) or artifact (~1% of trials) were modeled as a regressor of no interest in the fMRI analyses.

fMRI analysis.

fMRI analyses were carried out in SPM8 (Wellcome Department of Cognitive Neurology, London, United Kingdom) implemented in MATLAB R2014a. We applied a similar PAI approach using parametric modulation analyses as in Farrow and colleagues (2012). For each participant, three fixed-effects models were created with the following effects of interest: (1) a 7-column Subsequent Vividness (SubViv) model containing subsequently remembered items (hits) separately by valence with trial-level SubViv ratings as parametric modulators and one column containing all of the missed trials; (2) a 6-column HRD model containing all HRD events by stimulus valence (hits and misses collapsed within valence) with the trial-level HRD values as the parametric modulators for each column; and (3) a 13-column model containing all hits by valence with SubViv and HRD as the first and second parametric modulators (to control for the main effects)

followed by the trial-level PAI term (SubViv*HRD) and one column containing all of the missed trials. The third model allowed us to examine the PAI effect, that is, amygdala functional connectivity patterns above and beyond those patterns separately associated with SubViv or HRD. Each of the fixed-effects models also included a separate column comprised of the trials that showed a negative HRD value (possibly due to inspiration) or a HR artifact. All event-related encoding trials were modelled as 6s box-car functions convolved with the hemodynamic response functions. Finally, a matrix of regressors of no interest was added to the end of each fixed-effects model that controlled for item-level objective salience of the IAPS images (Kark and Kensinger, in press), seven head-motion parameters, and linear drift.

Next, functional connectivity analyses were conducted for each participant. Left and right amygdala seed regions (LAMY and RAMY) were generated using a 3D maximum probability atlas of the human brain (Hammers et al., 2003). Statistical maps of parametric functional connectivity of the amygdala were generated using the Generalized Psychophysiological Interactions Toolbox (gPPI Toolbox; McLaren et al., 2012). For each amygdala seed region, the gPPI toolbox was used to 1) generate task/psychological regressors, 2) estimate the BOLD signal in the amygdala seed regions to create the physiological variable, and 3) calculate the psychophysiological interaction terms by convolving the timecourse vectors with the corresponding parametric modulator vectors.

For all participants, six whole-brain functional parametric *t* images were saved from each of the three models to examine the main effects of SubViv, HRD, and PAI for each valence and amygdala seed. These *t* contrasts were entered into three separate

repeated-measures 2x3 ANOVAs at the random-effects with factors of hemisphere (Left, Right) and valence (Negative, Positive, Neutral). The results did not yield strong hemisphere-by-valence interactions; thus, we focus our findings on amygdala functional connectivity patterns collapsed across hemisphere.

1.4 RESULTS

Heart rate deceleration.

Analysis of variance showed a main effect of valence ($F(1.6, 42.4) = 4.0, p = 0.03$) and no main effect of memory ($p = 0.64$) or interaction ($p = 0.32$). As expected, negative items elicited the strongest HRD response ($M_{\text{neg}} = 0.48, M_{\text{neu}} = 0.43, M_{\text{pos}} = 0.37$) that were significantly greater than positive HRD responses ($t(26) = 2.32, p = .03$) and numerically greater than neutral HRD responses ($t(26) = 1.63, p = 0.12$). Average neutral and positive HRD response magnitudes were not significantly different ($t(26) = 1.6, p = 0.12$).

fMRI results: Effects of valence on amygdala functional connectivity (AFC).

Main effects of vividness. Neutral item vividness was associated with AVFC (shown in green, Figure 1A), including occipital gyri and the left inferior temporal gyrus. Positive item vividness was associated with AFC throughout the PFC (shown in blue, Figure 1A). AFC was not modulated by the main effect of negative item vividness. Peak

coordinates are listed in Table 1.

Main effects of heart rate deceleration. Consistent with prior research (Critchley et al., 2005; Lojowska et al., 2018), AFC increased as a function of arousal-related HRD in the insula and throughout the ventral visual stream, including V1 (shown in red, Figure 1B and see peak coordinates in Table 2). These effects were valence-specific in the left middle occipital gyrus and right occipito-temporal cortex (shown in magenta, Figure 1B) and greater than neutral stimuli in the left occipito-temporal cortex (shown in yellow, Figure 1B). Compared to negative valence, there was a strikingly different pattern for the neural correlates of HRD for neutral and positive stimuli: AFC increased with ventral parietal and frontal areas for neutral and positive stimuli, respectively (shown in green and blue, Figure 1B see peak coordinates in Tables 3 and 4).

Psycho-autonomic interaction. Negative hits were associated with AFVC PAI effects in a large portion ($k=491$) of the cuneus (including V1; $MNI_{xyz}=4,-72,16$), retrosplenial cortex (RSC), lingual gyrus, and superior occipital gyrus (shown in Figure 1C). Of these regions, V1, a cuneus/precuneus cluster, and a RSC cluster showed notable valence-specific effects (shown in yellow and magenta in Figure 1C and in call-out bar plots) that were also robust to sampling and survived controlling for scan-wise skin conductance metrics and respiration (see Table 5 for peak coordinates and further details). There were no suprathreshold PAI effects for neutral and positive stimuli.

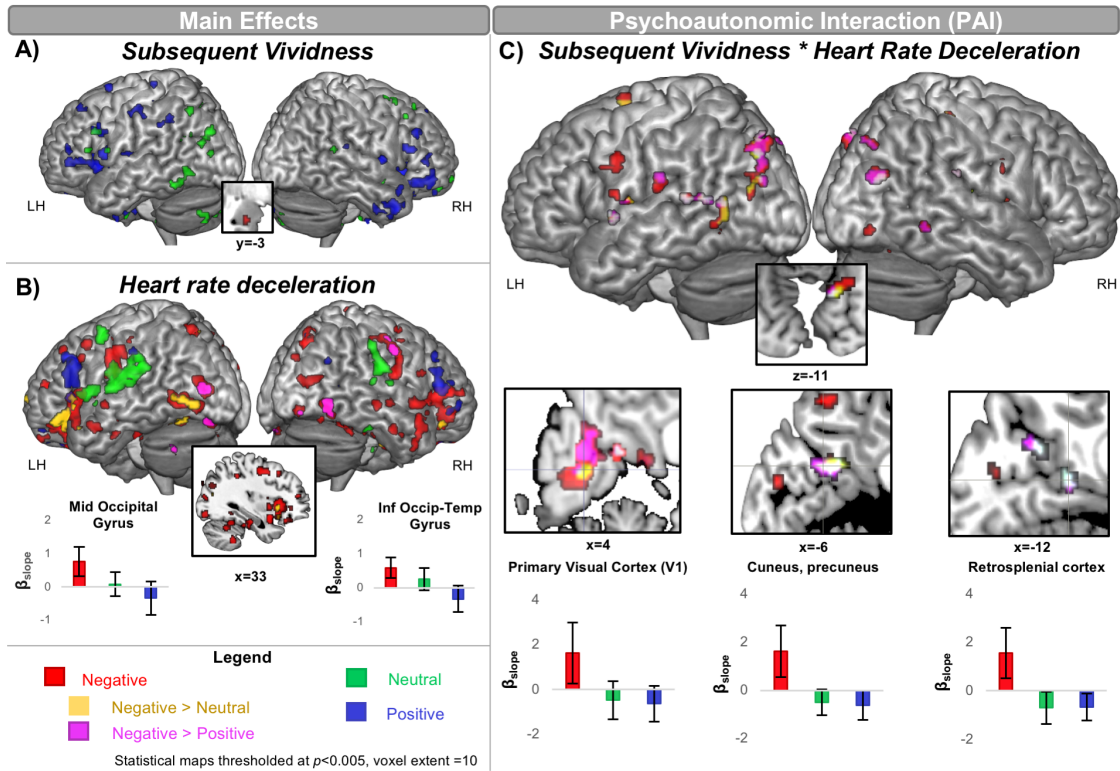


Figure 1. Statistical maps of amygdala parametric functional connectivity with subsequent vividness (**1A**), heart rate deceleration (**1B**), and their interactions (**1C**). Call-out plots for heart rate deceleration are shown for the left middle occipital gyrus and the right inferior occipito-temporal cortex (**1B**). Results are collapsed across the right and left amygdala, except in the coronal slice of the left amygdala in the top left panel, which depicts interhemispheric AFC with increasing subsequent vividness for negative stimuli. Error bars represent 95% within-subject confidence intervals. β_{slope} corresponds to the parameter estimate of the slopes. LH=Left hemisphere, RH=Right hemisphere. Statistical maps thresholded at $p < 0.005$, voxel extent=10.

Table 1. Main effects of subsequent vividness for neutral and positive memories.

Lobe	Hem	Region	BA	MNI	TAL	k
<i>Neutral Subsequent Memory Vividness</i>						
Occipital	L	Lingual gyrus	19	-16,-82,4	-16,-78,0	12
Occipital	L	Middle occipital gyrus	18	-28,-78,28	-27,-77,22	220
Occipital	L	Middle occipital gyrus	18	-34,-80,10	-33,-77,5	15
Temporal	L	Fusiform gyrus	37	-28,-38,-20	-27,-35,-18	34

Temporal	R	Fusiform gyrus	20	30,-36,-24	27,-33,-20	17
Temporal	R	Hippocampus, parahippocampal cortex	36, 54	32,-18,-18	29,-17,-13	29
Temporal	L	Inferior occipito-temporal cortex	20, 37	-52,-52,-18	-49,-48,-17	224
Temporal	L	Inferior temporal gyrus	20	-26,-6,-46	-25,-3,-38	13
Temporal	R	Superior and middle temporal gyrus	21, 22	48,2,-10	44,1,-4	59
Temporal	R	Superior temporal gyrus	22	68,-46,16	62,-46,15	14
Frontal	L	Inferior frontal gyrus	44	-58,16,30	-55,11,31	26
Frontal	L	Inferior frontal gyrus	45	-54,22,14	-51,18,18	20
Frontal	R	Medial frontal gyrus	10	16,68,-10	14,62,1	12
Frontal	L	Middle frontal gyrus	9	-44,10,28	-42,5,29	17
Frontal	R	Middle frontal gyrus	6	38,10,64	33,2,63	47
Frontal	R	Middle frontal gyrus	6	50,20,46	45,13,48	14
Frontal	R	Orbital frontal cortex	11	26,38,-16	23,35,-6	22
Frontal	R	Orbital frontal cortex	11	16,56,-16	14,52,-5	20
Frontal	L	Precentral gyrus	4	-36,-2,30	-35,-6,30	11
Frontal	L	Precentral gyrus	4	-56,6,12	-53,3,14	10
Frontal	R	Superior frontal gyrus	8	26,34,54	22,25,56	28
Parietal	L	Inferior parietal lobule	7	-34,-62,44	-33,-63,37	30
Parietal	B	Precuneus	7	0,-70,36	-2,-70,30	126
Parietal	L	Precuneus	7	-10,-68,54	-11,-70,46	25
Other	R	Caudate	N/A	10,10,16	8,6,19	53
Other	R	Caudate	N/A	14,12,-10	12,10,-4	23
Other	L	Cerebellum	N/A	-22,-74,-50	-21,-66,-47	92
Other	L	Cerebellum	N/A	-16,-54,-20	-16,-50,-19	42
Other	R	Cerebellum	N/A	16,-78,-42	14,-71,-40	29
Other	R	Cerebellum	N/A	26,-58,-40	23,-52,-36	21
Other	R	Posterior cingulate	23	16,-44,36	13,-46,33	63
Other	L	Thalamus	N/A	-6,-28,-2	-7,-28,0	16
Other	R	Thalamus	N/A	8,-24,0	6,-24,2	56

Other	R	Thalamus	N/A	24,-14,4	21,-15,7	10
<i>Positive Subsequent Memory Vividness</i>						
Temporal	R	Fusiform gyrus	20	32,-4,-40	29,-2,-31	11
Temporal	L	Inferior temporal gyrus	20	-42,-12,-44	-39,-9,-37	44
Temporal	R	Inferior temporal gyrus	20	52,-6,-36	48,-4,-28	25
Temporal	R	Parahippocampal cortex	36	28,-26,-20	25,-24,-16	12
Temporal	R	Parahippocampal cortex, uncus	28, 36	24,-2,-36	22,-1,-28	16
Temporal	L	Superior temporal gyrus	38	-32,2,-48	-30,4,-39	18
Temporal	R	Superior temporal gyrus	22, 38	50,12,-36	46,12,-26	138
Temporal	R	Temporal pole	38	40,8,-42	37,9,-32	16
Temporal	L	Transverse temporal gyrus	41	-50,-14,12	-47,-16,13	31
Temporal	L	Transverse temporal gyrus	42	-42,-28,8	-40,-28,8	11
Frontal	L	Inferior frontal gyrus	44	-48,8,28	-46,3,29	76
Frontal	R	Inferior frontal gyrus	44	60,24,16	54,19,21	33
Frontal	R	Inferior frontal gyrus	47	58,36,6	53,31,14	26
Frontal	L	Medial frontal gyrus	6	-2,18,50	-3,11,50	38
Frontal	L	Medial frontal gyrus	6	-4,-4,64	-5,-11,61	35
Frontal	R	Medial frontal gyrus	10	8,48,14	6,42,21	89
Frontal	R	Medial frontal gyrus	11	14,54,-22	12,50,-11	10
Frontal	L	Middle frontal gyrus	8	-36,32,50	-35,24,51	28
Frontal	L	Middle frontal gyrus	9	-48,40,12	-45,35,18	16
Frontal	R	Middle frontal gyrus	45	52,34,34	47,27,38	73
Frontal	R	Precentral gyrus	4	52,0,6	47,-3,10	141
Frontal	L	Superior frontal gyrus	6	-20,10,68	-20,2,65	30
Frontal	L	Superior frontal gyrus	6	-14,4,54	-15,-3,52	14
Frontal	R	Superior frontal gyrus	8	10,44,48	8,35,51	18
Parietal	R	Parietal operculum	N/A	56,-34,18	51,-35,18	10
Parietal	L	Post-central gyrus	2	-30,-26,48	-29,-30,44	241
Parietal	L	Post-central gyrus	2	-34,-32,70	-33,-38,63	12
Parietal	L	Supramarginal gyrus	40	-60,-50,40	-57,-52,34	31

Parietal	L	Supramarginal gyrus	40	-54,-42,36	-52,-44,32	10
Other	R	Anterior cingulate	24	6,20,22	4,15,26	94
Other	L	Caudate	N/A	-12,10,8	-12,7,12	23
Other	R	Caudate	N/A	16,4,14	14,1,17	20
Other	R	Cerebellum	N/A	0,-90,-34	-1,-83,-34	62
Other	R	Cerebellum	N/A	0,-50,-32	-1,-46,-29	18
Other	R	Cerebellum	N/A	10,-46,-26	8,-42,-23	12
Other	L	Cingulate gyrus	32	-8,36,22	-9,30,27	46
Other	L	Cingulate gyrus	24	-2,14,34	-3,8,36	16
Other	R	Cingulate gyrus	31	6,-2,36	4,-7,36	22
Other	R	Globus pallidus		16,2,-10	14,1,-4	11
Other	L	Insula	13	-32,-10,2	-31,-11,5	1053
Other	L	Insula	13	-34,-26,2	-33,-26,3	64
Other	L	Insula	13	-28,16,-12	-27,14,-6	22
Other	R	Insula	13	36,20,-4	32,17,3	399
Other	R	Insula	13	36,-16,-2	32,-17,1	129
Other	R	Putamen	N/A	28,6,-8	25,4,-2	12
Other	R	Thalamus	N/A	10,-14,0	8,-15,3	32

Hem=Hemisphere, B=Bilateral, L=Left hemisphere, R=Right hemisphere, MNI=Montreal Neurological Institute, TAL=Talairach and Tournoux, k=voxel extent

Table 2. Main effects of HRD for negative stimuli. Clusters showing a valence-specific (Negative HRD > Positive HRD) or negative emotional enhancement (Negative HRD > Neutral HRD) are displayed first (inclusively masked with Negative HRD at $p < 0.005$). The Negative HRD section of the table includes those clusters that showed no emotion or valence-specific enhancements in the whole-brain contrasts.

Lobe	Hem	Region	BA	MNI	TAL	k
Negative HRD > Positive HRD						
Occipital	R	Inferior occipital gyrus, fusiform gyrus	19	26,-80,-14	23,-75,-15	11
Occipital	R	Inferior occipito-temporal gyrus	20, 37	48,-68,-8	43,-65,-8	42
Occipital	L	Lingual gyrus, fusiform gyrus	18	-22,-84,-20	-21,-78,-22	18
Occipital	L	Middle occipital gyrus	18	-36,-84,6	-35,-80,1	48

Temporal	L	Superior temporal gyrus	21	-44,-8,-12	-42,-8,-8	11
Frontal	L	Inferior frontal gyrus	47	-22,18,-22	-21,17,-14	12
Frontal	R	Inferior frontal gyrus	47	24,8,-20	21,7,-13	18
Frontal	L	Temporal pole	38	-38,14,-22	-36,13,-15	23
Parietal	L	Inferior parietal lobule	40	-56,-16,18	-53,-18,18	10
Parietal	R	Postcentral gyrus	2	54,-20,48	48,-25,46	10
Parietal	R	Postcentral gyrus	2	66,-14,36	60,-18,36	30
Other	L	Cerebellum	N/A	-52,-66,-44	-49,-59,-42	20
Other	R	Globus pallidus	N/A	14,-2,-4	12,-3,1	18
Other	R	Insula	13	42,-4,-4	38,-5,1	10
Other	R	Insula	13	36,6,0	32,4,5	13
Negative HRD > Neutral HRD						
Occipital	L	Fusiform gyrus	37	-36,-70,-20	-34,-65,-20	28
Occipital	L	Middle and inferior occipital gyrus	19	-44,-78,-8	-42,-74,-11	101
Occipital	R	Superior occipital gyrus	30	30,-72,16	26,-70,12	13
Temporal	L	Parahippocampal cortex	36	-10,-34,-8	-10,-33,-6	10
Temporal	L	Superior temporal gyrus	21	-44,-6,-16	-42,-6,-11	10
Frontal	L	Inferior frontal gyrus	47	-48,20,2	-45,17,7	18
Frontal	R	Inferior frontal gyrus	47	40,34,-18	36,31,-8	24
Frontal	R	Inferior frontal gyrus, insula	13, 47	24,10,-20	21,9,-13	118
Frontal	L	Inferior frontal gyrus, temporal pole, insula	13, 38, 47	-40,12,-20	-38,11,-13	473
Frontal	L	Superior frontal gyrus	10	-10,68,10	-10,61,19	54
Frontal	R	Superior frontal gyrus	8	8,40,50	6,31,52	12
Parietal	L	Precuneus, superior parietal lobule	7	-24,-70,46	-24,-71,39	25
Other	L	Anterior cingulate	32	-12,46,10	-12,40,17	11

Other	B	Caudate, subgenual area	25	-2,10,-10	-3,8,-4	216
Other	L	Cingulate gyrus	32	-4,32,34	-5,25,37	39
Other	R	Cingulate gyrus	32	16,14,42	13,8,43	29
Other	R	Globus pallidus	N/A	14,-2,-2	12,-4,2	19
Other	L	Insula	13	-26,28,0	-25,24,6	22
Negative HRD						
Occipital	L	Calcarine sulcus	17	-12,-90,12	-12,-87,7	13
Occipital	L	Calcarine sulcus	30	-8,-64,10	-9,-62,7	17
Occipital	L	Cuneus	17	-24,-84,18	-24,-81,12	19
Occipital	L	Fusiform gyrus	19	-28,-66,-8	-27,-62,-9	10
Occipital	R	Fusiform gyrus	19	38,-70,-20	34,-65,-19	16
Occipital	R	Lingual gyrus	19	14,-60,6	12,-58,4	37
Occipital	R	Middle occipital gyrus	19	50,-80,10	45,-77,7	123
Occipital	R	Superior occipital gyrus	19	30,-88,32	26,-87,25	21
Occipital	R	Superior occipital gyrus	19	28,-72,30	24,-72,25	55
Temporal	L	Hippocampus	54	-24,-34,-4	-23,-33,-3	10
Temporal	L	Inferior temporal gyrus	20	-52,-18,-28	-49,-16,-23	19
Temporal	R	Inferior temporal gyrus	20	64,-6,-32	59,-5,-24	10
Temporal	R	Inferior temporal gyrus	20	66,-18,-30	60,-16,-23	27
Temporal	L	Middle temporal gyrus	21	-54,-22,-16	-51,-21,-13	33
Temporal	L	Middle temporal gyrus	21	-60,0,-22	-56,0,-16	41
Temporal	R	Middle temporal gyrus	21	70,-32,-10	64,-31,-7	32
Temporal	R	Middle temporal gyrus	21	58,-22,-6	53,-22,-2	103
Temporal	L	Parahippocampal cortex	36	-28,-40,-16	-27,-38,-14	18
Temporal	L	Parahippocampal cortex	36	-34,-28,-28	-32,-25,-24	29

Temporal	R	Parahippocampal cortex	36	24,-32,-12	21,-31,-9	50
Temporal	L	Parahippocampal cortex, hippocampus	36, 54	-16,-26,-10	-16,-25,-7	104
Temporal	R	Parahippocampal cortex, hippocampus	36, 54	32,-22,-22	29,-21,-17	54
Frontal	R	Inferior frontal gyrus	9	54,6,20	49,2,23	24
Frontal	R	Medial frontal gyrus	10	14,54,10	12,48,18	41
Frontal	L	Middle frontal gyrus	8	-40,30,40	-38,23,42	109
Frontal	L	Middle frontal gyrus	6	-32,8,52	-31,1,51	160
Frontal	L	Middle frontal gyrus	46	-42,44,16	-40,38,22	225
Frontal	R	Middle frontal gyrus	9	26,36,26	23,29,31	15
Frontal	R	Middle frontal gyrus	10	34,48,14	30,42,21	16
Frontal	R	Middle frontal gyrus	6	30,20,44	26,13,46	29
Frontal	L	Orbital frontal cortex	10	-6,62,-20	-6,58,-8	25
Frontal	L	Precentral Gyrus	6	-58,10,32	-55,5,33	16
Frontal	L	Precentral gyrus	6	-54,6,44	-52,0,43	65
Frontal	R	Precentral Gyrus	4	46,-6,58	41,-13,56	17
Frontal	R	Precentral gyrus	4	44,0,34	39,-5,35	52
Frontal	R	Precentral gyrus, middle frontal gyrus	4, 6	32,-8,50	28,-14,48	304
Frontal	R	Superior frontal gyrus	6	14,30,52	11,22,53	13
Frontal	L	Ventral medial prefrontal cortex	32	-4,26,-16	-4,24,-8	53
Frontal	R	Ventral medial prefrontal cortex	11	2,44,-26	1,41,-15	18
Parietal	R	Inferior parietal lobule	40	38,-30,36	34,-33,34	30
Parietal	L	Postcentral gyrus	3	-44,-14,48	-42,-19,45	38
Parietal	R	Postcentral gyrus	5	12,-38,76	9,-44,69	12
Parietal	R	Postcentral gyrus	3	60,-8,46	54,-14,45	12
Parietal	L	Postcentral gyrus, inferior parietal lobule	1, 40	-66,-16,32	-63,-19,30	333
Parietal	L	Posterior cingulate	31	-6,-64,26	-7,-64,22	11

Parietal	L	Superior parietal lobule	7	-30,-46,44	-29,-48,39	44
Parietal	R	Superior parietal lobule	7	32,-40,42	28,-43,39	19
Parietal	R	Superior parietal lobule	7	24,-48,58	20,-52,52	25
Parietal	R	Superior parietal lobule, superior occipital gyrus	7, 19	26,-78,44	22,-78,37	364
Other	R	Anterior cingulate	24	4,36,6	3,31,13	103
Other	R	Caudate	N/A	14,4,18	12,0,21	23
Other	L	Cerebellum	N/A	-52,-66,-44	-49,-59,-42	25
Other	L	Cerebellum	N/A	-16,-52,-28	-16,-48,-26	27
Other	L	Cerebellum	N/A	-20,-74,-46	-19,-67,-44	64
Other	L	Cerebellum	N/A	-34,-58,-38	-32,-52,-35	216
Other	R	Cerebellum	N/A	18,-76,-48	16,-68,-45	15
Other	R	Cerebellum	N/A	14,-62,-32	12,-57,-30	15
Other	R	Cerebellum	N/A	14,-76,-24	12,-71,-24	27
Other	R	Cerebellum	N/A	36,-44,-44	33,-39,-39	65
Other	L	Cingulate gyrus	23	-6,-14,38	-7,-18,37	11
Other	R	Posterior cingulate	31	8,-62,20	6,-61,17	19
Other	L	Putamen	N/A	-22,-12,6	-21,-13,8	16

Hem=Hemisphere, B=Bilateral, L=Left hemisphere, R=Right hemisphere, MNI=Montreal Neurological Institute, TAL=Talairach and Tournoux, k=voxel extent

Table 3. Main effects of HRD for positive stimuli. Clusters showing a valence-specific (Positive HRD > Negative HRD) or positive emotion enhancement (Positive HRD > Neutral HRD) are displayed first (inclusively masked with Positive HRD at $p < 0.005$). The Positive HRD section of the table includes those clusters that showed no emotion or valence-specific enhancements in the whole-brain contrasts.

Lobe	Hem	Region	BA	MNI	TAL	k
<i>Positive HRD > Negative HRD</i>						
Occipital	R	Lingual gyrus	19	24,-74,4	21,-71,1	11
Frontal	R	Dorsal medial prefrontal cortex	9	12,42,32	10,35,37	36

Other	L	Cerebellum		-2,-54,-20	-3,-50,-19	17
<i>Positive HRD > Neutral HRD</i>						
Occipital	R	Lingual gyrus	19	28,-74,0	25,-71,-2	37
Frontal	L	Dorsal medial prefrontal cortex	10	-2,50,28	-3,42,33	16
Frontal	R	Dorsal medial prefrontal cortex	9	10,42,30	8,35,35	38
Frontal	L	Inferior frontal gyrus	47	-48,22,4	-45,19,9	34
Frontal	L	Middle and inferior frontal gyrus	9, 44	-46,18,28	-44,13,30	37
Frontal	L	Superior frontal gyrus	6	-6,30,58	-7,21,58	41
Frontal	L	Ventral medial prefrontal cortex	11	0,56,-26	-1,53,-14	15
Parietal	R	Angular gyrus	39	48,-66,26	43,-66,22	11
Other	L	Cerebellum	N/A	-6,-68,-14	-7,-64,-15	30
<i>Positive HRD</i>						
Occipital	L	Lingual gyrus	19	-30,-68,0	-29,-65,-2	10
Temporal	L	Fusiform gyrus	37	-42,-44,-14	-40,-41,-13	42
Temporal	R	Middle temporal gyrus	21	42,-56,8	38,-55,7	19
Temporal	L	Superior temporal gyrus	22	-52,-26,2	-49,-26,3	15
Frontal	R	Dorsal medial prefrontal cortex	8	2,32,46	0,24,48	28
Frontal	R	Inferior frontal gyrus	46	50,38,16	45,32,22	12
Frontal	R	Inferior frontal gyrus	46	48,46,-2	44,41,7	114
Frontal	R	Inferior frontal gyrus	45	60,28,10	54,23,16	136
Frontal	R	Middle frontal gyrus	8	56,24,36	50,17,39	42
Frontal	L	Orbital frontal cortex	11	-18,56,-16	-17,52,-6	12
Frontal	L	Orbital frontal cortex	11	-8,44,-28	-8,42,-17	13
Frontal	L	Precentral gyrus	6	-44,0,48	-42,-6,46	18
Parietal	L	Inferior parietal lobule	40	-66,-36,34	-63,-38,30	10

Parietal	R	Precuneus	31	8,-66,32	6,-66,27	24
Parietal	R	Superior parietal lobule	7	18,-72,50	15,-73,43	52
Other	L	Caudate	N/A	-14,12,4	-14,9,9	19
Other	L	Cerebellum	N/A	-16,-56,-36	-16,-51,-33	11
Other	R	Cerebellum	N/A	14,-48,-38	12,-43,-34	12
Other	R	Cerebellum	N/A	40,-62,-38	36,-56,-35	14
Other	R	Cerebellum	N/A	14,-76,-38	12,-69,-36	30

Hem=Hemisphere, B=Bilateral, L=Left hemisphere, R=Right hemisphere, MNI=Montreal Neurological Institute, TAL=Talairach and Tournoux, k=voxel extent

Table 4. Main effects of HRD for neutral stimuli.

Lobe	Hem	Region	BA	MNI	TAL	k
Temporal	R	Inferior temporal gyrus	20	56,-36,-28	51,-33,-23	17
Temporal	L	Superior temporal gyrus	22	-54,-12,-6	-51,-12,-3	45
Temporal	R	Superior temporal gyrus	22	64,-20,8	58,-21,10	11
Frontal	L	Paracentral lobule	5	-4,-32,54	-5,-36,49	10
Frontal	L	Paracentral lobule	5	0,-14,66	-2,-21,62	21
Frontal	L	Precentral gyrus	4	-50,-6,48	-48,-11,46	110
Frontal	L	Precentral gyrus	6	-60,4,4	-57,2,7	124
Parietal	R	Inferior parietal lobule, superior temporal gyrus	22, 40	68,-28,20	62,-30,21	261
Parietal	L	Inferior parietal lobule, superior temporal gyrus, insula	13, 22, 40	-66,-42,22	-62,-42,19	786
Other	R	Cingulate gyrus	31	12,-22,40	10,-26,38	30
Other	L	Putamen	N/A	-20,14,-2	-19,12,3	13
Other	L	Putamen	N/A	-22,0,-12	-21,-1,-7	35
Other	R	Putamen	N/A	22,10,-6	19,8,0	76

Hem=Hemisphere, B=Bilateral, L=Left hemisphere, R=Right hemisphere, MNI=Montreal Neurological Institute, TAL=Talairach and Tournoux, k=voxel extent

Table 5. Valence-specific psycho-autonomic interaction (PAI) effects (Negative PAI > Positive PAI AND Neutral PAI, inclusively masked with Negative PAI at $p < 0.005$) followed by clusters that only showed an enhancement over one valence or the other. Listed last are clusters that showed a significant Negative PAI effect but not a significant whole-brain enhancement over Positive or Neutral PAI. Superscripted symbols denote clusters that survive additional control analyses (see legend below table).

Lobe	Hem	Region	BA	MNI	TAL	k
<i>Negative PAI > Positive PAI AND Negative PAI > Neutral PAI</i>						
Occipital	L	Cuneus (including V1), precuneus, retrosplenial cortex ^{^*~}	7, 17, 23, 29, 30	-8,-68,24	-9,-67,19	361
Occipital	R	Lingual gyrus	18	14,-68,-10	12,-64,-11	19
Occipital	R	Middle occipital gyrus [~]	19	42,-78,22	37,-77,17	58
Occipital	L	Superior occipital gyrus [~]	19	-36,-86,22	-35,-84,16	12
Occipital	L	Superior occipital gyrus, superior parietal lobule ^{^~}	7, 19	-20,-76,34	-20,-75,27	165
Temporal	L	Middle temporal gyrus	37	-56,-62,10	-53,-60,7	10
Temporal	L	Middle temporal gyrus [~]	21	-58,-56,12	-55,-55,9	21
Temporal	L	Parahippocampal cortex ^{^~}	36	-26,-48,-8	-25,-46,-8	29
Temporal	R	Parahippocampal cortex [~]	36	28,-38,-14	25,-36,-11	21
Temporal	L	Superior temporal gyrus [~]	22	-64,-44,12	-60,-44,10	15
Temporal	L	Superior temporal gyrus [~]	22	-54,2,4	-51,0,7	17
Parietal	L	Cuneus, retrosplenial cortex, lingual gyrus [^]	30	-12,-54,8	-12,-53,6	39
Parietal	R	Supramarginal gyrus ^{*~}	40	50,-30,24	45,-32,24	12
Other	L	Insula [~]	13	-44,-4,10	-42,-6,12	18
<i>Negative PAI > Positive PAI</i>						
Occipital	R	Superior occipital gyrus	19	28,-84,44	24,-84,36	15
Temporal	R	Middle temporal gyrus	22	54,-50,-8	49,-48,-7	17
Parietal	L	Inferior parietal lobule	40	-60,-30,24	-57,-32,22	12
<i>Negative PAI > Neutral PAI</i>						
Occipital	L	Superior occipital gyrus	19	-34,-82,38	-33,-81,30	13
Temporal	R	Transverse temporal gyrus ^{^*~}	41	46,-22,14	41,-24,15	15

Frontal	L	Middle frontal gyrus~	6	-22,-2,66	-22,-9,62	16
Parietal	R	Superior parietal lobule~	7	32,-32,58	28,-37,54	13
Other	R	Cingulate gyrus ^{^*} ~	32	10,20,36	8,14,38	16
Other	R	Insula~	13	42,-2,12	38,-5,15	14
<i>Negative PAI (no overlap with valence contrasts)</i>						
Occipital	L	Calcarine sulcus	17	-8,-86,16	-9,-83,11	20
Occipital	R	Fusiform gyrus	19	36,-80,-8	32,-76,-10	16
Temporal	L	Fusiform gyrus	37	-40,-60,-8	-38,-57,-9	12
Frontal	L	Cingulate gyrus	24	-8,8,40	-9,2,40	11
Frontal	L	Precentral gyrus	4	-62,-2,14	-59,-5,15	11
Frontal	L	Precentral gyrus	4	-58,-4,36	-55,-8,35	42
Frontal	R	Precentral gyrus	4	46,-4,32	41,-9,33	17
Parietal	L	Precuneus	7	-6,-66,54	-7,-68,46	16
Parietal	R	Superior parietal lobule	7	20,-52,52	17,-55,46	15

[^]Cluster overlaps with F-Contrast of the main effect of valence

*Survives controlling for skin conductance level (n=27) at p<0.005

~Survives controlling for respiration (n=21) at p<0.05

Hem=Hemisphere, B=Bilateral, L=Left hemisphere, R=Right hemisphere, MNI=Montreal Neurological Institute, TAL=Talairach and Tournoux, k=voxel extent

1.5 DISCUSSION

Using PAI analyses to examine interactions between trial-level metrics of arousal (i.e., HRD) and subsequent memory vividness, the current work provides strong evidence that arousal increases AVFC during encoding in a way that corresponds specifically to later vividness of negative, but not positive or neutral, memories. These results provide empirical support for William James' conjecture that the arousal of a negative event is

what “sears” it into memory. In fact, we found that the link between AVFC and subsequent vividness for negative memories *was contingent upon* the consideration of HRD: There was no main effect of negative memory vividness on AVFC, the relation to AVFC only emerged when the interaction between with HRD was considered. While we did not predict this contingency *a priori*, it is intriguingly consistent with affective “tagging” theories of negative memories: Arousal tags negative memory traces during encoding, which are then prioritized and selectively consolidated (Bennion et al., 2015). By utilizing trial-level changes in HRD, we were further able to show that these “tagging” effects are sensitive to the actual *magnitude* of the physiological arousal response, which goes beyond prior work using subjective arousal ratings or arousal categories based on normative data (i.e., high vs. low arousal).

We grounded these novel PAI findings in a replication of prior work demonstrating HRD main effects for negative stimuli in ventral visual regions (Lojowska et al., 2018) and the insula (Critchley et al., 2005). Together, these results underscore that not only does HRD relate to AFC in valence-specific ways, the implications for memory vividness are also valence-specific.

The current study provides foundational work for future investigations. First, although the effect in early visual cortex survived controlling for overall skin conductance level, item-level controls of event-related sympathetic responses (e.g., skin conductance or pupillary responses) could definitively confirm if this effect is specific to parasympathetic HRD, or if is more broadly related to autonomic arousal. Second, we can only infer based on prior work that affective valence is somehow gating V1 inputs and

thus possibly altering, for example, perception and field of view (Schmitz et al., 2009), perceptual vividness (Todd et al., 2013), visual sensitivity (Lojowska et al., 2018), or signal-to-noise ratios during encoding, all of which could influence the resolution of the information that enters memory stores (Xie and Zhang, 2017) to be selectively consolidated into long-term memory. Future work is needed to understand the content of the information that is enhanced in perception and memory for negative stimuli by AVFC that influences the subjective vividness of long-term memories.

1.6 REFERENCES

- Amaral, D.G., Behniea, H., Kelly, J.L., 2003. Topographic organization of projections from the amygdala to the visual cortex in the macaque monkey. *Neuroscience* 118, 1099-1120.
- Bennion, K.A., Payne, J.D., Kensinger, E.A., 2015. Selective effects of sleep on emotional memory: What mechanisms are responsible? *Translational Issues in Psychological Science* 1, 79-88.
- Bowen, H.J., Kark, S.M., Kensinger, E.A., 2018. NEVER forget: negative emotional valence enhances recapitulation. *Psychon Bull Rev* 25, 870-891.
- Critchley, H.D., Rotshtein, P., Nagai, Y., O'Doherty, J., Mathias, C.J., Dolan, R.J., 2005. Activity in the human brain predicting differential heart rate responses to emotional facial expressions. *Neuroimage* 24, 751-762.
- Cunningham, T.J., Crowell, C.R., Alger, S.E., Kensinger, E.A., Villano, M.A., Mattingly, S.M., Payne, J.D., 2014. Psychophysiological arousal at encoding leads to reduced reactivity but enhanced emotional memory following sleep. *Neurobiol Learn Mem* 114, 155-164.
- Farrow, T.F., Johnson, N.K., Hunter, M.D., Barker, A.T., Wilkinson, I.D., Woodruff, P.W., 2012. Neural correlates of the behavioral-autonomic interaction response to potentially threatening stimuli. *Front Hum Neurosci* 6, 349.
- Hammers, A., Allom, R., Koeppe, M., Free, S., Myers, R., Lemieux, L., Mitchell, T., Brooks, D., Duncan, J., 2003. Three-dimensional maximum probability atlas of

- the human brain, with particular reference to the temporal lobe. *Hum Brain Mapp* 19, 224-247.
- Hermans, E.J., Battaglia, F.P., Atsak, P., de Voogd, L.D., Fernandez, G., Roozendaal, B., 2014. How the amygdala affects emotional memory by altering brain network properties. *Neurobiol Learn Mem* 112, 2-16.
- Hermans, E.J., Henckens, M.J., Roelofs, K., Fernandez, G., 2013. Fear bradycardia and activation of the human periaqueductal grey. *Neuroimage* 66, 278-287.
- Inman, C.S., Bijanki, K.R., Bass, D.I., Gross, R.E., Hamann, S., Willie, J.T., in press. Human amygdala stimulation effects on emotion physiology and emotional experience. *Neuropsychologia*.
- James, W., 1890, pg. 670. *Principles of Psychology*. Holt, New York, NY.
- Kark, S.M., Kensinger, E.A., 2015. Effect of emotional valence on retrieval-related recapitulation of encoding activity in the ventral visual stream. *Neuropsychologia* 78, 221-230.
- Kark, S.M., Kensinger, E.A., in press. Post-encoding Amygdala-Visuosensory Coupling Is Associated with Negative Memory Bias in Healthy Young Adults. *J Neurosci*.
- Kark, S.M., Slotnick, S.D., Kensinger, E.A., submitted. Effects of emotional valence on true and false memory vividness.
- Lacey, J., Lacey, B., 1970. Some autonomic central nervous system interrelationships. In: Black, P. (Ed.), *Physiological correlates of emotion*. Academic Press, New York:, pp. 205-227.

- Lang, P.J., Greenwald, M.K., Bradley, M.M., Hamm, A.O., 1993. Looking at pictures: affective, facial, visceral, and behavioral reactions. *Psychophysiology* 30, 261-273.
- Lojowska, M., Ling, S., Roelofs, K., Hermans, E.J., 2018. Visuocortical changes during a freezing-like state in humans. *Neuroimage* 179, 313-325.
- McLaren, D.G., Ries, M.L., Xu, G., Johnson, S.C., 2012. A generalized form of context-dependent psychophysiological interactions (gPPI): a comparison to standard approaches. *Neuroimage* 61, 1277-1286.
- Mickley, K.R., Kensinger, E.A., 2008. Emotional valence influences the neural correlates associated with remembering and knowing. *Cogn Affect Behav Neurosci* 8, 143-152.
- Mickley Steinmetz, K.R., Addis, D.R., Kensinger, E.A., 2010. The effect of arousal on the emotional memory network depends on valence. *Neuroimage* 53, 318-324.
- Mickley Steinmetz, K.R., Kensinger, E.A., 2009. The effects of valence and arousal on the neural activity leading to subsequent memory. *Psychophysiology* 46, 1190-1199.
- Schmitz, T.W., De Rosa, E., Anderson, A.K., 2009. Opposing influences of affective state valence on visual cortical encoding. *J Neurosci* 29, 7199-7207.
- Shermohammed, M., Mehta, P.H., Zhang, J., Brandes, C.M., Chang, L.J., Somerville, L.H., 2017. Does Psychosocial Stress Impact Cognitive Reappraisal? Behavioral and Neural Evidence. *J Cogn Neurosci* 29, 1803-1816.

Todd, R.M., Schmitz, T.W., Susskind, J., Anderson, A.K., 2013. Shared neural substrates of emotionally enhanced perceptual and mnemonic vividness. *Front Behav Neurosci* 7, 40.

Xie, W., Zhang, W., 2017. Negative emotion enhances mnemonic precision and subjective feelings of remembering in visual long-term memory. *Cognition* 166, 73-83.

**2.0 POST-ENCODING AMYGDALA-VISUOSENSORY COUPLING IS
ASSOCIATED WITH NEGATIVE MEMORY BIAS IN HEALTHY YOUNG
ADULTS**

Published Article:

Kark, S.M., Kensinger, E.A., in press. Post-encoding Amygdala-Visuosensory Coupling
Is Associated with Negative Memory Bias in Healthy Young Adults. *J Neurosci*.

2.1 ABSTRACT

The amygdala is well-documented as the critical nexus of emotionally enhanced memory, yet its role in the creation of negative memory biases—better memory for negative as compared to positive stimuli—has not been clarified. While prior work suggests valence-specific effects at the moment of ‘online’ encoding and retrieval—with enhanced visuosensory processes supporting negative memories in particular—here we tested the novel hypothesis that the amygdala engages with distant cortical regions after encoding in a manner that predicts inter-individual differences in negative memory biases in humans. Twenty-nine young adults (males and females) were scanned while they incidentally encoded negative, neutral, and positive scenes, each preceded by a line-drawing sketch of the scene. Twenty-four hours later, participants were scanned during an Old/New recognition memory task with only the line-drawings presented as retrieval cues. We replicated and extended our prior work, showing that enhanced ‘online’ visuosensory recapitulation supports negative memory. Critically, resting state scans flanked the encoding task, allowing us to show for the first time that individual differences in ‘offline’ increases in amygdala resting state functional connectivity (RSFC) immediately following encoding relate to negative and positive memory bias at test. Specifically, post-encoding increases in amygdala RSFC with visuosensory and frontal regions were associated with the degree of negative and positive memory bias, respectively. These findings provide new evidence that valence-specific negative memory biases can be linked to the way that sensory processes are integrated into amygdala-centered emotional memory networks.

2.2 INTRODUCTION

We tend to remember the good and bad events in our lives long past the time when trivial events have slipped from our memories, but recent work suggests negative and positive memories are not always created equally in brain or behavior (Bowen et al., 2018). Despite the clinical relevance of understanding how disproportionate memory for negative events over positive events—a cognitive risk factor for depression (Gerritsen et al., 2012)—arises from individual differences in neural memory processes, these relationships have yet to be tested empirically. The bulk of task-based fMRI work on emotional memory has focused on the encoding of negative stimuli, with a focus on the amygdala, hippocampus, ventral visual stream, and prefrontal cortex (Murty et al., 2011). However, studies comparing memory for positive and negative events have suggested that while the amygdala is engaged by both valences (Hamann et al., 1999), the effect of arousal on the targets of amygdala-cortical coupling during encoding can depend on valence (Mickley Steinmetz et al., 2010). Our prior research has shown valence-specific memory effects during retrieval, with greater retrieval-related reactivation of encoding processes in visuosensory regions for negative events relative to positive and neutral ones (Bowen and Kensinger, 2017a, b; Kark and Kensinger, 2015), evidence that contributed to our proposed valence-based model of emotional memory (Bowen et al., 2018).

Decades of animal and human work in support of the *modulation hypothesis* of amygdala function has shown that the amygdala is the critical “nexus” of emotional memory formation and consolidation due to its ability modulate neural processes in medial temporal lobe (MTL) regions and distant cortical regions (Cahill and McGaugh,

1998; Hermans et al., 2014; McGaugh, 2000), including visual cortices (Dringenberg et al., 2004; Vuilleumier et al., 2004). Feedback projections from the amygdala to almost all levels of visual cortex are thought to enhance their response during emotional situations (Amaral et al., 2003; Silverstein and Ingvar, 2015) and likely continue to influence memory processes *after* the initial encoding experience itself (McGaugh, 2005; Müller and Pilzecker, 1900). Thus, the amygdala is well-positioned to exert long-lasting negative memory enhancing effects in visuosensory regions.

The work described above has monitored ‘online’ memory processes to reveal neural mechanisms that support emotional memory formation and retrieval during task. However, ‘offline’ post-encoding resting-state functional connectivity (RSFC) analysis has become increasingly utilized to reveal links between early consolidation processes and memory performance (Hermans et al., 2017; Murty et al., 2017; Tambini et al., 2010). Here, we use this approach in the emotional episodic memory realm to investigate the links between post-encoding changes in amygdala-cortical RSFC and behavioral measures of emotional memory bias across participants, an approach that has the potential to unveil ‘offline’ early consolidation processes that differentially predict long-term negative and positive memory outcomes.

We adjudicated between arousal-based and valence-based accounts of emotional modulation of early consolidation processes. An arousal-based account of emotional memory would predict the same link between post-encoding increases in amygdala RSFC and enhanced memory for negative and positive stimuli, while our valence-based account would predict a strong link between post-encoding increases in amygdala-visuosensory

RSFC and negative memory biases specifically, with a link to neutral memory falling between negative and positive. Based on previous work (Mickley Steinmetz et al., 2010), a secondary hypothesis was that amygdala-frontal RSFC enhancements would relate to positive memory biases.

Here, resting-state fMRI scans flanked the encoding scan and preceded the recognition scan of an emotional recognition memory paradigm with a 24-hour study-test delay. Participants incidentally encoded line-drawings of scenes (negative, positive, and neutral), each followed by the full image. At test, only old and new line-drawings were presented for an Old/New judgement. We root our novel test of the links between post-encoding increases in amygdala RSFC and valence-specific memory biases across participants in a replication-extension of our prior work (Kark and Kensinger, 2015) showing enhanced visuosensory recapitulation for negative memories.

2.3 METHODS

Participants

Thirty-three participants were recruited to participate in the control (no induced stress) condition of a larger study examining the effects of stress and sleep on emotional memory. All participants were right-handed, native English speakers between the ages of 18-29, with normal or corrected-to-normal vision and with no reported history of head injury, learning disorders, neurologic or psychiatric problems, or current medications affecting the central nervous system. Participants were screened for MRI environment

contradictions before entering the scanner. The Boston College Institutional Review Board approved this study and written informed consent of study procedures was obtained from all participants. Participants were compensated \$25/hour for their participation.

For inclusion in this set of analyses, participants needed to have usable data from encoding and retrieval fMRI scans, including above-chance recognition memory performance, as well as at least 5 minutes of usable RSFC data from pre- and post-encoding (Waheed et al., 2016). (Although additional measures were gathered as part of the larger study, they were not examined for this analysis and therefore were not required for data inclusion). Four participants were excluded from all of the present analyses: one due to chance-level memory performance (an overall d' value below zero; male, 25), one due to a brain structure anomaly (female, 23), one did not undergo a post-encoding RSFC scan due to time constraints and additionally did not have enough trials per condition for task fMRI analyses (female, 21), and one participant (male, 20) had excessive motion across resting state fMRI scans, resulting in less than 5 minutes of useable data for each resting scan. The final sample for the RSFC analyses was twenty-nine participants ages 18-29 ($M = 22.3$, $SD = 2.8$, 14 females). For the task-based fMRI analyses of subsequent memory and retrieval success, seven additional participants (3 females) were excluded because they did not have an ample number of trials across all of the memory conditions by valence (trials count requirement ≥ 8). The final sample for the memory task-fMRI analyses was twenty-two participants ($M = 22.2$, $SD = 2.8$, 11 females). However, to examine how brain-behavior patterns from the twenty-two participant sample expand to

the larger sample (with possibly noisier activation estimations), the data for these 7 participants will appear as open circles in the follow-up scatter plot for the memory retrieval fMRI analyses (see Figure 2B).

Experimental Design

Participants underwent fMRI scanning at the Harvard Center for Brain Science during both an incidental encoding task and a surprise recognition memory task approximately 24-hours later (see Figure 1A for depiction of the timeline for acquisition of data).

Encoding task

The encoding task is depicted in Figure 1B. Study stimuli were 300 images selected from the Internal Affective Picture System (IAPS; Lang et al., 2008) database and nearly identical to the set used in Kark and Kensinger (2015). In brief, participants viewed 150 line-drawings of IAPS images (50 negative, 50 neutral, 50 positive, each for 1.5s), followed by the full color photo of that line-drawing (3s). As an incidental encoding task, participants made a button press to indicate whether they would “Approach” or “Back Away” from each of the images. The negative and positive images were pre-selected using the normative data provided by IAPS (Lang et al., 2008) to ensure that the negative images were equally arousing ($M_{\text{neg}} = 5.54$, $M_{\text{pos}} = 5.43$, $t(198) = 1.32$, $p = 0.19$, independent samples t -test) and of similar absolute valence ($M_{\text{neg}} = 2.05$, $M_{\text{pos}} = 2.07$, $t(198) = 0.25$, $p = 0.80$, independent samples t -test) as the positive images.

The negative images were more arousing ($M_{\text{neut}} = 3.25$, $t(198) = 23.95$, $p < 0.001$, independent samples t -test) and higher in absolute valence ($M_{\text{neut}} = 0.42$, $t(198) = 19.27$, $p < 0.001$, independent samples t -test) than the neutral images. Similarly, positive images were more arousing ($t(198) = 22.97$, $p < 0.001$, independent samples t -test) and higher in absolute valence ($t(198) = 25.00$, $p < 0.001$, independent samples t -test) than neutral images. Line-drawing versions of the IAPS images were created using in-house MATLAB scripts (see Figure 1B and 1C for examples of IAPS images and their line-drawings). Resting state scans were collected immediately before and after the encoding task runs. During each of the three resting state scans, the stimuli presentation computer monitor was turned off (i.e., no fixation cross was presented) and participants were instructed to relax with their eyes open and think about anything that came to mind. The eye-tracking camera was on throughout the resting state scans and monitored by the experimenters to ensure that participants kept their eyes open for the majority of each rest scan.

Recognition task

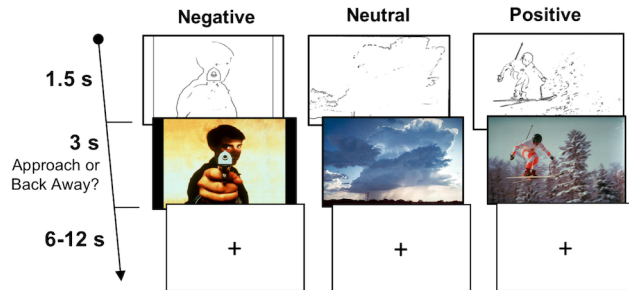
Twenty-four hours after encoding, participants returned to the scanner for a surprise recognition memory task. After a pre-retrieval resting state scan, participants were presented with all 150 of the old line-drawings (3s each, jittered fixation 1.5-9s) that they had seen during encoding randomly mixed with an equal number of new line-drawings. (Study lists were varied across participants such that studied line-drawings for some participants were the new line-drawings for other participants). For each line-

drawing, participants were instructed to use a 0-4 scale to indicate in one decision whether the line-drawing was new (0) or, if old, how vividly they remembered the colorful photo (1=“Not Vivid” to 4=“Extremely Vivid”). Here, we collapse across vividness ratings to compare old (1-4) to new (0) responses. To ensure participants understood that half of the line-drawings were old and half were new, we instructed them during the practice and instruction period that they should be pressing the 0 key “about half of the time”. The use of line-drawing cues—as opposed to re-presentation of the full colorful IAPS images—allowed us to 1) cue individual memories with less-emotionally laden visual cues and 2) trigger memories while minimizing visual and emotion induction confounds at the time of retrieval.

A) Scans used for current data analyses



B) Incidental Encoding Task



C) Sample Recognition Stimuli

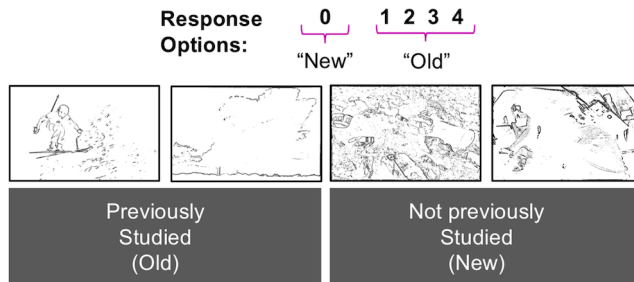


Figure 1. Scanning procedures and task structure. **1A)** Participants were scanned over the course of two days during an incidental encoding and a 24-hour surprise recognition memory task. RSFC scans were acquired before and after incidental encoding, as well as directly before retrieval. **1B)** Sample encoding trials. **1C)** Participants returned to the scanner 24 hrs later for a surprise recognition memory task in which all of the old line-drawings and an equal number of new line-drawings were presented one at a time. For each item, participants had 3 seconds to rate if a line-drawing was “Old” (1-4) or “New” (0), followed by a jittered fixation period (1.5-9s). Sample recognition stimuli are shown, with the depicted study history listed below in the gray boxes.

Post-recognition arousal and valence ratings

After the recognition scan, and outside of the scanner, participants completed post-scan ratings of arousal and valence (1-7 scales) of the 300 IAPS images. Results of these post-scan IAPS ratings confirmed that negative images were more arousing ($M_{\text{neg}} = 5.72$, $SD_{\text{neg}} = 0.61$, $M_{\text{neut}} = 4.0$, $SD_{\text{neut}} = 0.37$, $t(28) = 15.65$, $p < 0.001$, paired samples t -

test) and higher in absolute valence ($M_{\text{neg}} = 2.20$, $SD_{\text{neg}} = 0.38$, $M_{\text{neut}} = 0.62$, $SD_{\text{neut}} = 0.36$, $t(28) = 19.43$, $p < 0.001$, paired samples t -test) than the neutral images. Positive images also were more arousing ($M_{\text{pos}} = 4.60$, $SD_{\text{pos}} = 0.84$, $t(28) = 4.40$, $p < 0.001$, paired samples t -test) and higher in absolute valence ($M_{\text{pos}} = 1.77$, $SD_{\text{pos}} = 0.37$, $t(28) = 19.23$, $p < 0.001$, paired samples t -test) than the neutral images. However, despite being equated for arousal based on IAPS normative data (as reported above) negative images were rated as more arousing ($t(28) = 6.09$, $p < 0.001$, paired samples t -test) and higher in absolute valence ($t(28) = 6.06$, $p < 0.001$, paired samples t -test) than the positive images. The same pattern of results was observed in the subset of twenty-two participants in the memory task-based fMRI analyses.

Although the post-scan ratings of absolute valence and arousal were greater for negative stimuli, compared to positive stimuli, it is important to keep in mind that these ratings were made after participants had studied and retrieved the images, which could impact their valence and arousal strengths (e.g., perhaps these negative stimuli maintain their arousal even after multiple viewings, while positive stimuli show mitigation or habituation of arousal over repeated presentations). Nevertheless, in the fMRI data, valence-based patterns will be considered to occur when region of interest (ROI) analyses reveal a pattern of Negative greater than Neutral greater than Positive, not just Negative greater than Positive greater than Neutral, to ensure that they cannot simply be driven by lower arousal or absolute-valence in the positive images (since the positive images were rated as more arousing and of greater absolute-valence than the neutral images, as reported above). Moreover, for the replication fMRI analysis of Kark and Kensinger

(2015), we show the recapitulation results from an analysis that included individual ratings of subjective arousal as a nuisance regressor in the fixed-effects models of encoding and retrieval. Further, to ensure the reported across-subjects' effects were not driven by any valence differences of subjective arousal across participants (i.e., those with the greatest difference between negative and positive arousal ratings), we controlled for valence differences of arousal between-subjects (i.e., $Arousal_{neg-pos}$: average negative arousal ratings – average positive arousal ratings), where applicable.

MRI acquisition

Structural and functional images were acquired using a Siemens MAGNETOM Prisma 3T scanner with a 32-channel head coil. A localizer and auto-align scout were followed by collection of whole-brain T₁-weighted anatomical images (MEMPRAGE, 176 slices, 1.0mm³ voxels, TR = 2530 ms, Flip angle = 7 degrees, Field of view = 256 mm, base resolution = 256). The functional images were acquired using Simultaneous Multi-Slice blood-oxygen-level dependent (SMS-BOLD) scan sequences (Barth et al., 2016) provided by the Center for Magnetic Resonance Research at University of Minnesota (Feinberg et al., 2010; Moeller et al., 2010; Xu et al., 2013). All T₂-weighted EPI images were acquired in an interleaved fashion and included the whole brain, with the slices aligned 25 degrees above the anterior commissure–posterior commissure line in the coronal direction. The pulse sequences for the encoding and retrieval task-fMRI scans (69 slices, TR = 1500ms, 2.0 mm³ isotropic voxels, TE = 28 ms, Flip angle = 75 degrees, 208 mm field of view, base resolution = 104, multi-band acceleration factor = 3) differed

from the resting state EPI sequence (TR = 650ms, 64 slices, 2.3 mm³ voxels, TE = 34.8ms, flip angle = 52 degrees, field of view read = 207mm, multi-band acceleration factor = 8, base resolution = 90).

Statistical analysis

Memory performance and emotional memory bias

Effects of valence on memory performance (as calculated by $d' = z[\text{hit rate}] - z[\text{false alarm rate}]$) was tested using repeated-measures ANOVA with a factor of valence. Negative memory bias (Negative d' – Positive d') and Positive memory bias (Positive d' – Negative d') were calculated for each participant. Given that memory biases were calculated as difference scores, the fMRI data contrasts of interest were additionally masked where appropriate to ensure results were also correlated with memory performance of the single valence (e.g., Negative d' alone), and thus not driven by an inverse relationship with the other valence (e.g., Positive d'). Throughout the remainder of the analyses, *memory performance* refers to the d' score for a given valence category, whereas *memory bias* is the difference between d' scores between negative and positive stimuli.

fMRI pre-processing

Memory task-based fMRI. FMRI images from the encoding and retrieval scans were pre-processed and analyzed using SPM8 (Wellcome Department of Cognitive

Neurology, London, United Kingdom) implemented in MATLAB 2014a. All functional images were reoriented, realigned, co-registered, and spatially normalized to the Montreal Neurological Institute (MNI) template (re-sampled at 3 mm during segmentation and written at 2 mm during normalization), and smoothed using a 6 mm isotropic Gaussian kernel. The first 4 scans of each run were discarded to account for scanner equilibrium effects. Global mean intensity, rotation, and translation motion outliers were identified using Artifact Detection Tools (ART; available at www.nitrc.org/projects/artifact_detect). Global mean intensity outliers were defined as scans with a global mean intensity that differed by more than 3 standard deviations from the mean. Acceptable motion parameters were set to 3 mm for translation and 3 degrees for rotation. Framewise displacement (FWD)—the average rotation and translation parameter differences from scan to scan, using weight scaling (Power et al., 2012)—was calculated for each participant. Individual scan runs were eliminated if more than 5% of the timepoints were identified as having 1) an FWD value greater than 0.5 mm (Power et al., 2012) and 2) greater than 3 mm of movement/3 degree rotation. In total, 4 scan runs were excluded from the encoding analyses (two encoding runs for one participant, and one encoding run each for two other participants) and 5 scan runs were excluded from retrieval analyses (one run from 5 different participants). One participant was completely removed from the memory task-based fMRI analysis because 3 of their 6 retrieval runs showed excessive head motion based on these thresholds, resulting in too few trials for analysis. Participants were required to still have an ample number (≥ 8) of each response

type (hits and misses by valence) after any individual scan runs were removed due to motion.

Resting state fMRI. Resting state scans were pre-processed and denoised using the CONN Toolbox (Whitfield-Gabrieli and Nieto-Castanon, 2012; www.nitrc.org/projects/conn, RRID:SCR_009550) implemented in MATLAB 2015a and SPM12. To ensure the scanner had reached a steady state, the first 6 timepoints of each RSFC scan were discarded (Waheed et al., 2016). Functional scans were then realigned and unwarped, centered, segmented, normalized to MNI space, and smoothed with an 8 mm Gaussian smoothing kernel. Functional data were resampled to 2 mm isotropic voxels. Conservative functional outlier detection settings were utilized during the ART-based identification of outlier scans for scrubbing (global signal z -value threshold of 3, subject-motion threshold of 0.3 mm). Pre-processed resting scans for each participant were linearly detrended and a commonly used band pass filter (0.008-0.09 Hz) was applied after regression to isolate low-frequency fluctuations characteristic of resting state fMRI and attenuate signals outside of that range (Fox et al., 2005; Fox et al., 2006; Waheed et al., 2016). White matter and CSF noise sources were removed using the CONN Toolbox *aCompCor* method for noise removal. After artifact scrubbing, all participants included in the present analyses had at least 5.2 minutes ($M = 7.6$ minutes) of useable timepoints for each of the RSFC scans. One additional participant (male, 28)—also excluded from the memory task-fMRI analyses—was excluded from the follow-up analysis of pre-retrieval RSFC due to excessive motion resulting in less than 5 minutes pre-retrieval RSFC data.

Memory task-fMRI analyses

General linear models. For each participant, first-level models were created for encoding and retrieval separately. For both encoding and retrieval, each model contained twelve regressors of interest: hits and misses by the three valence categories, each with a parametric modulator for item reaction times to control for the time to make the Approach/Back Away decision (during encoding) or the memory judgement (during retrieval). Retrieval models additionally included correct rejections and false alarms, collapsed across valence. To control for low-level visual confounds, an additional nuisance regressor column contained item-level visual statistic information for the TRs that the images were on the screen (i.e., average image saliency for each IAPS image for the encoding models and edge density of the line-drawings for the retrieval models). Image saliency for each IAPS photo was calculated using the Saliency Toolbox (Itti and Koch, 2001) and the edge density of each line-drawing image was calculated as the proportion of black pixels within the image frame using MATLAB. Finally, 7 motion regressors (FWD, x, y, z roll, pitch yaw) were added before the linear drift regressors.

Analyses to test for replication of encoding-to-retrieval overlap. For encoding and retrieval separately, full-factorial 2x3 ANOVAs at the random-effects level were created with factors of memory (hits, misses) and valence (negative, neutral, positive). Encoding-to-retrieval overlap (or ‘recapitulation’) effects were operationalized like they were in the original study (Kark and Kensinger, 2015) as the spatial overlap of regions that exhibit differences due to memory at encoding (Hits > Misses, Dm effects; Paller and Wagner, 2002; Wagner et al., 1999) and Retrieval Success Activity at retrieval (Hits >

Misses). Practically, the encoding-to-retrieval overlap (or ‘recapitulation’) maps are a conjunction of encoding and retrieval maps (Encoding Dm \cap Retrieval Success) executed separately for each valence (e.g., Encoding Negative Dm \cap Negative Retrieval Success). Encoding-to-retrieval overlap maps were created for negative, neutral, and positive recapitulation effects separately (see Figure 2A, activity in red, white, and blue, respectively). The same approach was taken to analyze random-effects level recapitulation effects while controlling for subjective ratings of arousal in the fixed-effects models (see Figure 2A activity in magenta and cyan for negative and positive stimuli controlling for arousal, respectively).

Relations between valence-specific retrieval success activity and individual differences in emotional memory bias. Here, we conduct the first individual differences examination for links between valence-specific activity at the moment of successful retrieval and corresponding valence-specific memory biases. To test if those participants who recognized more negative stimuli than positive stimuli were those with greater retrieval success activity for negative stimuli in visuosensory regions, a whole-brain one-sample *t*-test was used to demarcate regions that showed a correlation between the first-level parameter estimates of Negative-Biased Retrieval Success Activity (e.g., Negative Retrieval Success > Positive Retrieval Success) and the magnitude the negative memory bias (e.g., Negative d' – Positive d'). To ensure the resulting clusters were not driven by the inverse relationship for positive memory effects, the resulting map was also inclusively masked with the results of an additional one-sample *t*-test to demarcate regions that also showed a correlation between Negative Retrieval Success Activity and

Negative d' (held at a reduced threshold of $p < 0.05$). We conducted a similar analysis to assess links between Positive-Biased Retrieval Success Activity and positive memory bias.

Resting state fMRI analyses

Whole brain seed-to-voxel RSFC analyses were conducted using left and right amygdala seeds from a maximum probability atlas of the human brain (Hammers et al., 2003).

These analyses produced Fisher r -to- Z transformed whole-brain maps of pre-encoding, post-encoding, and pre-retrieval amygdala RSFC for each participant. First-level r -to- Z RSFC maps outputted from CONN were entered into a factorial in SPM8 for group analysis with one factor (i.e., condition) with two levels (pre-encoding, post-encoding).

To test for valence specific memory biases, Negative d' , Neutral d' , and Positive d' were into the model as co-variates set to interact with the condition factor.

Baseline amygdala RSFC. We began the RSFC analyses with a replication of baseline amygdala RSFC patterns. We first examined group-level pre-encoding (Z_{Pre}) amygdala RSFC maps, as a comparison to prior work characterizing RSFC networks of the amygdala. For comparison with previous work reporting few changes in the amygdala RSFC following emotion picture viewing (Geissman et. al., 2018), next we examined overall pre-to-post encoding increases in amygdala RSFC ($Z_{Post} > Z_{Pre}$ masked with Z_{Post} thresholded at $p < 0.005$). These first two analyses were utilized to establish our group findings before exploring the novel inter-individual difference questions central to the purpose of the current study.

Post-encoding amygdala RSFC and emotional memory biases. The central purpose of the RSFC analysis was to test the hypothesis that individual differences in post-encoding amygdala coupling enhancements will relate to later emotional memory biases in a valence-specific manner. To test this hypothesis, we queried the factorial model in two ways to demarcate brain regions that showed correlations between pre-to-post encoding increases in amygdala RSFC and emotional memory biases. We first examined the whole-brain relationship of post-encoding increases in resting state that correlated with negative memory *performance* ($[Z_{\text{Post}} - Z_{\text{Pre}}] * \text{Negative } d'$), but not neutral or positive memory performance (by exclusively masking out the maps of $[Z_{\text{Post}} - Z_{\text{Pre}}] * \text{Neutral } d'$ and $[Z_{\text{Post}} - Z_{\text{Pre}}] * \text{Positive } d'$ each held at a reduced threshold of $p < 0.05$). Given that negative memory bias and pre-to-post encoding RSFC changes were difference measures, we further required post-encoding amygdala RSFC levels on their own to be correlated with negative memory performance (inclusively masked with the map of $Z_{\text{Post}} * \text{Negative } d'$). Critically, we further report the clusters that also show a valence-specific relationship between pre-to-post-encoding increases in amygdala RSFC and negative memory *bias* ($[Z_{\text{Post}} - Z_{\text{Pre}}] * [\text{Negative } d' - \text{Positive } d']$). That is, the greater the post-encoding increase in RSFC, the greater the difference between Negative d' and Positive d' for a given participant. The reverse approach was taken to test for regions that show a relationship between post-encoding amygdala coupling increases and positive memory *performance* ($[Z_{\text{Post}} - Z_{\text{Pre}}] * \text{Positive } d'$) and positive memory *bias* ($[Z_{\text{Post}} - Z_{\text{Pre}}] * \text{Positive } d' - \text{Negative } d'$) (inclusively masked with the map of $Z_{\text{Post}} * \text{Positive } d'$). We hypothesized valence-specific effects, by which parameter estimates of the slopes would

not only be greater for negative compared to positive (as revealed at the whole-brain level), but also with targeted ROIs showing parameter estimates of the slope for neutral falling in the middle of negative and positive.

Data reporting and visualization

Unless otherwise specified, whole-brain group analyses were interrogated at $p < 0.005$ (uncorrected). Monte Carlo Simulations (<https://www2.bc.edu/sd-slotnick/scripts.htm>) determined that a voxel extent of $k=40$ for memory task-fMRI analyses and $k=54$ for the resting-state fMRI analyses corrected results to $p < 0.05$. As in our original study (Kark and Kensinger, 2015), all conjunction analyses to assess the replication of encoding-to-retrieval overlap were thresholded at the joint probability $p < 0.005$ by setting the individual thresholds of each voxel at encoding and retrieval to $p = 0.0243$ (calculated using the Fisher equation; Fisher, 1973). Due to the resolution (2mm^3), voxels in brain stem regions are not reported in the tables. Follow-up ROI analyses were conducted using REX (<http://web.mit.edu/swg/software.htm>) to extract first-level parameter estimates for each subject for the conditions of interest to be entered into ANOVAs and t -tests and to extract the second-level parameter estimates of slopes to visualize the correlations between amygdala post-encoding RSFC by phase and memory performance by valence (see bar plots in Figure 4). Foci conversion (MNI to Talaraich coordinates) was implemented using the GingerAle (<http://www.brainmap.org/ale/>). Rendering of statistical maps was implemented using MRICroGL

(<http://www.mccauslandcenter.sc.edu/mricrogl/home>) and MRICRON (<http://people.cas.sc.edu/rorden/mricron/index.html>).

2.4 RESULTS

Memory performance and emotional memory bias

Overall recognition memory performance (d') varied across the 29 participants ($M = 0.74$, $SD = 0.33$, $SE = 0.06$, range: 0.17-1.52) and was lower than in our original 20-minute delay study ($M = 1.22$, $SE = 0.1$; Kark and Kensinger, 2015), which is not surprising given the longer study-test interval. As in our 2015 paper, we observed no significant group-level effects of valence on memory performance ($F(2,56) = 1.7$, $p = 0.19$, ANOVA) between negative ($M = 0.76$, $SD = 0.40$, $SE = 0.08$), positive ($M = 0.80$, $SD = 0.44$, $SE = 0.08$), and neutral stimuli ($M = 0.69$, $SD = 0.34$, $SE = 0.06$). Importantly, there was a range of memory bias scores (Negative d' - Positive d') scores across participants ($SD = 0.35$, range: -0.71 to +0.71); 13 participants showed a negative memory bias while 16 participants showed a positive memory bias (see full spread of negative and positive memory bias in the scatter plots in Figure 4, bottom). Individual differences in memory biases were not correlated with differences in post-scan ratings of arousal and absolute valence between the negative and positive IAPS images across the 29 participants (Arousal_{neg-pos}: $r(27) = .16$, $p = 0.41$; Absolute Valence_{neg-pos}: $r(27) = .19$,

$p = 0.34$, Pearson's correlation), suggesting that they arose from memory differences and not merely differences in emotional experience of the stimuli.

Memory task-based fMRI results

Replication of enhanced visuosensory recapitulation for negative memories

Before examining new questions regarding individual differences in emotional memory biases, we first sought to replicate our prior findings demonstrating enhanced recapitulation in visuosensory regions for negative memories (Bowen and Kensinger, 2017b; Kark and Kensinger, 2015) and confirm that enhanced group-level visuosensory recapitulation for negative events extends to a 24-hour study-test delay. Indeed, the conjunction analyses revealed encoding-to-retrieval overlap for negative memories in the bilateral ventral visual stream (inferior temporal and fusiform gyri), parahippocampal cortex, parietal areas, as well as lateral and orbital portions of the prefrontal cortex (see activity in red in Figure 2A and refer to Figure 3 in Kark and Kensinger, 2015).

Additional control analyses showed that many of these negative memory recapitulation regions—including ventral visual regions such as the inferior temporal gyri and parahippocampal cortex—remain significant even when the post-scan ratings of arousal were entered as a participant- and item-specific regressor in the fixed effects models (see activity in magenta in Figure 2A). However, two of the ventral visual stream clusters (of the right inferior temporal gyrus clusters and of the left fusiform gyrus clusters) no longer reached significance with item-level arousal metrics in the models. In another control analysis, there were no regions that showed arousal-memory interactions

across encoding and retrieval (i.e., a conjunction of positive parametric relation of arousal for Hits > Misses across both phases), further suggesting the majority of these recapitulation effects were not driven by systematic differences in arousal between the valences. However, future work with tighter controls is needed to clarify valence-arousal interactions. Notwithstanding, these replication results and additional control analyses were critical for three reasons: They allowed us to 1) root the central individual differences questions of the current study in a replication of prior work (Kark and Kensinger, 2015), 2) to further demonstrate that negative valence indeed enhances recapitulation in the present paradigm with a 24-hr study-test delay, suggesting that visuosensory enhancement remains relevant to negative memory processes long after encoding, and 3) to show that subjective arousal differences are not driving the valence differences in the distribution of the recapitulation effects.

Links between individual differences in negative memory bias and valence-specific retrieval success activity

With the recapitulation results replicated, we then moved on to ask new questions regarding links between valence-enhanced retrieval activity and emotional memory bias. Since we have consistently found group effects of visuosensory recapitulation for negative memories, we hypothesized that individual differences in negative memory bias would be associated with greater memory-related visuosensory activation at the time of retrieval. If visuosensory processes are linked with better memory for negative but not positive stimuli, those participants with greater success-related retrieval activity in visual

processing regions will be biased toward remembering more of the negative images, compared to the positive images. To test this hypothesis, we examined the whole-brain correlations between Negative > Positive Retrieval Success Activity (directional interaction contrast) and behavioral negative memory bias (Negative d' – Positive d'). We additionally masked this map with the relationship between Negative Retrieval Success Activity (Hits > Misses) correlated with Negative d' (at $p < 0.05$, see activity in yellow in Figure 2B), to ensure effects in the resulting clusters were not driven by an inverse correlation with positive memory. These analyses identified several visual cortex clusters including a large swath of the calcarine sulcus (MNI_{xyz} = 4, -88, -10, $k = 115$), the left lingual gyrus (MNI_{xyz} = -22, -82, -16, $k = 79$), and the right occipital fusiform gyrus (MNI_{xyz} = 20, -76, -10, $k = 50$), each with corresponding peaks that survived the inclusive masking technique (MNI_{xyz} = -6, -86, -10, $k=30$; MNI_{xyz}=-20, -82, -16, $k=25$; MNI_{xyz}=4, -92, -10 $k=18$, MNI_{xyz}= 24, -78, -10, $k=12$). No other clusters outside of the visual cortex were identified by the masking procedure. The same clusters were identified when a follow-up model included an across-subject covariate of post-scan rating differences of arousal between negative and positive stimuli (i.e., average negative arousal ratings – average positive arousal ratings). There were no suprathreshold voxels for the comparison assessing a relation between positive memory bias and valence-specific retrieval activity for positive stimuli. Together, these results suggest that those participants with greater memory-related activity in visuosensory regions are also those that remember more of the negative than positive stimuli at the time of retrieval. Importantly, these effects were not driven by participants who merely thought the

negative stimuli were more arousing than the positive stimuli, further suggesting a valence-specific enhancement in memory related to enhanced visuosensory memory-related activation at retrieval.

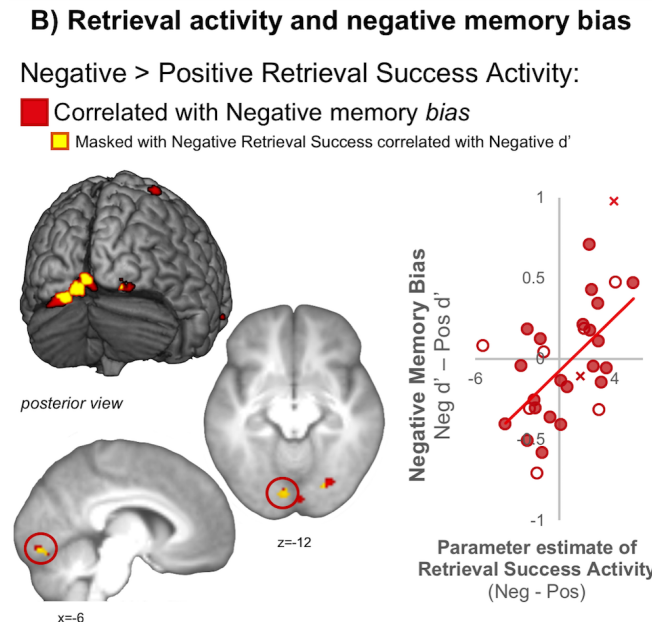
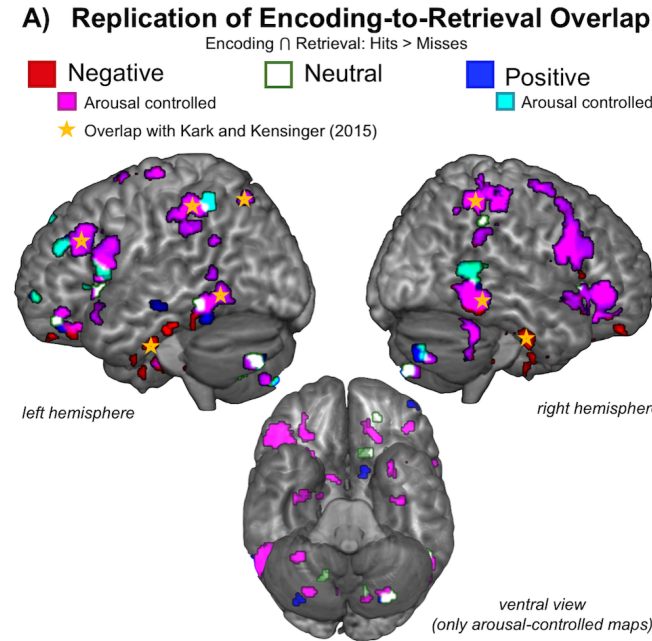


Figure 2. Memory task-based fMRI results. 2A) Replication of group-level whole-brain encoding-to-retrieval overlap effects for negative stimuli are plotted in red, with regions that directly overlap with clusters from our prior study (Kark and Kensinger, 2015) demarcated using yellow star symbols. Regions that survived controlling for item-level subjective arousal from the post-scan ratings are shown in magenta

for negative memories and cyan for positive memories. **2B)** Whole-brain correlations between individual differences in Negative > Positive Retrieval Success Activity and negative memory bias are shown in red, with yellow areas to identify clusters that also show a correlation between Negative Retrieval Success and Negative d' (inclusive masking technique thresholded at a $p < 0.05$). Individual data points from a cluster in the left calcarine sulcus (circled in red in the sagittal and axial slices) are visualized in a scatter plot (lower right). The scattered plot contains filled circles representing the $n=22$ participants included in the whole-brain analyses, but also open circles that represent the data for the seven participants excluded from the whole-brain retrieval analysis who might have noisier estimates of retrieval success activity due to a low number of misses. The red X's represent the $n=2$ participants who were not included in any of the group task or RSFC analyses but are plotted to observe how the pattern might extend if these participants were included in analysis.

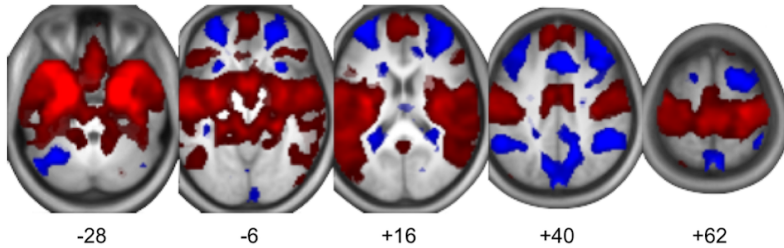
Resting state fMRI results

Before turning to the novel aspects of the present study, we first sought to root our individual differences analyses in a replication of past work of group-level amygdala RSFC patterns (Geissman et al., 2018). First, pre-encoding resting state networks resembled those previously reported (Geissmann et al., 2018; Roy et al., 2009), with positive RSFC of the bilateral amygdala with large swaths of ventro- and dorso-medial prefrontal cortex (PFC), temporal lobes, orbital and inferior PFC (shown in red in Figure 3A). Anticorrelations were observed in the middle frontal gyrus, parietal areas, and precuneus (shown in blue in Figure 3A). These findings suggest our group of participants show typical amygdala RSFC patterns at rest before encoding. Second, at the group-level, we found pre-to-post encoding increases in amygdala RSFC with regions such as the precuneus, inferior frontal gyrus, middle temporal gyrus, and insula (see Table 1 and Figure 3B). We found minimal group-level pre-to-post encoding increases in amygdala RSFC in visuosensory areas, with the exception of right amygdala RSFC increases with a portion of the right fusiform gyrus and the right temporal pole. While these changes suggest some reconfiguration of amygdala networks detectable at the group-level

following emotional picture viewing, these patterns but do not inform emotional memory processes specifically.

A) Pre-encoding (baseline) amygdala RSFC (Z_{Pre})

■ Positive Correlations ■ Negative Correlations



B) Post-encoding Δ amygdala RSFC ($Z_{Post} > Z_{Pre}$)

■ Left amygdala ■ Right amygdala

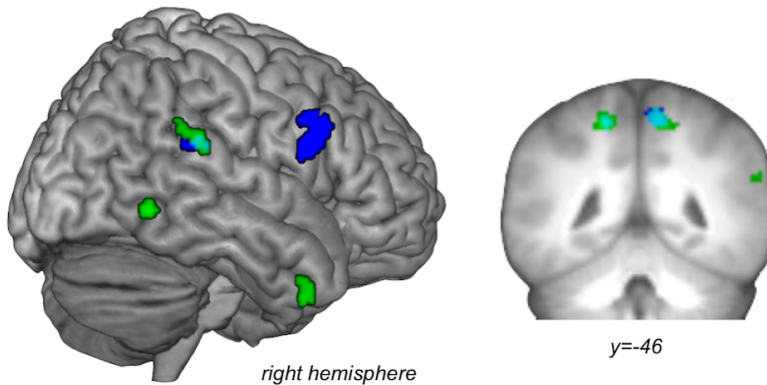


Figure 3. Group-level amygdala resting state functional connectivity results. 3A) Group-average amygdala RSFC during pre-encoding (baseline) replicates a typical widespread pattern of positive correlations (shown in red) and anti-correlations (shown in blue). **3B)** Depicts the group-level pre-to-post encoding increases in left (shown in blue) and right (shown in green) amygdala RSFC. Overlap between the left and right amygdala maps in the precuneus are shown in cyan.

Table 1. Group pre-to-post encoding increases in amygdala RSFC

Lobe	Region	Hem	BA	MNI (x,y,z)	TAL (x,y,z)	k
<i>Right amygdala</i>						
Frontal	Inferior frontal gyrus	L	47	-32,14,-26	-30,14,-18	12
	Precentral gyrus	R	6	32,-8,44	28,-13,43	16
		R	6	30,-6,60	26,-13,58	13
	Superior frontal gyrus, supplementary motor area	R*	6	12,0,60	9,-7,58	42
Parietal	Precuneus, superior parietal lobule	L*	7	-16,-44,54	-17,-47,48	104
	Paracentral Lobule	R	5	14,-32,52	11,-36,48	16
	Precuneus	R*	7	14,-44,54	11,-48,49	133
	Supramarginal gyrus, superior temporal gyrus	R*	22, 40	56,-38,22	50,-39,21	68
Temporal	Inferior temporal gyrus	R	37	50,-58,-8	45,-55,-7	37
	Temporal pole	R	21,38	44,8,-42	40,9,-32	44
Other	Insula	R	13	30,18,14	27,14,19	75
<i>Left amygdala</i>						
Frontal	Inferior frontal gyrus, precentral gyrus,	R	6,9	60,12,22	54,7,26	126
	Supplementary motor area	R*	6	10,0,56	8,-7,54	57
Parietal	Precentral gyrus	L	6	-34,-10,36	-33,-14,35	16
	Precuneus, post-central gyrus	L*	5,7	-16,-44,54	-17,-47,48	28

	Precuneus, pre- and post-central gyrus	R*	7,31	16,-28,48	13,-32,45	167
	Supramarginal gyrus, superior temporal gyrus	R*	22, 40	46,-34,24	41,-36,23	166
Other	Parietal operculum	L	13	-38,-30,22	-37,-31,21	16

*Signifies overlap between the left and right amygdala maps

Individual differences in post-encoding amygdala RSFC and emotional memory biases

After establishing that our task effects replicate our prior work (Kark and Kensinger, 2015) and the pre-encoding amygdala RSFC is consistent with previously-reported patterns (Geissmann et al., 2018), we then moved on to address the critical analyses: Examining links between individual differences in immediate post-encoding amygdala RSFC increases and long-term valence-specific emotional memory biases. We hypothesized that offline amygdala-visuosensory and amygdala-frontal RSFC enhancements during post-encoding rest—compared to pre-encoding rest—would be associated with later negative and positive memory biases, respectively. Consistent with this hypothesis, negative memory *performance* (Negative d') was correlated with post-encoding enhancements of right amygdala RSFC with early visual cortex (BA17; spanning the cuneus, calcarine sulcus, occipital pole) as well as the superior, middle, and inferior occipital gyri (BA18/19; results for neutral and positive memory performance exclusively masked out, see activity in red in Figure 4 and Table 2). The whole-brain analyses further demarcated two right visual regions (lingual gyrus/inferior occipital gyrus [BA18/19], $k=103$; inferior/middle occipital gyrus [BA19], $k=147$) that showed a

whole-brain correlation between negative memory *bias* (Negative d' – Positive d') and post-encoding increases of right amygdala RSFC (see plots and activity in yellow in Figure 4). The whole-brain RSFC effects of the left amygdala were not as wide spread as the right amygdala; however, the only cortical region to show a relation between post-encoding enhancements of left amygdala RSFC and negative memory bias was the same right lingual gyrus/inferior occipital gyrus region ($MNI_{xyz} = +28, -88, -18, k=20$) that showed the effect with the right amygdala.

While negative memory performance and negative memory bias were associated with amygdala-visuosensory increases in RSFC, positive memory performance was associated with right amygdala-frontal post-encoding increases in RSFC, including the dorsal anterior cingulate cortex (dACC), ventrolateral PFC, inferior frontal gyrus, orbital frontal cortex, and medial prefrontal cortex (see Table 2). Whole-brain analyses identified voxels ($k=37$) within the dACC as associated with positive memory bias (see symbol to demarcate significant bias in Table 2). The same dACC region showed a whole-brain correlation between left amygdala increases in RSFC and positive memory performance ($MNI_{xyz} = -4, 36, 26, k = 32$), but only a sub-threshold relation to positive memory bias (whole-brain threshold $p = 0.05, k = 16$). Further, post-encoding RSFC increases of the left amygdala with the superior frontal gyrus showed a significant relationship to positive memory bias ($MNI_{xyz} = -22, 18, 38, k = 16$). Overall, these results suggest a similar pattern of RSFC effects of the right and left amygdala. Follow-up analyses of pre-retrieval RSFC of the right amygdala suggest no significant link between pre-retrieval amygdala-visuosensory levels of RSFC and negative memory bias ($r(26) = -$

0.15, $p = 0.44$, Pearson's correlation) or amygdala-dACC levels RSFC and positive memory bias ($r(26) = 0.02$, $p = 0.93$, Pearson's correlation). These data suggest the principal findings are detectable shortly after encoding and there is no significant relationship between to pre-retrieval configuration of the amygdala RSFC networks with these areas and valence-specific memory performance. Together, these results provide new evidence of valence-specific effects of amygdala functional connectivity enhancements with distant brain regions *after* encoding on subsequent behavioral memory biases.

Given prior work establishing links between memory vividness and occipital activity (Richter et al., 2016), we tested if the present visuosensory-amygdala RSFC links with negative memory *bias* were also related to biases in negative memory vividness (i.e., negative memory vividness - positive memory vividness). Results returned no significant relationship between right amygdala post-encoding RSFC increases with the two visuosensory clusters that showed a relation to a greater negative memory *bias* (right lingual gyrus/inferior occipital gyrus: $r(27) = -.07$, $p = 0.71$; right inferior/middle occipital gyrus: $r(27) = -.07$, $p = 0.73$, Pearson's correlations). Similarly, follow-up analysis returned no significant relationship between right amygdala post-encoding increases with the dACC and greater positive memory vividness, compared to negative memory vividness ($r(27) = -.27$, $p = .16$, Pearson's correlation). However, we instructed participants to make vividness ratings based not only on memory for visual details but also thoughts, feelings, or reactions to the original photo, making it impossible to draw conclusions about the content of the memoranda driving vividness for each trial. Our null

results could reflect that participants use one aspect of vividness to rate negative vividness (e.g., visual details) and another aspect (e.g., thoughts or feelings) to rate positive vividness.

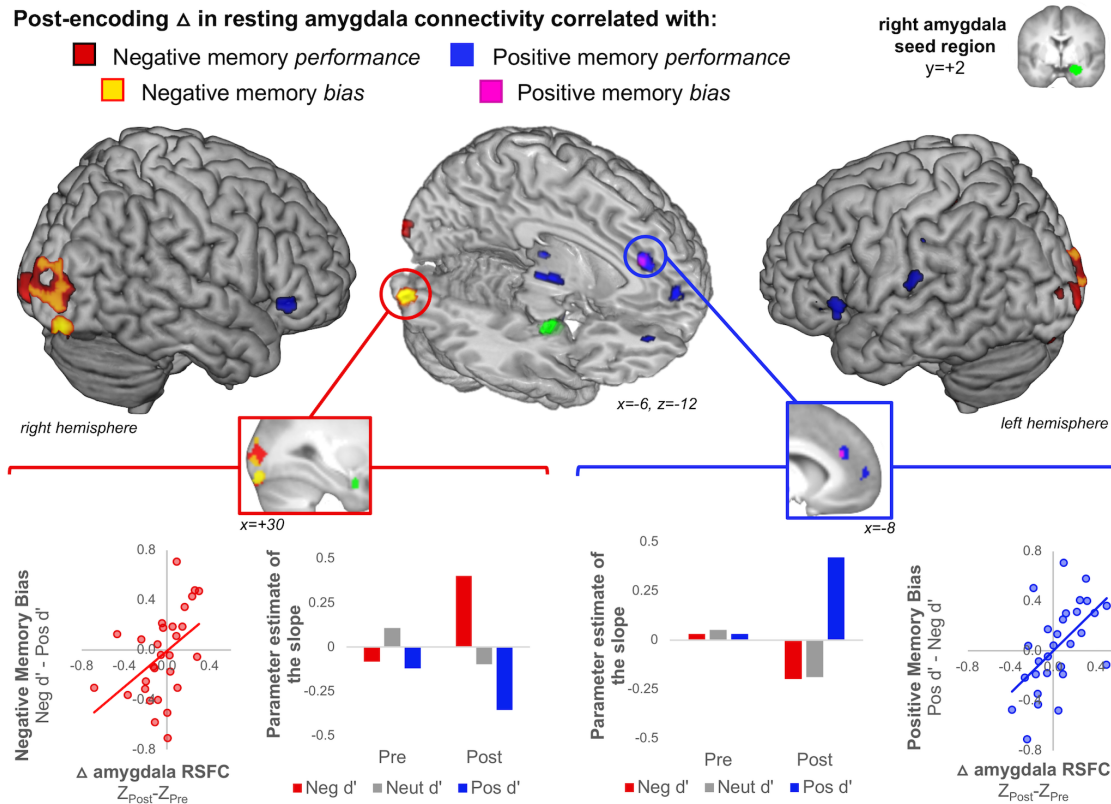


Figure 4. Post-encoding enhancement of right amygdala connectivity and valence-specific emotional memory biases. The right amygdala seed region is shown in green. Whole-brain correlations between post-encoding increases in amygdala connectivity and a) Negative memory performance (Negative d') are shown in red and b) Positive memory performance (Positive d') effects are shown in blue. Whole-brain correlations that additionally show Negative memory bias (Negative $d' - \text{Positive } d'$) are shown in the inferior occipital and lingual gyri in yellow while Positive memory bias (Positive $d' - \text{Negative } d'$) are shown in the dACC in violet. The bar plots display the random-effects level parameter estimates of the slope for the correlations between amygdala RSFC and memory performance by valence (negative, neutral, positive) and phase (pre-encoding, post-encoding). The scatter plots depict the relationship between the magnitude of post-encoding amygdala RSFC enhancement ($Z_{\text{Post}} - Z_{\text{Pre}}$) and magnitude of the given emotional memory bias.

Table 2. Across-subject correlations between post-encoding increases in right amygdala resting state functional connectivity and emotional memory performance (exclusively masking out the effects for the other two valences). Links with emotional memory biases are indicated with superscripted symbols.

Lobe	Region	Hem	BA	MNI (x,y,z)	TAL (x,y,z)	k
<i>Negative memory performance</i>						
Occipital	Calcarine sulcus, cuneus	L	17, 18	0,-102,-6	-1,-96,-10	79
	Middle occipital gyrus	L	18	-30,-98,8	-29,-94,2	11
	Cuneus, superior and middle occipital gyri	R *	17,18,19	20,-100,18	17,-97,12	492
	Lingual gyrus, inferior occipital gyrus, fusiform gyrus	R * ^	18,19	28,-88,-18	25,-82,-19	108
Parietal	Post-central gyrus	L	3	-22,-32,52	-22,-36,47	60
Frontal	Superior frontal gyrus, supplementary motor area	R	6	16,-4,58	13,-11,56	21
Temporal	Temporal pole	R	38	18,8,-50	16,10,-40	21
Other	Cerebellum	L	NA	-26,-90,-26	-25,-83,-27	12
<i>Positive memory performance</i>						
Frontal	Inferior frontal gyrus	L	45	-54,22,0	-51,19,5	38
		L	46	-38,36,0	-36,32,7	11
		R	45	52,30,-4	47,26,4	57
	Superior frontal gyrus (anterior)	L	10	-10,56,6	-10,50,14	33
	Orbital frontal gyrus	R	11	10,46,-16	9,42,-6	13

Other	Cerebellum	R	NA	12,-56,-38	10,-51,-35	34
	Dorsal anterior cingulate	L * #	32	-10,38,24	-10,32,29	104
	Mid-cingulate	L	31	-2,-14,46	-3,-19,44	11
	Thalamus	L	NA	-16,-14,2	-16,-15,4	104
	Thalamus	L	NA	-2,-24,8	-3,-25,9	17
Parietal	Post-central gyrus	L	40	-58,-22,20	-55,-24,19	63
		L	2	-46,-20,34	-44,-23,32	19
Temporal	Transverse temporal gyrus	R	41	40,-28,4	36,-28,6	17

*Signifies whole-brain relation to emotional memory bias (k-values of sub-clusters reported in-text).

^Left amygdala pre-to-post RSFC shows whole-brain correlation with negative memory bias (k=20).

#Left amygdala pre-to-post RSFC shows whole-brain correlation with positive memory performance (k=32).

Control analyses

We ran several control analyses to confirm that the relationship between post-encoding increases in amygdala RSFC and negative memory biases were not driven by individual valence differences in univariate encoding levels of amygdala or visuosensory 1) activity, 2) functional connectivity 3) “background connectivity”, 4) valence-differences in the post-scan subjective ratings of valence and arousal across participants, or 5) parallel changes in hippocampal or other subcortical connectivity with these areas. Encoding functional connectivity models were created using the gPPI toolbox (available at <http://brainmap.wisc.edu/PPI>; McLaren et al., 2012). Encoding “background connectivity” was calculated similar to previously reported methods (Al-Aidroos et al., 2012; Duncan et al., 2014; Murty et al., 2017) by extracting signal from the right amygdala, right lingual gyrus/inferior occipital gyrus, and dACC, from fixed-effect

model residuals, which are thought to represent task- and noise-filtered signal. These signals were band-pass filtered [0.01 - 0.08 Hz] and pairwise correlation coefficients were *r*-to-*z* transformed and saved as the metric of background connectivity for each participant. These control metrics of interest were entered as covariates in four separate follow-up random-effects models to confirm that the whole-brain links between individual differences in pre-to-post encoding increases in right amygdala RSFC and emotional memory biases remained suprathreshold when controlling for these possible across-subject explanations of the effects. The principal valence-specific links of right amygdala RSFC links with negative and positive memory biases remained significant in the inferior occipital gyrus and DACC, respectively, when these additional random-effects factorial models controlled for 1) encoding activity differences between negative and positive hits and 2) functional connectivity differences in the right amygdala, right lingual gyrus/inferior occipital gyrus, and DACC between negative and positive hits, as well as 3) encoding background connectivity differences of the RAMY with these target regions, and 4) valence differences in post-scan ratings of arousal and absolute valence (e.g., average negative arousal ratings – average positive arousal ratings). RSFC analysis of other subcortical seed regions (i.e., hippocampus and putamen) with the principal visuosensory clusters associated with negative memory biases returned no significant link with negative memory bias (all $r_s < .3$, $p_s > 0.1$, Pearson's correlations). A similar pattern was observed for positive memory bias and post-encoding RSFC increases with the dACC cluster. These data suggest the principal negative memory bias effects might be specific to the amygdala and were not driven by hippocampal (but see *Exploratory*

mediation analysis) or putamen influences of increased post-encoding RSFC with these valence-specific cortical targets.

Follow-up analysis of post-encoding resting state fMRI scans available from the original 20-minute study-test delay study (Kark and Kensinger, 2015) using a separate set of participants shows no significant correlation between post-encoding right amygdala-visuosensory RSFC and negative memory bias ($r(20) = -0.24$, $p = 0.28$, Pearson's correlation) or right amygdala-dACC RSFC and positive memory bias ($r(20) = -0.1$, $p = 0.67$, Pearson's correlation). These data suggest that a delay longer than 20 minutes might be required to observe a relation between post-encoding amygdala RSFC increase with these ROIs and long-term memory. However, future work is needed to directly confirm the need for an extended delay, since these RSFC scans were collected on a different scanner and used different acquisition parameters (47 slices, TR=3000ms, 100 images, 3mm³ voxels) and pre-encoding scans were not collected. Together, these follow-up analyses demonstrate that the principal findings are not driven by differences *during* encoding or by subjective reactivity differences to the images as valence categories, and likely reflect enhanced amygdala engagement following encoding that is relevant to later behavior in a valence-specific fashion.

Exploratory mediation analysis

We have presented evidence that negative memory biases are associated with visuosensory engagement both online during retrieval and offline during post-encoding rest periods: Specifically, we have demonstrated that negative memory bias is related to

both 1) greater retrieval success activation in visuosensory areas for negative compared to positive stimuli as well as 2) greater enhancements of visuosensory-amygdala connectivity during post-encoding offline rest periods. Although these visuosensory areas that showed a significant relation with negative memory bias were not directly spatially overlapping—possibly due to differences of engagement while at rest as compared to during task or after a period of consolidation—we utilize these metrics to capture individuals who show a visuosensory tendency in the brain with regard to negative memory bias. With these across-subjects metrics, we conducted an exploratory, *post hoc* mediation analysis to test if post-encoding amygdala-visuosensory RSFC increases (Figure 4) and visuosensory negative-biased retrieval activity (Figure 2B) independently influence behavioral negative memory bias (unmediated) or if post-encoding right amygdala RSFC increases set-up visuosensory brain areas for a negative memory bias mode at retrieval (see Model 1 below in Figure 5). That is, do changes in amygdala-visual RSFC immediately following encoding (independent X variable) influence negative memory bias (dependent Y variable) via biases in visual retrieval activity (mediator M variable)?

Mediation methods. For the Visuosensory-Amygdala Δ RSFC variable (X), we chose the magnitude of right amygdala post-encoding change with the right lingual gyrus/inferior occipital gyrus region (MNI_{xyz} = 28, -88, -16, shown in yellow in the pop-out plot in Figure 4 and sagittal slice in Figure 5). We chose this particular area because it 1) fell nearer to the right hemisphere clusters that showed visuosensory negative-biased retrieval activity (Figure 2b) and 2) because it fell nearer to the terminal area of the

inferior longitudinal fasciculus (Catani et al., 2003), which structurally connects the amygdala and occipital cortex. For the Visuosensory Negative-Biased Retrieval Activity variable (M), we averaged the parameter estimates (Negative Retrieval Success > Positive Retrieval Success directional contrasts) from the right hemisphere clusters that showed a correlation with behavioral negative memory bias ($MNI_{xyz} = 24, -78, -10$ and $MNI_{xyz} = 4, -92, -10$, circled on the axial slice in Figure 5), since amygdala effects tend to be strongest ipsilaterally (Amaral et al., 2003; Kilpatrick and Cahill, 2003; Vuilleumier et al., 2004).

We then tested the hypothesized mediation model (Model 1, shown in Figure 5A), with the metric of Behavioral Negative Memory Bias (Negative d' – Positive d') as the dependent variable (Y). In Model 1, post-encoding amygdala-visuosensory RSFC increases (X, Visuosensory-Amygdala Δ RSFC) predict Behavioral Negative Memory Bias via Visuosensory Negative-Biased Retrieval Activity (M). In Model 2, Visuosensory Negative-Biased Retrieval Activity predicts Behavioral Negative Memory Bias via Visuosensory-Amygdala Δ RSFC on the prior day.

We utilized regression analysis and a bootstrapping estimation method to determine significance of the mediation model using PROCESS (<http://www.processmacro.org/index.html>; Hayes, 2018), regression path analyses modelling tool we implemented in SPSS 24. Mediation is determined significant if the confidence interval does not contain 0. Unstandardized regression coefficients (b values) and bootstrapped 95% confidence intervals (10,000 iterations) were used to determine significance and standardized coefficients (β) are reported for comparisons across studies.

Mediation results. In Model 1 (see Figure 5A), Visuosensory Amygdala Change in RSFC (X) was a significant predictor of Visuosensory Negative-Biased Retrieval Success Activity ($b = 7.51$, $SE = 2.79$, $p = 0.01$, $CI_s = [1.69, 13.34]$, $\beta = 0.52$) and explained 27% of the variability of retrieval activity ($R^2=0.27$). Visuosensory Amygdala Change in RSFC no longer predicted negative memory bias ($b = 0.38$, $SE = 0.30$, $p = 0.22$, $CI_s = [-.24, 0.99]$, $\beta=0.26$) when Visuosensory Negative-Biased Retrieval Success bias was added to the model as a mediator ($b = 0.05$, $SE = 0.02$, $p = 0.03$, $CI_s = [0.01, .09]$, $\beta = 0.48$), suggesting a complete mediation. The indirect effect was found to be significant using a bootstrap estimation approach with 10,000 samples ($b=0.36$, $SE_{boot}=0.20$, $CI_{sboot} = [0.08, 0.87]$, $\beta=0.25$). That is, a one standard deviation difference in post-encoding right amygdala RSFC was associated with 0.1 greater difference in negative memory bias (Negative d' – Positive d'), as mediated by visuosensory retrieval success activity. Approximately 42% of the variance in behavioral negative memory bias was accounted for by these two predictors ($R^2 = .42$). The indirect effects were also significant and indicated a full mediation when additional models were run with the two retrieval clusters averaged to create the M variable were run separately (when M values were extracted from $MNI_{xyz} = 4, -92, -10$: $b=0.35$, $SE_{boot}=0.20$, 95% $CI_{sboot} = [0.07, 0.88]$, $\beta=0.24$; $MNI_{xyz} = 24, -78, -10$: $b=0.29$, $SE_{boot}=0.17$, 95% $CI_{sboot} = [0.04, 0.71]$, $\beta=0.20$), suggesting neither cluster drove the indirect effect when collapsed across those two clusters. A full mediation suggests post-encoding enhancements of Visuosensory-Amygdala Δ RSFC predict later Visuosensory Negative-Biased Retrieval Activity, which in turn predicts the magnitude of the Behavioral Negative Memory Bias. In other words,

post-encoding processes set-up the brain for a negative-biased retrieval mode, which drives the gap between remembering more of the bad than the good.

While Model 1 makes the most sense both theoretically and chronologically (i.e., post-encoding processes precede retrieval activity), we also evaluated the possibility that the association between retrieval activity bias and negative memory bias could be mediated by a prior history of post-encoding increases in amygdala RSFC, and not that amygdala RSFC increases cause retrieval activity biases. Using the same approach but with Visuosensory Negative-Biased Retrieval Activity as the independent variable (X) and Visuosensory-Amygdala Δ RSFC as the mediator (M), the indirect effect in Model 2 was not found to be significant ($b = 0.01$, $SE_{boot} = 0.01$, $CI_{Sboot} = [-0.01, .04]$, $\beta = 0.13$).

Additional first-stage moderated mediation model. We further explored for hippocampal contributions to these links. Although post-encoding increases in right hippocampal RSFC (Visuosensory-Hippocampal Δ RSFC) with the right lingual gyrus/inferior occipital gyrus region were not statistically significant ($r(27) = .28$, $p = 0.14$, Pearson's correlation), post-encoding increases of Visuosensory-Hippocampal Δ RSFC moderated the relationship between Visuosensory-Amygdala Δ RSFC and Visuosensory Negative-Biased Retrieval Activity (see Figure 5B for plot of the interaction). A moderated mediation model further revealed that the indirect effect of X on Y through M shown in Figure 5A was only significant at average or greater-than-average levels of Visuosensory-Hippocampal Δ RSFC ($W_{average-1SD}$: $b=0.22$, $SE_{boot} = 0.22$, $CI_{Sboot}=[-.25 0.64]$; $W_{average}$: $b=0.44$, $SE_{boot} = 0.26$, $CI_{Sboot}=[.02 1.05]$; $W_{average+1SD}$: $b=0.67$, $SE_{boot} = 0.43$, $CI_{Sboot}=[.10 1.68]$). Although these findings require further

examination with a larger sample size, these results provide preliminary evidence that greater visuosensory-hippocampal increases in post-encoding RSFC augment the indirect effect that visuosensory-amygdala RSFC exerts on negative memory biases.

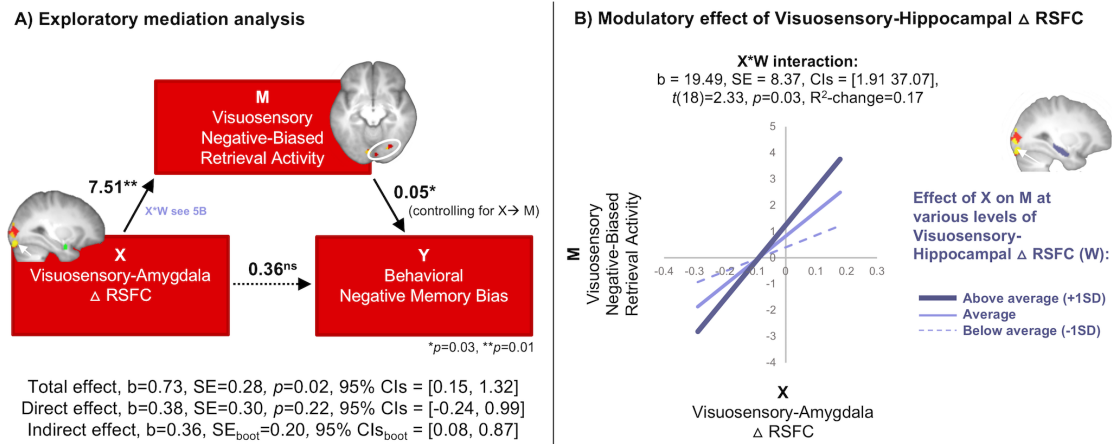


Figure 5. Exploratory moderated mediation analysis. 5A) Exploratory Mediation analysis. Visuosensory Negative-Biased Retrieval Activity in right occipital cortex (average of two right hemisphere visuosensory regions shown in the axial slice, top) completely mediated the relationship between pre-to-post encoding increases in Visuosensory-Amygdala RSFC and Behavioral Negative Memory Bias, which suggests post-encoding amygdala-visuosensory RSFC enhancements set-up the brain for a negative-biased retrieval mode visuosensory regions at the time of retrieval. The path values represent the unstandardized regression coefficients. Significance of the indirect effect was determined by the bootstrapped 95% CIs (10,000 samples). **5B)** Additional first-stage moderated mediation analysis. Follow-up analysis of pre-to-post encoding changes of the right hippocampus and the right visuosensory region (shown in sagittal slice) revealed a significant moderated mediation, whereby the effect of post-encoding amygdala-visuosensory RSFC on Visuosensory Negative-Biased Retrieval Activity depended on the level of pre-to-post encoding changes of visuosensory-hippocampal RSFC. The significant X*W interaction is plotted at various levels of visuosensory-hippocampal changes in RSFC.

2.5 DISCUSSION

The present study is the first to demonstrate not only valence-specific emotional memory retrieval patterns but also valence-specific links between post-encoding increases in

amygdala-cortical RSFC and long-term episodic emotional memory biases. These results emphasize that negative memories differ from positive not only in the way the content is initially encoded but also in how that content is consolidated over time and brought to mind at retrieval. Primarily, we demonstrate that behavioral negative memory bias was specifically associated with ‘offline’ post-encoding RSFC increases of the amygdala with occipital areas, and that activation of similar visual regions at the time of retrieval was also linked to negative memory bias.

These findings are consistent with a growing body of work demonstrating that immediate post-learning functional connectivity of the MTL can have long-term consequences on subsequent memory (Staresina et al., 2013; Tambini and Davachi, 2013; Tambini et al., 2010; Tambini et al., 2017), including fear memory (de Voogd et al., 2016; Hermans et al., 2017). Here we show that some of these effects are dissociable along the dimension of emotional valence. These results may provide new avenues for understanding or remediating negative memory biases, by revealing that negative memory biases can be linked to the way that sensory processes are integrated into amygdala-centered emotional memory networks.

Post-encoding amygdala-cortical RSFC predicts emotional memory

The key finding was a valence-based dissociation in the link between post-encoding amygdala RSFC increases and long-term emotional memory biases: Greater amygdala engagement with occipital and frontal areas immediately following encoding was differentially associated with greater negative and positive memory biases,

respectively. Inferior occipital and medial frontal areas show dense reciprocal connections with the amygdala along the inferior longitudinal fasciculus and uncinate fasciculus, respectively (Catani et al., 2003; Ghashghaei et al., 2007), making these offline functional changes in connectivity anatomically plausible. While we can only speculate why the individual differences in negative memory biases play out in more posterior visual processing regions, one possibility is that participants with a stronger negative memory bias are bringing to mind more fine-grained visual features of the negative stimuli to support memory. Similar areas of the inferior and middle occipital gyri have been associated with sensitivity to spatial frequency information (Rotshtein et al., 2007) and retrieval of color (Ueno et al., 2007), raising the possibility that those participants with greater posterior visuosensory engagement bring to mind these visual features. In contrast, group-level recapitulation effects in relatively more anterior visual regions might reflect reactivation of higher-order visual representations (Wheeler and Buckner, 2003).

Positive memory performance was associated with post-encoding amygdala RSFC increases with frontal regions, with a specific positive memory bias effect associated with amygdala-dACC RSFC. These findings are broadly consistent with prior work (Mickley Steinmetz et al., 2010) but extend amygdala-frontal influences on memory into post-encoding periods. Perhaps amygdala enhancement of frontal areas involved in gist- or heuristic-based memory processing associated with positive stimuli (Kensinger and Schacter, 2008) and the experience of positive emotions (Ashby et al.,

1999; Fredrickson and Branigan, 2005) tips the scale toward overall better recognition memory of positive stimuli.

Amygdala-visuosensory RSFC may influence negative memory bias via retrieval activity

The exploratory mediation analysis suggests those participants with greater post-encoding amygdala-visuosensory RSFC have greater memory-related visuosensory activity for negative stimuli compared to positive stimuli during retrieval, resulting in a more pronounced negative memory bias. Although these visuosensory areas were not directly overlapping, individuals with a tendency toward visuosensory engagement may exhibit a greater negative memory bias. The change over time in the exact visuosensory areas could plausibly be consistent with systems consolidation, such that initial changes in one set of regions may trigger changes over time in distal regions. The exploratory moderated mediation result was broadly consistent with a systems consolidation view as well, suggesting a role for the hippocampus in moderating the indirect effects of amygdala-visuosensory RSFC on negative memory bias through retrieval activity. While exploratory, these results may help to guide further research that can settle recent debates about the role of amygdala-hippocampal interactions in emotional memory (e.g., Inman et al., 2018; Yonelinas and Ritchey, 2015).

Modulatory role of the amygdala

Our study provides new evidence in humans that in the minutes following an emotional experience, long-term behavioral emotional memory outcomes are influenced

by increases in post-encoding amygdala coupling with neocortical regions, and the regions of interaction determine the dominant valence to-be remembered later. The present findings are broadly consistent with the *modulation hypothesis of amygdala function* and are also aligned with Müller and Pilzecker's *perseveration-consolidation hypothesis* (1900), which proposed that neural activity can continue for hours after initial learning, suggesting a role of the amygdala *after* encoding (McGaugh, 2005). Pelletier and colleagues (2005) suggest “that the memory-modulating role of the BLA would not depend on the specific activation of particular groups of BLA neurons, but on the activity patterns taking place in BLA projection sites when the emotional arousal occurred”. Yet the present results also provide intriguing evidence that, while emotional arousal undoubtedly enhances amygdala activation and engagement with distant brain regions, the target sites of those interactions may depend on valence (Tye, 2018).

Limitations and future work

There are a few limitations and important next steps in this research. Although these data are consistent with memory consolidation theories and could reflect early consolidation processes, future work is needed to confirm that RSFC changes reflect ‘offline’ memory consolidation processes. Future work is needed to formally test in a within-subjects design if the link between post-encoding amygdala RSFC and valence-specific memory biases require a long period of consolidation to be observed. Although RSFC studies provide an important window into memory consolidation, it is challenging to separate off-line consolidation effects from those elicited by participants’ thoughts or

rehearsals following encoding. For instance, it is possible that the amygdala-frontal RSFC connectivity increase corresponds with positive memory biases not because of changes to intrinsic network connectivity but because those participants who employ an active emotion regulation strategy post-encoding end up remembering more of the good than the bad. Future work is needed to adjudicate between consolidation and other rehearsal or regulatory accounts of these data. Notwithstanding, the current results provide the first evidence that amygdala-visuosensory coupling following an event predicts negative memory bias and further highlights the need for valence-based accounts of emotional memory.

More generally, it will be important for future research to examine whether the pattern of results revealed here requires a longer delay. If these results reflect systems consolidation, then the link between emotional memory bias and post-encoding amygdala-neocortical interactions might depend on a lengthy study-test delay. In the fear conditioning literature, it is broadly accepted that long-term systems consolidation memory is assessed over days and weeks rather than minutes or hours (Dudai et al., 2015; Nader, 2003), yet shorter delays are common when assessing episodic emotional memory. Future episodic emotional memory work could consider that same-day testing might not be ideal for examining how “long-term” emotional episodic memory effects are instantiated in neocortical areas.

Another direction for future research will be to clarify which aspects of memory are enhanced via these interactions with the amygdala. Recent work has emphasized differences in the effects of negative valence on subjective memory vividness, the

precision of visual feature encoding, and the precision of visual retrieval (Cooper et al., in press). Future work can test if post-encoding MTL-visuosensory interactions bear influence not only on memory discrimination, as revealed here, but also on memory measures such as visual specificity (Kensinger and Schacter, 2007; Leal et al., 2014), continuous color (Richter et al., 2016) or salience judgements (Cooper et al., in press), that might underlie differences between negative and positive memories.

While the present work lays a preliminary foundation to explain variability in emotional memory biases, none of the participants in the present study reported a history of affective disorders, so it will be important to decipher if these basic valence-specific memory mechanisms map onto the exaggerated negative memory biases observed in psychopathology (Haas and Canli, 2008) or to the positive memory biases in aging that rely more heavily on prefrontal and cingulate engagement (Kensinger and Schacter, 2008), each of which can be maintained over many months.

Conclusions

The current study is the first to demonstrate that post-encoding amygdala RSFC patterns are linked with behavioral measures of valence-specific emotional memory biases. The dominant valence remembered by an individual depends on the regions showing the strongest RSFC with the amygdala post-encoding, with posterior visuosensory and frontal connectivity differentially supporting negative and positive memory biases, respectively. We circumvented and controlled for stimulus-bound differences, reducing the likelihood that these valence effects would be driven by low-

level visual differences or greater subjective feelings of arousal for negative images. These findings suggest valence-specific effects occur outside the context of encoding and retrieval tasks during ‘offline’ periods following encoding—possibly contributing to early consolidation processes. These data support a new valence-based account of emotional memory enhancement (Bowen et al., 2018) and provide evidence for valence-specific differences in amygdala connectivity that give rise to remembering more of the bad than the good.

2.6 REFERENCES

- Al-Aidroos, N., Said, C.P., Turk-Browne, N.B., 2012. Top-down attention switches coupling between low-level and high-level areas of human visual cortex. *Proc Natl Acad Sci U S A* 109, 14675-14680.
- Amaral, D.G., Behniea, H., Kelly, J.L., 2003. Topographic organization of projections from the amygdala to the visual cortex in the macaque monkey. *Neuroscience* 118, 1099-1120.
- Ashby, F.G., Isen, A.M., Turken, A.U., 1999. A neuropsychological theory of positive affect and its influence on cognition. *Psychol Rev* 106, 529-550.
- Barth, M., Breuer, F., Koopmans, P.J., Norris, D.G., Poser, B.A., 2016. Simultaneous multislice (SMS) imaging techniques. *Magn Reson Med* 75, 63-81.
- Bowen, H.J., Kark, S.M., Kensinger, E.A., 2018. NEVER forget: negative emotional valence enhances recapitulation. *Psychon Bull Rev* 25, 870-891.
- Bowen, H.J., Kensinger, E.A., 2017a. Memory-related functional connectivity in visual processing regions varies by prior emotional context. *Neuroreport* 28, 808-813.
- Bowen, H.J., Kensinger, E.A., 2017b. Recapitulation of emotional source context during memory retrieval. *Cortex*, 91, 142-156.
- Cahill, L., McGaugh, J.L., 1998. Mechanisms of emotional arousal and lasting declarative memory. *Trends Neurosci* 21, 294-299.
- Catani, M., Jones, D.K., Donato, R., Ffytche, D.H., 2003. Occipito-temporal connections in the human brain. *Brain* 126, 2093-2107.

- Cooper, R.A., Kensinger, E.A., Ritchey, M., in press. Memories fade: The relationship between memory vividness and remembered visual salience. *Psychol Sci*.
- de Voogd, L.D., Fernandez, G., Hermans, E.J., 2016. Awake reactivation of emotional memory traces through hippocampal-neocortical interactions. *Neuroimage* 134, 563-572.
- Dringenberg, H.C., Kuo, M.C., Tomaszek, S., 2004. Stabilization of thalamo-cortical long-term potentiation by the amygdala: cholinergic and transcription-dependent mechanisms. *Eur J Neurosci* 20, 557-565.
- Dudai, Y., Karni, A., Born, J., 2015. The Consolidation and Transformation of Memory. *Neuron* 88, 20-32.
- Duncan, K., Tompary, A., Davachi, L., 2014. Associative encoding and retrieval are predicted by functional connectivity in distinct hippocampal area CA1 pathways. *J Neurosci* 34, 11188-11198.
- Feinberg, D.A., Moeller, S., Smith, S.M., Auerbach, E., Ramanna, S., Gunther, M., Glasser, M.F., Miller, K.L., Ugurbil, K., Yacoub, E., 2010. Multiplexed echo planar imaging for sub-second whole brain FMRI and fast diffusion imaging. *PLoS One* 5, e15710.
- Fisher, R., 1973. *Statistical Methods for Research Workers*, 14 ed. Hafner Press, New York.
- Fox, M.D., Snyder, A.Z., Vincent, J.L., Corbetta, M., Van Essen, D.C., Raichle, M.E., 2005. The human brain is intrinsically organized into dynamic, anticorrelated functional networks. *Proc Natl Acad Sci U S A* 102, 9673-9678.

- Fox, M.D., Snyder, A.Z., Zacks, J.M., Raichle, M.E., 2006. Coherent spontaneous activity accounts for trial-to-trial variability in human evoked brain responses. *Nat Neurosci* 9, 23-25.
- Fredrickson, B.L., Branigan, C., 2005. Positive emotions broaden the scope of attention and thought-action repertoires. *Cogn Emot* 19, 313-332.
- Geissmann, L., Gschwind, L., Schicktanz, N., Deuring, G., Rosburg, T., Schwegler, K., Gerhards, C., Milnik, A., Pflueger, M.O., Mager, R., de Quervain, D.J.F., Coyne, D., 2018. Resting-state functional connectivity remains unaffected by preceding exposure to aversive visual stimuli. *Neuroimage* 167, 354-365.
- Gerritsen, L., Rijpkema, M., van Oostrom, I., Buitelaar, J., Franke, B., Fernandez, G., Tendolkar, I., 2012. Amygdala to hippocampal volume ratio is associated with negative memory bias in healthy subjects. *Psychol Med* 42, 335-343.
- Ghashghaei, H.T., Hilgetag, C.C., Barbas, H., 2007. Sequence of information processing for emotions based on the anatomic dialogue between prefrontal cortex and amygdala. *Neuroimage* 34, 905-923.
- Haas, B.W., Canli, T., 2008. Emotional memory function, personality structure and psychopathology: a neural system approach to the identification of vulnerability markers. *Brain Res Rev* 58, 71-84.
- Hamann, S.B., Ely, T.D., Grafton, S.T., Kilts, C.D., 1999. Amygdala activity related to enhanced memory for pleasant and aversive stimuli. *Nat Neurosci* 2, 289-293.
- Hammers, A., Allom, R., Koeppe, M., Free, S., Myers, R., Lemieux, L., Mitchell, T., Brooks, D., Duncan, J., 2003. Three-dimensional maximum probability atlas of

- the human brain, with particular reference to the temporal lobe. *Hum Brain Mapp* 19, 224-247.
- Hayes, A.F., 2018. *Introduction to Mediation, Moderation, and Conditional Process Analysis*, 2nd ed. Guilford Press, New York, NY.
- Hermans, E.J., Battaglia, F.P., Atsak, P., de Voogd, L.D., Fernandez, G., Roozendaal, B., 2014. How the amygdala affects emotional memory by altering brain network properties. *Neurobiol Learn Mem* 112, 2-16.
- Hermans, E.J., Kanen, J.W., Tambini, A., Fernandez, G., Davachi, L., Phelps, E.A., 2017. Persistence of Amygdala-Hippocampal Connectivity and Multi-Voxel Correlation Structures During Awake Rest After Fear Learning Predicts Long-Term Expression of Fear. *Cereb Cortex* 27, 3028-3041.
- Inman, C.S., Manns, J.R., Bijanki, K.R., Bass, D.I., Hamann, S., Drane, D.L., Fasano, R.E., Kovach, C.K., Gross, R.E., Willie, J.T., 2018. Direct electrical stimulation of the amygdala enhances declarative memory in humans. *Proc Natl Acad Sci U S A* 115, 98-103.
- Itti, L., Koch, C., 2001. Computational modelling of visual attention. *Nat Rev Neurosci* 2, 194-203.
- Kark, S.M., Kensinger, E.A., 2015. Effect of emotional valence on retrieval-related recapitulation of encoding activity in the ventral visual stream. *Neuropsychologia* 78, 221-230.

- Kensinger, E.A., Schacter, D.L., 2007. Remembering the specific visual details of presented objects: neuroimaging evidence for effects of emotion. *Neuropsychologia* 45, 2951-2962.
- Kensinger, E.A., Schacter, D.L., 2008. Neural processes supporting young and older adults' emotional memories. *J Cogn Neurosci* 20, 1161-1173.
- Kilpatrick, L., Cahill, L., 2003. Amygdala modulation of parahippocampal and frontal regions during emotionally influenced memory storage. *Neuroimage* 20, 2091-2099.
- Lang, P.J., Bradley, M.M., Cuthbert, B.N., 2008. International affective picture system (IAPS): Affective ratings of pictures and instruction manual. Technical Report A-6. University of Florida, Gainesville, FL.
- Leal, S.L., Tighe, S.K., Jones, C.K., Yassa, M.A., 2014. Pattern separation of emotional information in hippocampal dentate and CA3. *Hippocampus* 24, 1146-1155.
- McGaugh, J.L., 2000. Memory--a century of consolidation. *Science* 287, 248-251.
- McGaugh, J.L., 2005. Emotional arousal and enhanced amygdala activity: new evidence for the old perseveration-consolidation hypothesis. *Learn Mem* 12, 77-79.
- McLaren, D.G., Ries, M.L., Xu, G., Johnson, S.C., 2012. A generalized form of context-dependent psychophysiological interactions (gPPI): a comparison to standard approaches. *Neuroimage* 61, 1277-1286.
- Mickley Steinmetz, K.R., Addis, D.R., Kensinger, E.A., 2010. The effect of arousal on the emotional memory network depends on valence. *Neuroimage* 53, 318-324.

- Moeller, S., Yacoub, E., Olman, C.A., Auerbach, E., Strupp, J., Harel, N., Ugurbil, K., 2010. Multiband multislice GE-EPI at 7 tesla, with 16-fold acceleration using partial parallel imaging with application to high spatial and temporal whole-brain fMRI. *Magn Reson Med* 63, 1144-1153.
- Müller, G.E., Pilzecker, A., 1900. Experimentelle beitrage zur lehre vom geda'chtnis. *Zeitschrift fuer Psychologie* 1, 1-288.
- Murty, V.P., Ritchey, M., Adcock, R.A., LaBar, K.S., 2011. Reprint of: fMRI studies of successful emotional memory encoding: a quantitative meta-analysis. *Neuropsychologia* 49, 695-705.
- Murty, V.P., Tompary, A., Adcock, R.A., Davachi, L., 2017. Selectivity in Postencoding Connectivity with High-Level Visual Cortex Is Associated with Reward-Motivated Memory. *J Neurosci* 37, 537-545.
- Nader, K., 2003. Memory traces unbound. *Trends Neurosci* 26, 65-72.
- Paller, K.A., Wagner, A.D., 2002. Observing the transformation of experience into memory. *Trends Cogn Sci* 6, 93-102.
- Pelletier, J.G., Likhtik, E., Filali, M., Pare, D., 2005. Lasting increases in basolateral amygdala activity after emotional arousal: implications for facilitated consolidation of emotional memories. *Learn Mem* 12, 96-102.
- Power, J.D., Barnes, K.A., Snyder, A.Z., Schlaggar, B.L., Petersen, S.E., 2012. Spurious but systematic correlations in functional connectivity MRI networks arise from subject motion. *Neuroimage* 59, 2142-2154.

- Richter, F.R., Cooper, R.A., Bays, P.M., Simons, J.S., 2016. Distinct neural mechanisms underlie the success, precision, and vividness of episodic memory. *Elife* 5.
- Rotshtein, P., Vuilleumier, P., Winston, J., Driver, J., Dolan, R., 2007. Distinct and convergent visual processing of high and low spatial frequency information in faces. *Cereb Cortex* 17, 2713-2724.
- Roy, A.K., Shehzad, Z., Margulies, D.S., Kelly, A.M., Uddin, L.Q., Gotimer, K., Biswal, B.B., Castellanos, F.X., Milham, M.P., 2009. Functional connectivity of the human amygdala using resting state fMRI. *Neuroimage* 45, 614-626.
- Silverstein, D.N., Ingvar, M., 2015. A multi-pathway hypothesis for human visual fear signaling. *Front Syst Neurosci* 9, 101.
- Staresina, B.P., Alink, A., Kriegeskorte, N., Henson, R.N., 2013. Awake reactivation predicts memory in humans. *Proc Natl Acad Sci U S A* 110, 21159-21164.
- Tambini, A., Davachi, L., 2013. Persistence of hippocampal multivoxel patterns into postencoding rest is related to memory. *Proc Natl Acad Sci U S A* 110, 19591-19596.
- Tambini, A., Ketz, N., Davachi, L., 2010. Enhanced brain correlations during rest are related to memory for recent experiences. *Neuron* 65, 280-290.
- Tambini, A., Rimmele, U., Phelps, E.A., Davachi, L., 2017. Emotional brain states carry over and enhance future memory formation. *Nat Neurosci* 20, 271-278.
- Tye, K.M., 2018. Neural Circuit Motifs in Valence Processing. *Neuron* 100, 436-452.
- Ueno, A., Abe, N., Suzuki, M., Hirayama, K., Mori, E., Tashiro, M., Itoh, M., Fujii, T., 2007. Reactivation of medial temporal lobe and occipital lobe during the retrieval

- of color information: A positron emission tomography study. *Neuroimage* 34, 1292-1298.
- Vuilleumier, P., Richardson, M.P., Armony, J.L., Driver, J., Dolan, R.J., 2004. Distant influences of amygdala lesion on visual cortical activation during emotional face processing. *Nat Neurosci* 7, 1271-1278.
- Wagner, A.D., Koutstaal, W., Schacter, D.L., 1999. When encoding yields remembering: insights from event-related neuroimaging. *Philos Trans R Soc Lond B Biol Sci* 354, 1307-1324.
- Waheed, S.H., Mirbagheri, S., Agarwal, S., Kamali, A., Yahyavi-Firouz-Abadi, N., Chaudhry, A., DiGianvittorio, M., Gujar, S.K., Pillai, J.J., Sair, H.I., 2016. Reporting of Resting-State Functional Magnetic Resonance Imaging Preprocessing Methodologies. *Brain Connect* 6, 663-668.
- Wheeler, M.E., Buckner, R.L., 2003. Functional dissociation among components of remembering: control, perceived oldness, and content. *J Neurosci* 23, 3869-3880.
- Whitfield-Gabrieli, S., Nieto-Castanon, A., 2012. Conn: a functional connectivity toolbox for correlated and anticorrelated brain networks. *Brain Connect* 2, 125-141.
- Xu, J., Moeller, S., Auerbach, E.J., Strupp, J., Smith, S.M., Feinberg, D.A., Yacoub, E., Ugurbil, K., 2013. Evaluation of slice accelerations using multiband echo planar imaging at 3 T. *Neuroimage* 83, 991-1001.
- Yonelinas, A.P., Ritchey, M., 2015. The slow forgetting of emotional episodic memories: an emotional binding account. *Trends Cogn Sci* 19, 259-267.

3.0 EFFECTS OF EMOTIONAL VALENCE ON TRUE AND FALSE MEMORY VIVIDNESS

Submitted Manuscript:

Kark, S.M., Slotnick, S.D., Kensinger, E.A., submitted. Effects of emotional valence on true and false memory vividness.

3.1 ABSTRACT

Emotional memories tend to be re-experienced with a stronger sense of subjective vividness, compared to neutral memories. Even false emotional memories, those not linked to a specific, genuine experience, can be associated with this same rich sense of vividness. Indeed, behavioral studies tend to find that emotional true and false memories are largely indistinguishable. Neuroimaging work has shown that successful (i.e., true) retrieval of negative memories is associated with retrieval-related activation in the ventral visual stream. However, it remains unknown if activation in these regions 1) bears a valence-specific influence on the *vividness* of these true memories and 2) is uniquely tied to veridical memory or also drives illusory negative memories. To address these questions, we used fMRI to investigate the effects of valence (negative, neutral, positive) on the regions that tracked with true and false memory vividness. Twenty-nine participants incidentally encoded line-drawings of emotional and neutral images, each followed by the full colorful version of the image. Twenty-four hours later, participants underwent a surprise recognition memory fMRI scan in which all of the old line-drawings were presented inter-mixed with an equal number of new line-drawings. For each line-drawing, participants were asked to rate if it was Old or New and also rate memory vividness on a 1-4 scale. We used parametric modulation analysis to investigate the parametric effect of vividness as a function of memory accuracy and valence. We replicated prior work showing parametric effects of vividness in the hippocampus, inferior parietal lobule, prefrontal cortex, and retrosplenial cortex/precuneus, regardless of valence, and early visual cortex (V1) distinguished true from false vividness for

neutral memories. Negative memories showed a valence-specific effect of vividness in the occipito-temporal cortex, including the inferior temporal gyrus and parahippocampal cortex. Parahippocampal cortex activation was linked with both true and false vividness for negative memories. There were no regions that showed a greater parametric effect of vividness for false memories greater than true memories. The current findings demonstrate that activation in ventral visual regions relates to negative memory vividness and does so for both true and false memories; indeed, the neural processes that tracked with memory vividness were largely indistinguishable for true and false memories.

3.2 INTRODUCTION

The word vividness stems from the Latin root *viv*, meaning “spirited, animated, alive”. When a memory springs to mind, it is the rich sense of vividness that allows us to ‘re-experience’ past events in the present moment. Recent work has shown that the level of activation in regions associated with visual processing and visual imagery is positively correlated with this subjective sense of memory vividness (e.g., early visual cortex, ventral visual regions, precuneus/retrosplenial cortex; Buchsbaum et al., 2012; Richter et al., 2016; St-Laurent et al., 2015). However, memory is a reconstructive process that is prone to errors and distortions (Schacter, 1999) and a strong sense of vividness can also accompany false memories (Dodson et al., 2007; Kahn et al., 2004; Neisser and Harsch, 1992), which occur when a person falsely endorses an event or stimulus that is not rooted in an authentic prior experience. False eye-witness testimony in criminal cases—which are often emotionally negative by nature—can be delivered with high confidence (Loftus, 1979; Semmler et al., 2004; Wells and Olson, 2003) and a strong sense of emotion (Laney and Loftus, 2008), which can result in faulty testimony, false accusations, and wrongful convictions (Kaplan et al., 2016). Negative valence has been associated with an increased rate of false memories, compared to positive and neutral memories (Knott et al., 2018; Porter et al., 2003), an effect that is amplified in patients with a history of trauma exposure, post-traumatic stress disorder, and depression (Otgaar et al., 2017) and in aging (Gallo et al., 2009). If on the surface the subjective experience of an emotional memory can be the same but the authenticity of the memory can vary, what neural

processes differentiate true from false emotional memories? Are there shared neural processes that support emotional memory vividness regardless of memory authenticity? While it is well-established that emotional memories are re-experienced with a strong sense of memory vividness (Phelps and Sharot, 2008), to our knowledge there is no prior functional magnetic resonance imaging (fMRI) work available examining the neural effects of emotional valence on true and false subjective memory vividness. In the laboratory, behavioral work examining the effect of emotion on false memory is typically investigated by assessing or manipulating mood or emotional state (e.g., Forgas et al., 2005; Mirandola and Toffalini, 2016; Zhang et al., 2018), implanting emotional false memories (Laney and Loftus, 2008), or utilizing stimuli that are inherently emotional (e.g., words lists, pictures) to elicit false memories (e.g., modified versions of the Deese-Roediger-McDermott [DRM] paradigm, Deese, 1959; Roediger and McDermott, 1995). Paradoxically, these studies suggest that while negative and positive mood states can protect against false memory, negative content tends to elicit more false memories than neutral or positive content (Bookbinder and Brainerd, 2016), which recent work suggests might be driven by automatic neural processing for negative stimuli (Knott et al., 2018). Examining the neural correlates of true and false memory vividness as function of emotional valence will increase both the understanding the emotional modulation of accurate reconstruction of vivid veridical memories as well as the signals that give rise or reflect a sense of memory for something that never happened.

Successful negative memory retrieval

Recent work from four separate studies has shown that successful retrieval of negative memories, compared to positive memories, is associated with greater retrieval-related reactivation in ventral visual processing regions (Bowen and Kensinger, 2017; Kark and Kensinger, 2015, in press; Loos et al., 2019). Recent work also suggests individuals with greater reactivation in visual cortex during retrieval exhibit a more pronounced negative memory bias (i.e., better memory for negative items compared to positive items, Kark and Kensinger, in press), highlighting the effect of these sensory areas on behavioral differences at the moment of retrieval. While negative and positive memories can both have an arousal-related boost in subjective vividness, we have posited that the brain regions that support negative memory formation and retrieval are often valence-specific (i.e., the 'NEVER' model, Bowen et al., 2018). More specifically, we have proposed that negative valence enhances engagement of sensory-specific processes during encoding and recapitulation of these processes during retrieval. For positive memories, previous work suggests valence-specific prefrontal cortex enhancements (Kark and Kensinger, in press; Mickley Steinmetz et al., 2010) and little or no retrieval-related recapitulation in visual regions (Bowen and Kensinger, 2017; Kark and Kensinger, 2015, in press).

However, these studies, like other investigations of emotional memory, examined the neural processes that led to the successful formation and successful retrieval of emotional memories (i.e., remembered compared to forgotten), and not necessarily activity linked with the degree of subjective memory vividness or strength. During encoding, subsequent recollection of negative stimuli, compared to positive stimuli, has been specifically

associated with activation of the inferior temporal gyrus and parahippocampal cortex (Mickley and Kensinger, 2008). The results of another study examining emotional source recollection, compared to familiarity, reported enhanced retrieval-related recapitulation in ventral visual regions for negative stimuli, compared to positive stimuli, suggesting negative valence enhances the vividness and detail of negative memories (Bowen and Kensinger, 2017). If these valence-specific processes are indeed linked to memory vividness in valence-specific ways, then there should be a stronger link between visual processing region activity and memory vividness for negative memories compared to positive memories. The existing literature cannot adequately address this possibility, because most studies of emotional memory that have examined the neural correlates of memory strength have either not included positive stimuli or have allowed large differences between the negative and positive stimuli on the dimension of arousal.

Overlapping behavioral and neural characteristics of true and false memories.

One challenge of distinguishing true from false memories is that these two forms of memory share overlapping behavioral and neural characteristics. Behavioral research suggests that classifying the authenticity of a memory based on subjective recollective experience alone is nearly impossible (Heaps and Nash, 2001, p. 921). For instance, both forms of memory have been associated with high levels of reported confidence (Loftus and Pickrell, 1995) and retrieval of item-specific details (Geraci and McCabe, 2006). Prior work has shown that, on average, confidence levels, sensory detail, and emotional intensity to a true negative memory can be greater than an implanted negative false

memory (Laney and Loftus, 2008). However, these recollective characteristics were not unique to true negative memories, as a majority of negative false memories were rated as extremely vivid, emotional, and were accompanied with rich sensory imagery (Laney and Loftus, 2008), a finding that has since been extended to strong sense of false memory for committing a crime (Shaw and Porter, 2015). Psychophysiological (e.g., skin conductance) data also suggests that emotion responsivity profiles cannot reliably distinguish true from false emotional memories (McNally et al., 2004).

Electrophysiological data have also shown that negative false memories, like true memories, are associated with recollection-related event-related potentials (Zheng et al., 2018). These findings suggest that, although less frequent in their occurrence, negative false memories can *look* and *feel* like negative true memories, a finding that is particularly worrisome in the legal setting where jurors can conflate eyewitness confidence or sincere emotion with accuracy (Lacy and Stark, 2013).

Neuroimaging of true and false memories

Given the behavioral and psychophysiological overlap between true and false memories, neuroimaging has proven useful to investigate the relation between memory and reality by examining their neural similarities and differences (Garoff-Eaton et al., 2006; Kurkela and Dennis, 2016). However, in addition to the often-indistinguishable subjective reports of true and false memories, neuroimaging studies of true and false memory often report considerable neural overlap for true and false memories, and very sparse activity, if any, that is greater for false memories compared to that of true memories (for a review see

Kurkela and Dennis, 2016). Specifically, neural overlap is often observed in higher-order visual processing regions, the medial temporal lobes, and top-down control processes of the prefrontal and parietal cortices, with some mixed evidence regarding the extent to which activation levels in each of these regions distinguish true from false memory (Kurkela and Dennis, 2016). Similar levels of engagement in these regions during high-confidence false recollection is thought to reflect content borrowing, a faulty reconstruction of studied items that are misattributed to a lure item during recognition (Dennis et al., 2012; Lampinen et al., 2005). Together, these findings suggest false memories do not necessarily emanate from outside of typical memory regions, but often activate many of the same brain regions that support true memory—although it is important to acknowledge that the function of that activation might differ between the two forms of memory (e.g., reactivation of true memory representations as compared to content borrowing in the case of false memory).

While there is considerable overlap in the neural processes supporting true and false memory, behavioral work has shown that true memories on average are more sensory-oriented, as evidenced by a greater number of subjective sensory details (Johnson and Raye, 1981; Norman and Schacter, 1997). Previous neuroimaging work suggests inferior-superior network differences and bottom-up/top-down distinctions in the brain between true and false memories: True memories are more automatic recapitulations with associated modality-specific sensory signals (inferior and bottom-up processes) while false memories involve more controlled cognitive processes (superior and top-down processes; see Dennis et al., 2012). Correspondingly, multiple fMRI studies have found

that sensory reactivation of the early visual cortex distinguishes true from false visual memories (Slotnick and Schacter, 2004; Ye et al., 2016), but this true from false memory distinction diminishes in more anterior portions of the ventral visual stream associated with higher-order visual processing (but see Kurkela and Dennis, 2016), such as occipitotemporal cortex (Dennis et al., 2012; Slotnick and Schacter, 2004) and the parahippocampal cortex (Karanian and Slotnick, 2017).

True and false memory effects in the parahippocampal cortex have been mixed, with some studies showing greater activity for true compared to false memories for neutral stimuli (Cabeza et al., 2001; Cabeza and St Jacques, 2007; Iidaka et al., 2012; Slotnick and Schacter, 2004; Turney and Dennis, 2017) and other studies suggesting similar levels of engagement regardless of memory accuracy (Karanian and Slotnick, 2014, 2017; Stark et al., 2010; Ye et al., 2016). Based on prior work showing enhanced visual processing region engagement in support of negative memory encoding and retrieval, including the parahippocampal cortex (Kark and Kensinger, 2015, in press), it is reasonable to predict that negative valence enhances the link between the level of activation at retrieval and subjective memory strength to a greater extent than positive valence. What is unclear is whether this negative valence enhancement of visual processing regions would be specific to true negative memories—conferring a kind of accuracy protection—or if signals emanating from these areas also drive or reflect a false sense of vividness for negative stimuli. That is, do negative true and false memories activate similar areas of the brain?

Assessments of emotional memory have typically examined the effects of valence while holding memory constant (i.e., only examining valence differences within remembered items) or examined success (i.e., hits compared to misses) and did not have a sufficient number of false alarm trials for analysis of accuracy. Here, we deciphered the processes that were important for successful and accurate emotional memory vividness from those that extended to vividness for illusory emotional memories.

Current study

In the present study, we investigated the effects of emotional valence on the neural processes that support true and false memory vividness. We used a challenging long-term emotional recognition memory paradigm, which allowed us to elicit a sufficient number of trials for parametric modulation analysis of trial-level vividness ratings. We hypothesized that while positive and negative memories can be remembered with similar levels of vividness, the brain regions supporting vividness would be valence-specific (i.e., linked to visual processing-related activation for negative memories and to frontal activation for positive memories). Participants incidentally encoded scenes (negative, neutral, and positive) that were each preceded by a line-drawing sketch of the scene. Twenty-hours later, participants were scanned during a surprise recognition memory task in which all of the old line-drawing sketches and an equal number of new line-drawing sketches were presented for a memory and vividness judgment. We begin with a replication of prior work by examining true and false memory vividness, regardless of valence, here extending those findings to a study-test delay of 24 hours. We then present

findings demonstrating a valence-specific effect of vividness in the ventral visual stream for negative memories, compared to positive memories. Finally, we present evidence that negative true and false memory vividness is positively correlated with activation levels in many of the same brain regions, but exploratory analyses suggested functional connectivity patterns may distinguish true from false memory vividness patterns.

3.3 METHODS

Participants.

Thirty-three participants were recruited as a control group as part of a larger study examining the effects of pre-encoding stress and sleep on the neural correlates of emotional memory (Kark and Kensinger, in press). The control participants included in the present analyses did not undergo the stress manipulation prior to encoding.

Participants were healthy, right-handed young adult native speakers of English with normal or corrected-to-normal vision. Participants were not taking medications that could affect the central nervous system and reported no history of psychiatric or neurological problems, learning disorders, or head injury. All participants were screened for contraindications for safety in the MRI environment. This study was approved by the Institutional Review Board of Boston College and informed consent of study procedures

was obtained from all participants. Participants underwent MRI scanning at the Harvard Center for Brain Science (CBS) and were compensated \$25/hour for their participation.

From the thirty-three control participants recruited, three participants were excluded from consideration for the fMRI analyses: one participant was excluded from analysis due to a structural anomaly (female, 23), one participant was excluded from analysis due to chance-level memory performance (a d' value below zero; male, 25), and one participant exhibited excessive motion requiring removal of half of their retrieval scans (male, 24). One additional participant (male, 24) did not have enough trials per response type to be included in the fMRI parametric analysis of true memory vividness (see *Inclusion in fMRI Analyses*). In total, twenty-nine participants (15 females) aged 18-29 ($M = 22.03$, $SD = 2.77$) were included in the true memory vividness analysis. Of the twenty-nine participants, nineteen participants (10 females) had a sufficient number of false memory responses by valence and vividness level to be included in the whole-brain parametric analysis of the effects of valence on false memories (see *Inclusion in fMRI Analyses*).

Stimuli.

The incidental encoding stimuli were 300 images of scenes (100 negative, 100 neutral, and 100 positive) selected from the International Affective Picture System (IAPS; Lang et al., 2008). The line-drawing sketches of these IAPS images were created using an in-house MATLAB script (The MathWorks, Natick, MA) and Adobe Photoshop (San Jose, CA). The negative images were pre-selected to be more arousing ($M_{\text{neg}} = 5.54$, $M_{\text{neut}} =$

3.25, $t(198) = 23.95$, $p < 0.001$, independent samples t -test) and of greater absolute valence than the neutral images ($M_{\text{neg}} = 2.05$, $M_{\text{neut}} = 0.42$, $t(198) = 19.27$, $p < 0.001$, independent samples t -test). The positive images were similarly pre-selected to be more arousing ($M_{\text{pos}} = 5.43$, $t(198) = 22.97$, $p < 0.001$, independent samples t -test) and of greater absolute valence ($M_{\text{pos}} = 2.07$, $t(198) = 25.00$, $p < 0.001$, independent samples t -test) than the neutral images. Critically, in order to make direct valence comparisons the negative and positive IAPS images were pre-selected to be equally arousing ($t(198) = 1.32$, $p = 0.19$, independent samples t -test) and of similar absolute valence ($t(198) = 0.25$, $p = 0.80$, independent samples t -test).

Task procedures.

Following screening and informed consent procedures, participants completed an incidental encoding task while undergoing fMRI scanning. During the encoding task, participants were shown line-drawings of IAPS images (1.5s), followed by the full colorful IAPS image (3s). To ensure participants were actively engaging with the encoding stimuli, they were asked to indicate whether they would ‘Approach’ or ‘Back Away’ from each of the scenes depicted in the IAPS images.

Twenty-four hours later, participants returned for a scanned surprise recognition memory test. Participants were shown all of the old line-drawings seen the day before, intermixed with an equal number of new line-drawings they had not seen previously. For each line-drawing, participants were given 3s to make a one-step Old/New and vividness rating (0 = “New”, 1 = “Old, Not Vivid”, 2 = “Old, Somewhat vivid”, 3 = “Old, Vivid”, 4

= “Old, Extremely Vivid”). Participants were instructed that “vividness ratings can be based on how vividly you remember the visual details in the photo and/or how vividly you remember your reaction or thoughts about the photo.” Before the recognition task began, participants were also told that, since half of the images were previously studied and half were not, they should be pressing the “0” key to indicate that items were “New” about half of the time. There were two study lists that varied across participants and the new line-drawings seen at test were always from the unstudied list of IAPS images. Participants completed brief practice versions of the encoding and recognition tasks on day 1 and day 2, respectively, before entering the scan room. They additionally were reminded of the instructions immediately before the scans commenced. A jittered fixation was presented between encoding (6-12s) and retrieval (1.5-9s) trials. After the recognition memory scan, participants were removed from the scanner and completed subjective ratings of arousal and valence of the IAPS image in a separate testing room.

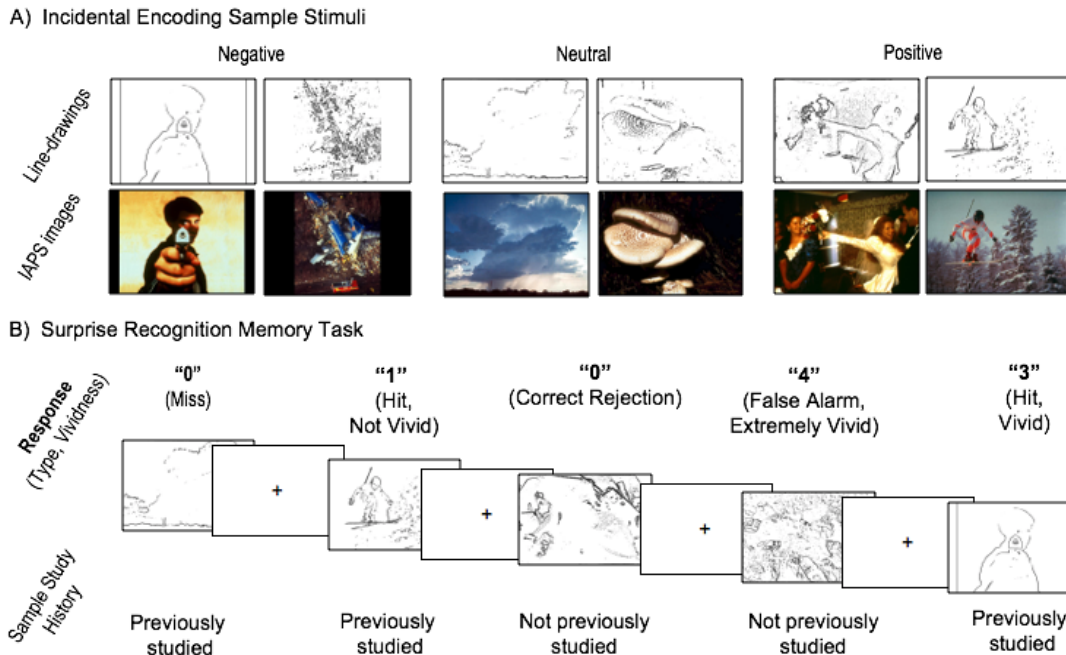


Figure 1. Sample stimuli and recognition memory vividness responses. 1A) Sample line-drawings and their corresponding IAPS images of each valence studied during the incidental encoding task. **1B).** Depiction of the recognition memory task with sample line-drawings. Sample responses and their corresponding response types and vividness levels are listed above the line-drawings, based on the study history listed at the bottom.

MRI Acquisition

All MRI images were acquired using a 32-channel head coil on a Siemens MAGNETOM Prisma 3T scanner. Scanning sessions began with a functional localizer and auto-align scout, followed by collection of whole-brain T₁-weighted anatomical images (MEMPRAGE, 1.0mm³ isotropic voxels, 176 slices, TR = 2530 ms, FoV= 256 mm, Flip angle = 7 degrees, base resolution = 256). The T₂-weighted EPI images functional images collected during the encoding and recognition tasks were acquired using Simultaneous Multi-Slice blood-oxygen-level dependent scan sequences (SMS-BOLD; Barth et al., 2016). The whole-brain EPI images were collected in an interleaved fashion, with the

slices aligned coronally 25 degrees above the AC-PC line (69 slices, TR = 1500ms, 2.0 mm³ isotropic voxels, TE = 28 ms, Flip angle = 75 degrees, 208 mm field of view, base resolution = 104, multi-band acceleration factor = 3). The SMS-BOLD scanning protocols were provided to Harvard CBS from provided by the Center for Magnetic Resonance Research at University of Minnesota (Feinberg et al., 2010; Moeller et al., 2010; Xu et al., 2013).

MRI Data Preprocessing and Motion Correction.

Images were pre-processed and analyzed using SPM8 (Wellcome Department of Cognitive Neurology, London, United Kingdom) implemented in MATLAB 2014a (The MathWorks, Natick, MA). All functional images were reoriented, realigned, co-registered, and spatially normalized to the Montreal Neurological Institute (MNI) template (re-sampled at 3 mm during segmentation and written at 2 mm during normalization). All functional images in both studies were smoothed using a 6 mm isotropic Gaussian kernel.

Global mean intensity and motion outliers were identified using Artifact Detection Tools (ART) (available at www.nitrc.org/projects/artifact_detect). Global mean intensity outliers were defined as scans with a global mean intensity that differed by more than 3 standard deviations from the mean. Acceptable motion parameters were set to 3 mm for translation and 3 degrees for rotation. Scan runs were eliminated if more than 5% of the timepoints showed a framewise-displacement greater than 0.5mm (Power et al., 2012) AND greater than 3 degree rotation/3 mm of movement. Seven motion regressors

(framewise displacement, x, y, z, roll, pitch, yaw) were included at the fixed effects level to regress out motion effects. As mentioned previously, one participant was removed from analysis because 3 of the 6 retrieval runs showed excessive motion based on these thresholds (male, 24). In total, five participants (2 females) had one scan run each that needed to be removed due to excessive motion

Inclusion in fMRI Analyses

To be included in the whole-brain parametric fMRI analyses participants were required to have: 1) A sufficient number of trials per response type (≥ 10 hits, false alarms for each type of valence), 2) Used at least 3 of the 4 vividness levels per response type (i.e., excluded if only used two or fewer of the four vividness levels for a given response type), and 3) At least 5 trials per response type were at least "somewhat vivid" (a rating of 2 or higher). The third criterion was implemented to reduce false positives and ensure that the parameter estimate of the slope for a given participant would not be disproportionately estimated from "not vivid" false memories, for example, sixteen trials of Not Vivid false alarms ("1" responses) and only one Moderately Vivid false alarm ("3" response) and one Highly Vivid false alarm ("4"). Of the twenty-nine participants included in the true memory vividness analysis, four participants did not meet Criterion 2 (3 females), five did not meet Criterion 3, and one met neither Criterion 2 nor 3 (1 female). Three of the ten participants excluded also did not meet Criterion 1. Therefore, nineteen participants were included in the final sample for the whole-brain parametric modulation analysis that examined false memory vividness by valence. To ensure the core false memory vividness

findings are robust to sampling differences, we focus our conclusions on the patterns that hold when Criterion 3 was dropped for false memory analyses (increasing the sample to $n=24$). To provide data transparency, we plotted the data from the five participants that did not meet Criterion 3 using open circles in the figure call-out plots.

Fixed-effects fMRI models

Fixed-effects general linear models were created for each participant that modelled hits and false alarms by valence with reaction times and vividness ratings entered as parametric modulators. Vividness ratings were entered as the second parametric modulator, with reaction times entered first, to be able to examine for positive relations between brain activity and subjective vividness while controlling for neural differences related to reaction time. Misses and correct rejections were collapsed across valence and modelled as two separate regressors. To mitigate any effects of visual complexity on the neural correlates of subjective memory vividness, an additional nuisance regressor that included an edge density metric (proportion of black pixels to total image pixels) for each of the line-drawing epochs was added to the vividness retrieval models. Finally, for all fixed-effects models, each participant's seven motion parameters (framewise displacement, x, y, z, pitch, roll, yaw) were added as nuisance regressors to mitigate the effects of motion on the effects of interest. Additional follow-up models were run that included a regressor for item-level post-scan ratings of subjective arousal. We focus our conclusions and discussion on the regions that remained significant when controlling for item-level arousal.

For all participants, at least five fixed-effects contrasts were saved to be entered into one sample t -tests at the random-effects level: Negative Hits Vividness > zero (Parametric Negative), Neutral Hits Vividness > zero (Parametric Neutral), and Positive Hits Vividness > zero (Parametric Positive), Negative Hits Vividness > Positive Hits Vividness (Parametric Negative Valence-Specific), and Positive Hits Vividness > Negative Hits Vividness (Parametric Positive Valence-Specific). For the nineteen participants with sufficient trials to examine the effects of valence on both true and false memory vividness, three additional fixed-effects contrasts examining False Memory Vividness for each valence (i.e., positive parametric) were created. To ensure the patterns reported are robust to sampling differences, the discussion will focus on areas that were also significant when the maps described below were inclusively masked with the corresponding map for the $n=24$ group at a reduced threshold of $p<.05$. These parametric contrasts were entered along with the True Memory Vividness parametric contrasts into a 2 x 3 repeated-measures ANOVA with factors of memory accuracy (hits, false alarms) and valence (negative, neutral, positive).

Random-effects fMRI analyses.

Examining valence-invariant true memory vividness. For the twenty-nine participants included in the examination of the effects of valence on true memory vividness (i.e., only examining the hits), a conjunction analysis was used to demarcate the activity that tracked true memory vividness (i.e., a positive parametric effect for hits) for

each valence category (Parametric Negative \cap Parametric Neutral \cap Parametric Positive). This conjunction analysis revealed valence similarity.

Next, we interrogated the true and false memory vividness 2 x 3 repeated-measures ANOVA model to isolate regions that distinguished true and false memory vividness. To isolate a true memory vividness effect, we conjoined the *F*-Contrast of the Main Effect of Memory (i.e., requiring that the ANOVA revealed some difference between true and false memory vividness) with two *T*-Contrasts: 1) the *T*-Contrast of True Memory Vividness > False Memory Vividness ensured that the directionality of the main effect was such that there was a greater correspondence to true than to false memory vividness, and 2) the *T*-Contrast of True Memory Vividness > zero further ensured that a difference between true and false memory vividness was not driven by a positive relation between activation and true memory vividness, rather than a negative relation between activation and false memory vividness. In order to identify True Memory Vividness Effects that were robust to sampling, we finally conjoined the resulting map with the valence similarity map from the full participant sample described in the paragraph above. Similarly, we conjoined the positive parametric maps for false memory vividness for each valence to reveal valence similarity in false memory vividness. To examine positive parametric effects specific to false memory vividness compared to true memory vividness, the *F*-Contrast of the Main Effect of Memory map was inclusively overlaid with two additional contrasts (*T*-Contrast of False Memory Vividness > zero and *T*-Contrast False Memory Vividness > True Memory Vividness) to

identify any areas with a greater effect for false memory vividness compared to true memory vividness.

Effects of valence on true and false memory vividness. To reveal valence-specific differences, two one-sample *t*-tests at the random-effects level examined Negative Valence-Specific True Vividness Effects (Negative True Vividness > Positive True Vividness) and Positive Valence-Specific True Vividness Effect (Positive True Vividness > Negative True Vividness). To be considered an effect of interest, we required that correlations were significantly above zero (e.g., Negative True Vividness > zero) and significantly different than the comparison valence (e.g., Negative True Vividness > Positive True Vividness).

The approach above was used to identify regions that show a valence-specific effect of true memory vividness when memory was held constant, and isolates further effects *within* those clusters. We next focused exclusively on the analyses afforded by the random-effects 2 x 3 ANOVA model that included both true and false memory vividness for each valence: The ability to examine the similarities and differences of true and false memory vividness as a function of valence. We sought to test if vividness patterns for emotional false memories, and negative false memories in particular, resembled the patterns seen for true memories, or if there are largely separate processes in the generation of vivid emotional memories. First, we probed the whole-brain Memory Accuracy x Valence Interaction *F*-Contrast without any further masking, to reveal any areas where the patterns were specific to memory accuracy and valence levels. Next, *T*-Contrasts were used to identify regions that showed greater vividness for true compared

to false memory vividness and false memory greater than true memory vividness within each valence category. These maps outlined the areas that distinguish true from false memory vividness. Finally, to examine spatial overlap in areas supporting both true and false memory for a particular valence we conjoined the statistical maps of true and false memory vividness within each valence category and further conjoined those maps with the *F*-Contrast for the Main Effect of Valence. Overlap with the Main Effect of Valence would suggest a given pattern for true memory vividness also extends to false memory vividness for a given valence, whereas overlap with the map of the Interaction effects would imply the differences between negative and positive memory vividness vary as a function of memory accuracy. Follow-up analyses outside of SPM8 were conducted on regions of interest in visual processing regions and medial temporal lobe areas.

Visualization and Follow-Up Analyses

All whole-brain maps were thresholded at $p < 0.005$ (uncorrected) and, to avoid false negatives in reporting, all clusters with 10 or more contiguous voxels are reported. Ten thousand Monte Carlo Simulations (<https://www2.bc.edu/sd-slotnick/scripts.htm>) were conducted based on the acquisition volume, individual voxel threshold, and a computed null contrast spatial autocorrelation value of 7mm (Slotnick, 2017). This yielded a cluster extent threshold of 40 voxels for the parametric modulation analyses, which was corrected for multiple comparisons to $p < 0.05$. As such, we focus our discussion on the cortical activations with a cluster extent of at least 40 voxels. Given the relatively circumscribed area of the medial temporal lobe and our a priori hypotheses, we relaxed

the emphasis on the voxel extent threshold for medial temporal lobe regions. The rendering of the statistical maps for the current figures created using MRIcroGL (<https://www.mccauslandcenter.sc.edu/mricrogl/home>) and MRICRON (<https://www.nitrc.org/projects/mricron>). For follow-up region of interest statistics, parameter estimates of the slopes were extracted from each participant's fixed-effects model using REX (<http://web.mit.edu/swg/software.htm>). SPM8 coordinates reported in Montreal Neurological Institute (MNI) space were converted to Talairach space (TAL) space using GingerALE Version 2.3.6 (<http://www.brainmap.org/ale/>). Coordinates for regions of the brain stem are not reported, given the limited resolution (2mm³) of the brain images for localizing this structure.

3.4 RESULTS

Behavioral Results.

There was no significant difference in memory performance, $d' = z(\text{HitRate}) - z(\text{FalseAlarmRate})$, between negative and neutral stimuli ($t(27) = 1.24, p = 0.23$), negative and positive stimuli ($t(27) = 0.13, p = 0.90$), or positive and neutral stimuli ($t(27) = 0.85, p = 0.40$). For vividness ratings, a repeated-measures 2 x 3 ANOVA with memory accuracy (hits, false alarms) and valence (negative, neutral, positive) as factors revealed main effects of memory accuracy $F(1, 27) = 200.33, p < 0.001, \eta^2 = 0.88$, with greater vividness for hits ($M = 2.69, SE = 0.10$) than false alarms ($M = 1.9, SE = 0.09$), and of valence $F(2, 54) = 15.41, p < 0.001, \eta^2 = 0.36$, with higher vividness for positive

($M = 2.43$, $SE = 0.09$) relative to negative ($M = 2.26$, $SE = 0.10$) or neutral ($M = 2.21$, $SE = 0.09$) stimuli.

Neural correlates of valence-invariant true memory vividness.

We first examined the effects of true memory vividness that were common to all three of the valence categories. The valence similarity map (Parametric Negative \cap Parametric Neutral \cap Parametric Positive Vividness) returned widespread effects throughout regions previously associated with strong recollective memory, including the hippocampus, retrosplenial cortex/precuneus, posterior cingulate, and inferior parietal areas including the angular and supramarginal gyri (see Table 1 and activity shown in blue in Figure 2). We additionally found activation in bilateral orbital frontal cortex, medial and lateral prefrontal cortex, and the middle and inferior temporal gyri. Several of these clusters—namely the right inferior frontal gyrus and the left inferior parietal lobule—also showed a main effect of memory accuracy, with a significantly greater link between activity and vividness for true memories compared to false memories (see regions denoted with asterisks in Table 1 and activity shown in cyan in Figure 2).

We conducted follow-up analyses within *a priori* regions of interest within the hippocampus and retrosplenial cortex/precuneus—regions susceptible to emotional modulation and have been associated with memory vividness (Todd et al., 2013) and visual imagery and scene reconstruction (Maddock, 1999), respectively—to examine the effects of memory accuracy and valence. Analysis of both regions revealed only a main effect of memory accuracy (greater links to true than false memory vividness, for

hippocampus: $F(1,18) = 5.35, p = 0.03, \eta^2 = 0.23$; for retrosplenial/precuneus: $F(1,18) = 6.12, p = 0.02, \eta^2 = 0.25$) and no main effect of valence (hippocampus: $F(2, 36) = 0.46, p = 0.64, \eta^2 = 0.03$; retrosplenial/precuneus: $F(2, 36) = 1.14, p = 0.33, \eta^2 = 0.06$) or memory accuracy-by-valence interaction (hippocampus: $F(2, 36) = 0.29, p = 0.75, \eta^2 = 0.02$; retrosplenial/precuneus: $F(2, 36) = 1.23, p = 0.31, \eta^2 = 0.06$).

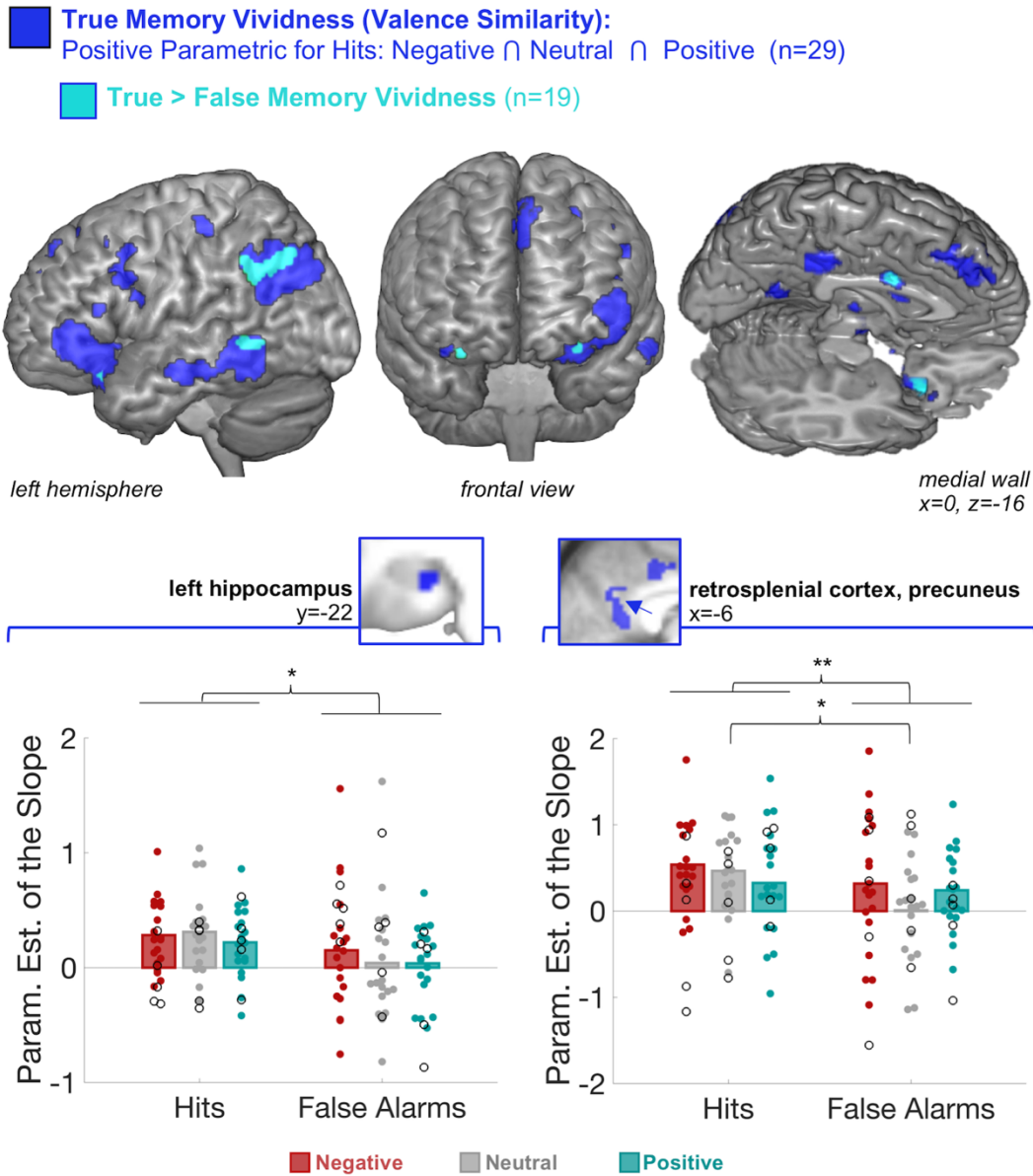


Figure 2. Valence-invariant effects of memory vividness. **Top.** Many regions (blue) showed a positive parametric relation with vividness for negative, neutral, and positive stimuli (n=29). A subset of these regions (cyan) showed a stronger relation to vividness for true memories than false memories (n=19 sample). **Bottom.** The call-out bar graphs show the average and individual parameter estimates of the slopes between activity and vividness rating by valence and memory accuracy for the participants with an ample number of false alarm trials extracted *a priori* regions of interest (hippocampus and retrosplenial cortex [see black arrow on sagittal slice]). The open circles represent individual data points for the five participants that were excluded from the analysis of true and false memory by valence for not having an ample number of high vividness trials and possibly noisier estimates of the slope. * $p < 0.05$, ** $p < .025$.

Table 1. Regions that showed a significant positive parametric relation of true memory vividness (hits only, n=29) across all valences. Regions that showed a main effect of memory are denoted with superscripted symbols (see legend).

Lobe	Region	Hem	BA	MNI	TAL	k
Frontal	Dorsal medial prefrontal cortex	L	8	0,28,50	-2,20,51	268
Frontal	Inferior frontal gyrus, middle frontal gyrus, orbital frontal cortex*	L	10, 46, 47	-42,42,-2	-40,38,5	865
Frontal	Inferior frontal gyrus, middle frontal gyrus	L	6, 8, 9	-42,14,36	-40,8,37	142
Frontal	Inferior frontal gyrus, orbital frontal cortex**, insula	R	11, 13, 47	28,14,-18	25,13,-10	85
Frontal	Inferior frontal gyrus	R	47	46,26,-8	42,23,0	26
Frontal	Inferior frontal gyrus	L	45	-50,26,14	-47,21,18	11
Frontal	Inferior frontal gyrus	R	47	38,24,-20	34,22,-11	10
Frontal	Superior frontal gyrus	L	8	-28,20,48	-27,13,48	18
Parietal	Retrosplenial cortex, precuneus, posterior cingulate^	L	7, 29, 30	-8,-56,12	-9,-55,10	121
Parietal	Superior lateral occipital cortex, supramarginal gyrus, angular gyrus**	L	19, 39, 40	-38,-70,32	-37,-70,26	1252
Parietal	Post-central gyrus, pre-central gyrus	L	1, 2, 3	-40,-26,56	-39,-31,51	94
Parietal	Angular gyrus, superior occipital gyrus	R	19, 39	48,-60,26	43,-60,23	16
Temporal	Hippocampus^	L	35	-26,-22,-18	-25,-21,-14	33
Temporal	Middle and inferior temporal gyri*	L	20, 21, 37	-58,-52,-4	-55,-50,-5	528
Other	Anterior cingulate*	L	24	2,2,30	0,-3,31	49
Other	Caudate body	L	NA	-10,8,12	-10,5,15	60
Other	Posterior cingulate	L	31	-2,-30,38	-3,-33,35	185
Other	Thalamus	L	NA	0,-18,4	-1,-19,6	10

BA=Brodman area, Hem=Hemisphere, k=voxel extent, MNI=Montreal Neurological Institute coordinate system, TAL=Talairach & Tournoux coordinate space.

*Cluster also shows a significant whole-brain main effect of memory (*k \geq 10, **k \geq 40 threshold from simulations) in the analysis of a subset of participants (n=19) with a sufficient number of false alarm trials (shown in cyan in Figure 2). ^Significant main effect of memory in a follow-up 2 x 3 ANOVA outside of SPM8 for plotting region of interest call-out plots in Figure 2 (bottom).

Valence-specific effects of true memory vividness. We next examined valence-specific effects, comparing negative to positive valence.

Negative-valence specific effects. Consistent with our hypothesis, activation in ventral visual regions tracked more strongly with negative memory vividness than positive memory vividness: The whole-brain comparison of Negative True Vividness > Positive True Vividness (inclusively masked with Negative True Vividness > zero) defined an area of occipito-temporal cortex that included the inferior and middle temporal gyri, the left parahippocampal cortex, and the left superior occipital gyrus (see Table 2 and activity shown in red in Figure 3). The left occipito-temporal cortex area—a cluster largely posterior to the effects observed across valences in Figure 2A—directly overlapped with clusters that have previously shown encoding-to-retrieval overlap for negative memories across two studies (Kark & Kensinger, 2015; Kark & Kensinger, in press). The middle frontal gyrus, precuneus, and superior and inferior parietal lobule also showed this valence-specific pattern (see Table 2). All of these regions continued to show this valence-specific effect at the group level when the fixed-effects models included a trial-level regressor of participant’s post-scan arousal ratings of the IAPS images. Critically, further evidence that these results were driven by valence rather than arousal came from follow-up analyses, revealing that the parametric relation tracked with valence, with the parameter estimate of the slope for neutral stimuli falling nominally between that of negative and positive stimuli (see plots in Figure 3, bottom).

Positive-valence specific effects. The Positive True Vividness > Negative True Vividness contrast outlined several clusters that spanned precentral gyrus and superior

frontal gyrus as well as the superior parietal and paracentral lobules (see Table 2 and activity shown in cyan in Figure 3), even when item-level arousal was controlled for in the fixed-effects models.

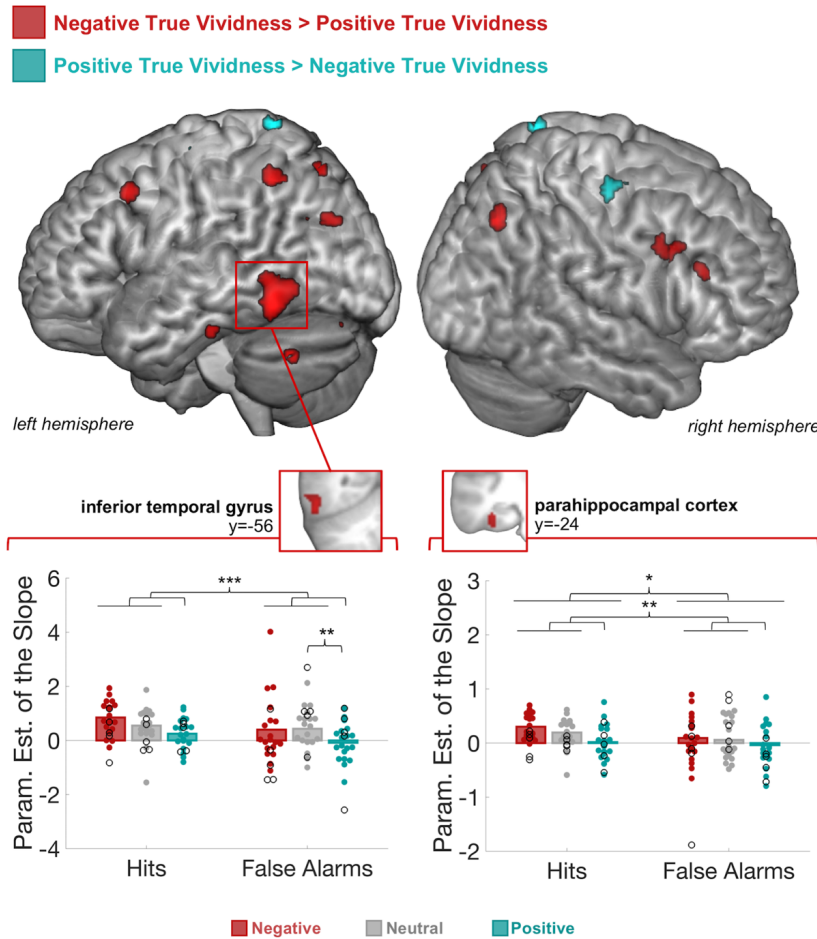


Figure 3. Effects of valence on true memory vividness. **Top.** Valence-specific true memory vividness comparisons were observed for true memory vividness (shown in red) and positive memory vividness (shown in cyan). **Bottom.** The call-out bar graphs show the average and individual parameter estimates of the slopes between activity and vividness rating by valence and memory accuracy for the participants with an ample number of false alarm trials for *a priori* regions of interest in the ventral visual stream. The open circles represent individual data points for the five participants that were excluded from the analysis of true and false memory by valence for not having an ample number of high vividness trials and possibly noisier estimates of the slope. Follow-up repeated measures ANOVA results are displayed. * $p < .05$, ** $p < .025$, *** $p < .01$.

Table 2. Valence-specific effects of true memory vividness (hits only, n=29).

Lobe	Region	Hem	BA	MNI	TAL	k
<i>Negative True Vividness > Positive True Vividness</i>						
Temporal	Inferior temporal gyrus (occipito-temporal), middle temporal gyrus [^]	L	21, 37	-52,-56,-18	-49,-52,-18	226
Temporal	Parahippocampal cortex [^]	L	36	-38,-22,-18	-36,-21,-14	51
Occipital	Superior occipital gyrus	L	19	-34,-80,26	-33,-78,20	22
Frontal	Middle frontal gyrus	L	9	-52,14,38	-50,8,38	39
Frontal	Middle frontal gyrus	R	9	56,30,28	51,23,33	21
Frontal	Middle frontal gyrus	R	6	38,10,32	34,5,34	115
Parietal	Inferior parietal lobule, precuneus	L	7, 40	-28,-60,28	-27,-60,23	262
Parietal	Precuneus	L	7	-22,-72,52	-22,-73,44	17
Parietal	Superior parietal lobule	R	7	30,-68,46	26,-69,40	51
Other	Cerebellum	L	N/A	-52,-64,-42	-49,-57,-40	19
Other	Cerebellum	L	N/A	-10,-76,-28	-10,-70,-28	48
<i>Positive True Vividness > Negative True Vividness</i>						
Frontal	Paracentral lobule	R	6	12,-20,54	9,-25,51	31
Frontal	Precentral gyrus	L	4	-30,-14,60	-30,-20,56	13
Frontal	Superior frontal gyrus, precentral gyrus	R	4, 6	24,-12,52	21,-18,50	105
Parietal	Superior parietal lobule	L	7	-16,-50,76	-17,-55,67	26

BA=Brodmann area, Hem=Hemisphere, k=voxel extent, MNI=Montreal Neurological Institute coordinate system, TAL=Talairach & Tournoux coordinate space.

[^]Significant main effect of valence in a follow-up memory accuracy-by-valence 2 x 3 ANOVA outside of SPM8 for plotting region of interest call-out plots in Figure 3 (bottom).

Effects of valence on true and false memory vividness.

In the previous section we reported valence-specific effects of negative memory vividness when only true memory was examined. We next sought to investigate if the effects of memory accuracy depended on valence. The conjunction analysis returned no false memory vividness effects that were similar across all three valence categories. The whole brain *F*-Contrast of the Memory Accuracy x Valence Interaction yielded no cortical activations. Given that this null result could have been due to low power, we conducted follow-up analyses separately examining the effect of memory accuracy on neutral, negative, and positive stimuli.

Neutral memory vividness. Replicating past research using neutral memoranda, neutral true memory vividness, compared to neutral false memory vividness, was tied to increased activation in early visual processing regions, medial and lateral parietal areas, and medial and lateral prefrontal cortex (see Table 3 and activity in cyan in the middle panel of Figure 4). Specifically, we found evidence for a greater link between memory vividness and activity in the calcarine sulcus (V1) for true compared to false neutral memories (see call-out plot in Figure 4, middle panel), which is broadly consistent with the idea that early visual cortex reactivation during retrieval distinguishes true from false memories (Slotnick and Schacter, 2004). Unexpectedly, this true-false memory vividness distinction in early visual cortex was strongest for neutral memories as evidenced by a memory-by-valence interaction ($F(2, 36) = 4.76, p = 0.015, \eta^2 = 0.21$), such that activity in this area of the calcarine sulcus did not distinguish negative and positive true from false memory vividness ($ps > 0.78$) and that the effect for neutral true memory vividness

was stronger than for negative true memory vividness ($t(18) = 2.24, p = 0.038$) and positive true memory vividness ($t(18) = 2.25, p = 0.037$) (see call out plot in Figure 4, bottom of the middle panel).

While we found relatively widespread patterns of a neutral true-false memory vividness distinction, we observed overlap for true and false neutral memory vividness in the bilateral inferior temporal gyrus, with a cluster of the left posterior inferior temporal gyrus also showing overlap with the F -Contrast of a Main Effect of Valence (shown in white on the left hemisphere in the middle panel of Figure 4). Interestingly, a follow-up ANOVA of the parameter estimates for neutral items from the calcarine sulcus and left posterior inferior temporal gyrus returned a significant memory accuracy-by-region interaction ($F(1, 18) = 7.82, p = 0.012, \eta^2 = 0.30$), suggesting the patterns for neutral memory vividness differ in early visual regions (distinguish true and false) and later visual regions (do not distinguish true and false). No regions varied more strongly with false than true neutral memory vividness.

Negative memory vividness. Before turning to the whole-brain comparisons of the effect of valence on true and false memory vividness, we conducted follow-up analyses on the visual regions that showed valence-specific effects in the previous section (see *Negative-valence specific effects* and activity shown in red in Figure 3). To compare these valence patterns of true memory vividness in visual regions to false memory vividness patterns, we extracted parameter estimates of the slopes from the nineteen participants with sufficient false alarm trials for analysis and conducted a 2 x 3 repeated-measures ANOVA with factors of memory accuracy (hits, false alarms) and valence

(negative, neutral, positive). The three visual processing regions that showed Negative True Vividness > Positive True Vividness each showed a main effect of valence (Left inferior temporal gyrus: $F(2, 36) = 6.05, p = 0.005, \eta^2 = 0.25$; Left parahippocampal cortex: $F(2, 36) = 4.44, p = 0.019, \eta^2 = 0.20$, Left superior occipital gyrus: $F(2, 36) = 4.43, p = 0.019, \eta^2 = 0.20$), reflecting greater effects for negative and neutral vividness, compared to positive vividness, regardless of memory accuracy. Results of three paired-samples *t*-tests suggest the effects for negative true memory vividness were not greater than false negative memory vividness in these areas (all *ps* > .07). These findings suggest that negative memory vividness is associated with greater activation in these higher-level visual processing regions, compared to positive memories, but that these effects do not distinguish true from false negative memory vividness. Interestingly, these regions did not show a significant enhancement for negative relative to neutral memory vividness, but rather a main effect of valence that reflected a relative drop-out of positive memory vividness from showing a link between activity and vividness in these regions.

Next, we conducted whole-brain analysis to demarcate regions that distinguished negative true from false memory vividness. Within negative items, increased true memory vividness was associated greater activity in bilateral ventral visual regions—including a small portion of the left inferior temporal gyrus cluster that showed a valence-specific effect for negative memory vividness in the previous section—as well the inferior frontal gyrus, anterior cingulate, and superior parietal lobule (see Table 3 and activity shown in cyan in the left panel of Figure 4). Further examination of the parameter estimates of the slopes extracted from the right fusiform gyrus cluster suggest this

difference between true and false vividness might be specific to negative memories as there were no significant differences between neutral and positive true and false memory vividness in this cluster ($ps > 0.32$). However, a memory accuracy-by-valence interaction ($F(2, 36) = 3.20, p = 0.05, \eta^2 = 0.15$) was only at trend levels and the fusiform cluster was relatively small.

While there was some evidence for regions that distinguished true from false memory vividness, conjunction analysis of true and false negative memory vividness confirmed substantial overlap (see Table 4 and activity shown in magenta in Figure 4, left panel). Most notably, we found true and false memory vividness overlap in bilateral parahippocampal cortex. The effect appeared strongest in the right hemisphere, with a significant whole-brain main effect of valence observed in the right parahippocampal cortex (see area outlined in white and call-out plot in Figure 4, left panel). Follow-up analyses showed a significant main effect of memory accuracy ($F(1, 18) = 4.71, p = 0.04, \eta^2 = 0.21$) and a trend toward a memory accuracy-by-valence interaction ($F(2, 36) = 2.66, p = 0.08, \eta^2 = 0.13$). While there were no differences in the parametric estimates of the slope for true and false negative memories in the right parahippocampal cortex ($t(18) = 0.84, p = 0.41$), neutral and positive stimuli showed stronger effects for true compared to false memory vividness (Neutral: $t(18) = 2.46, p = 0.024$; Positive: $t(18) = 2.1, p = 0.049$). No regions varied more strongly with false than true negative memory vividness.

Positive memory vividness. Activity in the middle temporal gyrus and angular gyrus distinguished true from false memory vividness for positive items. Although not an *a priori* hypothesis, we found that bilateral hippocampal activation was associated with

greater positive memory vividness for true compared to false memories (see activity in cyan in Figure 4, right panel). While right hippocampal activation did not significantly distinguish true from false memory vividness for negative or neutral stimuli ($p > 0.84$), follow-up analysis returned a main effect of memory accuracy ($F(1, 18) = 5.85$, $p = 0.03$, $\eta^2 = 0.25$) and only a trend toward a memory accuracy-by-valence interaction ($F(2, 36) = 2.27$, $p = 0.12$, $\eta^2 = 0.11$). By contrast, conjunction analyses showed that activation within multiple frontal regions (e.g., medial prefrontal cortex, superior frontal gyrus, and orbital frontal cortex) tracked with false as well as true memory vividness (see activity shown in magenta in Figure 4, right panel). No regions varied more strongly with false than true positive memory vividness.

Emotional memory vividness. For both negative and positive items, there was widespread activation corresponding to both true and false memory vividness (see Table 4 and activity shown in magenta in Figure 4, left and right panels) in large clusters of the temporal-occipital-parietal junction (e.g., middle temporal gyrus, superior occipital gyrus, and angular gyrus), ventral medial prefrontal cortex, and orbital frontal cortex. No regions showed stronger tracking of false than true emotional memory vividness.

Amygdala and memory vividness

Given the well-established role of the amygdala in emotional memory and the recent debate over the role of the amygdala in modulating memory (for discussion see Kensinger and Kark, 2018), we conducted follow-up analyses in the left and right amygdala to determine the link between activity and vividness in this paradigm. The role

of the amygdala in negative memory retrieval is mixed: Some studies have found amygdala engagement during retrieval is linked with accuracy for details (Kensinger and Schacter, 2007), while other studies have concluded that the amygdala is not necessarily linked to negative memory accuracy (Sharot et al., 2004) and purport that the majority of amygdala influence occurs around the time of encoding (Kark and Kensinger, 2015, in press). While these equivocal findings could be rooted in methodological differences across studies, here we test if amygdala activation at the moment of retrieval bears any influence on the link with subjective vividness, and if those effects vary as a function of accuracy and valence. To test this prediction, we conducted follow-up region of interest analyses of the amygdala. Analysis of the parameter estimates of the slope extracted the left and right amygdala seed regions (Hammers et. al., 2003) suggest no effect of valence on the relationship between activity levels and subjective vividness for hits (left amygdala: $F(2, 84) = 1.26, p = 0.29$; right amygdala: $F(2, 84) = 0.81, p = 0.45$, One-way ANOVA). In a 2 x 3 repeated-measures ANOVA with factors of memory accuracy and valence, the left amygdala showed a main effect memory accuracy ($F(1, 18) = 5.84, p = .027, \eta^2 = .245$), but no main effect of valence ($F(2, 36) = 0.39, p = .678, \eta^2 = .021$), or memory accuracy-by-valence interaction ($F(2, 36) = 0.73, p = .49, \eta^2 = .04$), and the right amygdala showed no main effects or an interaction ($ps > 0.09$), suggesting that a link between the amygdala and vividness might occur when memories are veridical, at least in in this paradigm.

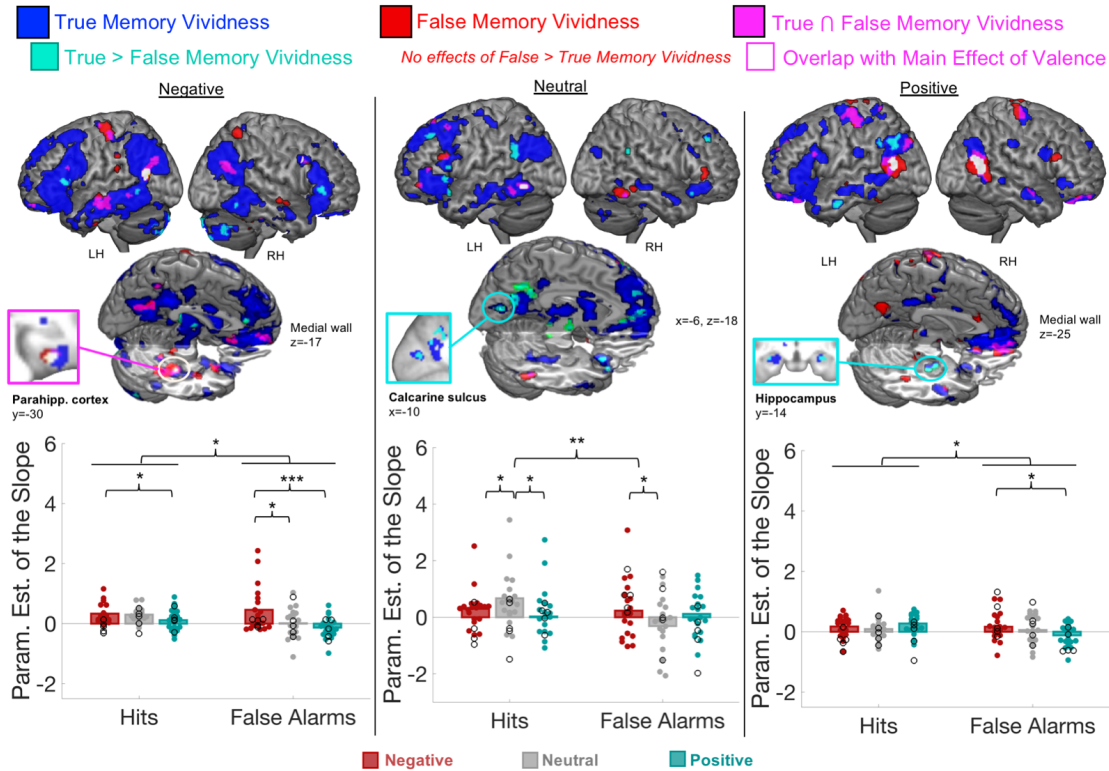


Figure 4. Effects of valence on true and false memory vividness. **Top.** Visualization of the positive parametric relation between activity for true memory vividness (shown in blue), false memory vividness (shown in red), and for true and false memory (shown in violet). Regions shown in cyan additionally show a greater link between activity and vividness for true as compared to false memory vividness. Regions depicted in white show a whole-brain main effect of valence (i.e., a similar pattern for true and false memory). **Bottom.** Call-out plots for regions of interest (parahippocampal cortex [left panel], calcarine sulcus [middle panel], hippocampus [right panel]) plot average and individual data points of the parameter estimates as a function of valence and memory accuracy. Results of follow up tests outside of SPM are displayed. * $p < .05$, ** $p < .025$, *** $p < .01$.

Table 3. Regions that showed a greater positive parametric effect for true memory vividness than false memory vividness by valence (n=19).

Lobe	Region	Hem	BA	MNI	TAL	k
<i>Negative True Memory Vividness > Negative False Memory Vividness</i>						
Temporal	Fusiform gyrus, inferior temporal gyrus	L	20, 37	-40,-58,-10	-38,-55,-11	12
Temporal	Fusiform gyrus, inferior temporal gyrus	R	20, 37	42,-48,-6	38,-46,-5	35
Temporal	Inferior temporal gyrus, middle temporal gyrus	L	37	-50,-54,-4	-47,-51,-5	19
Temporal	Parahippocampal cortex	L	36	-20,-26,-6	-20,-25,-4	13

Frontal	Inferior frontal gyrus	L	44, 45	-40,24,8	-38,20,13	104
Frontal	Inferior frontal gyrus	R	45	58,34,2	53,29,10	28
Parietal	Superior parietal lobule, superior occipital gyrus	L	19, 39	-26,-72,20	-25,-70,15	214
Other	Anterior cingulate	B	24	6,28,16	4,23,21	58
Other	Caudate	L	N/A	-14,6,14	-14,3,17	18
Other	Caudate	L	N/A	-12,10,0	-12,8,5	10
Other	Cerebellum	L	N/A	-32,-82,-50	-30,-74,-48	27
Other	Cerebellum	L	N/A	-10,-94,-30	-10,-87,-31	24
Other	Cerebellum	L	N/A	-18,-90,-44	-17,-82,-43	19
Other	Cerebellum	L	N/A	-46,-76,-40	-43,-69,-39	15
Other	Cerebellum	R	N/A	8,-88,-32	7,-81,-32	102
Other	Cerebellum	R	N/A	26,-86,-48	23,-78,-46	43
Other	Cerebellum	R	N/A	52,-70,-40	47,-64,-37	39
Other	Cerebellum	R	N/A	8,-82,-46	7,-74,-44	33
Other	Thalamus	L	N/A	-18,-12,6	-18,-13,8	51
Other	Thalamus	L	N/A	0,-12,4	-1,-13,7	36
Other	Thalamus	L	N/A	-10,-30,12	-10,-31,12	47
<i>Neutral True Memory Vividness > Neutral False Memory Vividness</i>						
Occipital	Calcarine sulcus	L	17	-10,-76,10	-11,-73,6	31
Temporal	Fusiform gyrus	L	37	-26,-40,-20	-25,-37,-18	26
Temporal	Middle temporal gyrus, angular gyrus	L	22, 39	-64,-54,24	-61,-54,20	101
Frontal	Anterior cingulate, ventral medial and orbital frontal	B	10, 24, 32	10,36,-12	8,33,-3	292
Frontal	Dorsal medial prefrontal cortex	L	8	-8,50,30	-9,42,35	20
Frontal	Inferior frontal gyrus	L	45	-50,20,-2	-47,17,3	28
Frontal	Inferior frontal gyrus	L	44	-48,16,10	-46,13,14	11

Frontal	Inferior frontal gyrus	R	47	44,24,-16	40,22,-7	12
Frontal	Inferior frontal gyrus, superior temporal gyrus	L	47	-44,16,-18	-41,15,-11	11
Frontal	Insula, frontal operculum	R	13	30,18,-16	27,16,-8	63
Frontal	Middle frontal gyrus	L	8	-28,36,44	-27,28,46	87
Frontal	Superior frontal gyrus	R	8	24,38,40	21,30,44	13
Parietal	Precuneus	L	7	-6,-58,40	-7,-59,35	120
Parietal	Retrosplenial cortex, posterior cingulate	L	31	-6,-64,22	-7,-63,18	57
Parietal	Retrosplenial cortex, posterior cingulate	R	30, 31	14,-60,22	12,-60,19	61
Parietal	Supramarginal gyrus	R	40	58,-44,28	52,-45,26	15
Other	Anterior cingulate	B	24	0,24,20	-1,19,24	14
Other	Cingulate gyrus	B	24	-2,-8,38	-3,-13,37	26
<i>Positive True Memory Vividness > Positive False Memory Vividness</i>						
Temporal	Hippocampus	L	N/A	-26,-16,-18	-25,-15,-14	17
Temporal	Hippocampus	R	N/A	30,-14,-20	27,-13,-15	28
Temporal	Middle temporal gyrus	L	21	-48,-8,-26	-45,-7,-21	40
Parietal	Angular gyrus	L	39	-58,-66,30	-55,-66,24	12
Parietal	Angular gyrus, middle temporal gyrus	L	39	-44,-66,36	-42,-66,30	91
Frontal	Subgenual area	B	25	0,18,-14	-1,16,-7	15
Parietal	Supramarginal gyrus	L	40	-54,-50,36	-52,-51,31	12

B=Bilateral, BA=Brodmann area, Hem=Hemisphere, k=voxel extent, MNI=Montreal Neurological Institute coordinate system, TAL=Talairach & Tournoux coordinate space.

Table 4. Regions that showed a positive parametric effect of vividness for true and false memories by valence.

Lobe	Region	Hem	BA	MNI	TAL	k
<i>Negative True Memory Vividness \cap Negative False Memory Vividness</i>						
Occipital	Superior occipital gyrus, middle temporal gyrus, angular gyrus	R	19, 39	48,-60,24	43,-60,21	118
Occipital	Superior occipital gyrus, middle temporal gyrus, angular gyrus*	L	19, 39	-46,-70,28	-44,-69,22	163
Temporal	Middle temporal gyrus	L	21	-58,-46,-8	-55,-44,-8	13
Temporal	Middle temporal gyrus	L	21	-56,-26,-12	-53,-25,-10	26
Temporal	Middle temporal gyrus	L	21	-64,-12,-12	-60,-12,-9	67
Temporal	Parahippocampal cortex	L	36	-26,-32,-14	-25,-30,-12	17
Temporal	Parahippocampal cortex*	R	36	38,-14,-26	34,-13,-20	33
Temporal	Parahippocampal cortex*, fusiform gyrus	R	20, 36	34,-30,-24	31,-28,-19	88
Frontal	Inferior frontal gyrus, temporal pole	R	38, 47	28,12,-22	25,11,-14	17
Frontal	Middle frontal gyrus	L	9	-42,20,24	-40,15,27	18
Frontal	Middle frontal gyrus*	R	9	36,12,32	32,6,34	117
Frontal	Orbital frontal cortex, subgenual area	B	11, 25	-8,28,-18	-8,26,-10	51
Frontal	Ventral medial prefrontal cortex	B	10, 11	4,38,-16	3,35,-7	96
Parietal	Postcentral gyrus	L	3	-36,-26,58	-35,-31,53	78
Parietal	Retrosplenial cortex, precuneus	B	7, 30	-12,-60,20	-13,-59,16	281
<i>Neutral True Memory Vividness \cap Neutral False Memory Vividness</i>						
Temporal	Inferior temporal gyrus	R	37	50,-48,-18	45,-45,-15	16
Temporal	Inferior temporal gyrus, middle temporal gyrus	L	20, 37	-54,-48,-16	-51,-45,-15	56
Temporal	Inferior temporal gyrus*	L	37	-50,-58,-10	-47,-55,-11	38
Temporal	Superior occipital gyrus	L	19	-34,-64,30	-33,-64,25	18
Frontal	Inferior frontal gyrus	L	46	-50,40,6	-47,35,12	10
Frontal	Middle frontal gyrus	L	6	-40,18,56	-39,10,55	19

<i>Positive True Memory Vividness \cap Positive False Memory Vividness</i>						
Occipital	Superior occipital gyrus	L	19	-36,-84,38	-35,-83,30	52
Temporal	Superior occipital gyrus, middle temporal gyrus, angular gyrus**	L	19, 39	-48,-64,16	-46,-63,12	102
Temporal	Middle temporal gyrus, superior occipital gyrus, middle temporal	R	19, 39	54,-62,18	49,-61,16	264
Frontal	Dorsal medial prefrontal cortex, superior frontal gyrus	L	9, 10	-12,48,34	-12,40,38	87
Frontal	Inferior temporal gyrus	L	44	-48,18,24	-46,13,26	20
Frontal	Orbital frontal cortex, subgenual area	L	11, 25	10,2,-10	8,1,-5	46
Frontal	Precentral gyrus	R	4	34,-16,70	30,-23,66	10
Frontal	Precentral gyrus, post-central gyrus	L	4, 6	-38,-24,58	-37,-29,53	225
Frontal	Superior frontal gyrus	L	10	-10,60,8	-10,53,16	10
Frontal	Ventral medial prefrontal cortex	B	10, 11	6,46,-18	5,43,-8	233

B=Bilateral, BA=Brodmann area, Hem=Hemisphere, k=voxel extent, MNI=Montreal Neurological Institute coordinate system, TAL=Talairach & Tournoux coordinate space.

*Cluster shows significant overlap with the *F*-Contrast of the main effect of valence (* $k \geq 10$, ** $k \geq 40$) (shown in white in Figure 4).

Exploratory analysis: Effect of memory accuracy on parahippocampal cortex parametric functional connectivity and negative memory vividness

In this study, we reported a main effect of a valence in the right parahippocampal cortex, suggesting this region is important for both true and false negative memory vividness and that negative true and false memories share similar neural processes with regard to subjective memory strength. However, some theories of false memory would predict differential functional connectivity profiles of medial temporal lobe regions for true as compared to false memories, such as an inferior-superior distinction, with greater functional connectivity with inferior sensory areas driving vividness for true negative

memories and greater functional connectivity with superior control regions with increased vividness for false memories (Dennis et al., 2015). To test this exploratory hypothesis, we utilized the Generalized PPI (gPPI) Toolbox (McLaren et al., 2012; <https://www.nitrc.org/projects/gppi>) to save whole-brain parametric functional connectivity maps for negative hits vividness and negative false alarms vividness separately for each participant. We used two, group-level one-sample *t*-tests to demarcate regions that showed increased functional connectivity of the right parahippocampal cortex seed region for negative true memories and negative false memories. Follow-up analyses outside of SPM8 were conducted on six regions of interest (visual processing and frontal) to test for regions that showed a significant difference between true and false negative memory vividness.

The positive parametric functional connectivity map of the right parahippocampal cortex revealed increased functional connectivity with visual processing and frontal regions with increasing levels of vividness (see Table 5 and activity shown in blue in Figure 5). The visual processing patterns were mostly restricted to early visual regions. The analysis of negative false memory vividness functional connectivity returned no suprathreshold voxels. Given potential power issues for estimating parametric functional connectivity of false memory vividness, we visualize negative true vividness effects of parahippocampal cortex functional connectivity exclusively masking out any effects for negative false memory vividness at a reduced threshold ($p < 0.05$) (see Figure 5 patterns in blue). We conducted follow-up paired samples *t*-tests in six regions of interest (four visuosensory and two frontal clusters) and applied a Bonferroni correction for multiple

comparisons ($p < .05/6$). The only cluster to showed a significant enhancement for negative true memory vividness compared to negative false memory vividness was the anterior cingulate ($t(18)=3.17, p=0.005$). Together, these exploratory results suggest that while activity in the right parahippocampal cortex is associated with true and false negative memory vividness, the right parahippocampal cortex signal shows accuracy-distinguishing functional connectivity with the anterior cingulate, possibly reflecting greater retrieval monitoring for negative true memory vividness. However, given the limited power, future work is needed to determine if medial temporal lobe signals engaged for true and false memories differ on the basis of functional connectivity patterns with cortex.

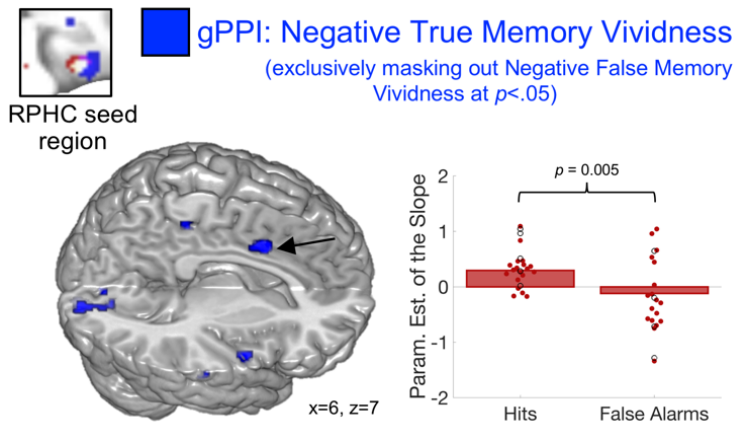


Figure 5. Exploratory functional connectivity analysis of the right parahippocampal cortex for true and false memories. The positive parametric relationship for negative true memory vividness is shown in blue. There were no suprathreshold voxels for negative false memory vividness. The call out plot shows the significant difference between the average parameter estimates of the slope for the functional connectivity of the right parahippocampal cortex with the anterior cingulate between true and false memory vividness. The right parahippocampal cortex seed region is shown in white on the coronal slice in the top left corner.

Table 5. Parametric functional connectivity of the right parahippocampal cortex for negative true memory vividness, exclusively masking out any effects for negative false memory vividness.

Lobe	Region	Hem	BA	MNI	TAL	k
Occipital	Calcarine sulcus	L	17	-14,-92,8	-14,-88,3	80
Occipital	Calcarine sulcus	L	17	-14,-76,12	-14,-74,8	12
Occipital	Calcarine sulcus	R	17	10,-80,8	8,-77,4	13
Occipital	Cuneus, precuneus	R	17, 31	24,-62,18	21,-61,15	22
Occipital	Lingual gyrus, calcarine sulcus	R	17, 18	18,-90,-6	15,-85,-9	162
Occipital	Middle occipital gyrus	L	19	-44,-86,18	-42,-83,12	12
Occipital	Superior occipital gyrus, angular gyrus	R	19, 39	42,-72,36	37,-72,31	68
Temporal	Middle temporal gyrus	R	39	38,-60,32	34,-61,28	10
Temporal	Parahippocampal cortex, hippocampus	L	28	-20,-14,-28	-19,-12,-22	60
Temporal	Superior temporal gyrus	R	22	58,2,2	53,0,7	30
Temporal	Superior temporal gyrus	R	22	70,-22,4	64,-23,7	13
Frontal	Dorsal anterior cingulate**	R	24, 32	6,12,38	4,6,39	72
Frontal	Inferior frontal gyrus, precentral gyrus	R	6	62,2,24	56,-2,27	35
Frontal	Paracentral lobule	R	5	6,-32,54	4,-36,50	21
Frontal	Precentral gyrus	L	4	-48,-16,26	-46,-19,25	13
Frontal	Superior frontal gyrus	R	6	22,-10,70	18,-17,66	14
Other	Cerebellum	R	N/A	28,-58,-48	25,-52,-43	10
Other	Globus pallidus	R	N/A	10,2,-10	8,1,-5	19

BA=Brodman area, Hem=Hemisphere, k=voxel extent, MNI=Montreal Neurological Institute coordinate system, TAL=Talairach & Tournoux coordinate space.

**Significant follow-up *t*-test comparing true and false negative memory vividness parametric functional connectivity.

3.5 DISCUSSION

The current study investigated the neural correlates of true and false memory vividness with a focus on valence-specific effects. Prior work has demonstrated enhanced activation of ventral visual regions supports encoding and retrieval of negative memories, which motivated the main study questions: Does the magnitude of retrieval activity in these regions bear a valence-specific influence on the subjective sense of *vividness* for those memories, or if successfully retrieved, do ventral visual regions show a similar relation to vividness regardless of valence? Further, are those signals unique to veridical memory vividness or do ventral visual signals also drive or reflect negative false memory vividness?

We began with an analysis of true compared to false memory vividness, to both root our findings in a replication of past work and extend those findings to a 24-hour study-test delay. Regardless of valence, true memory vividness was associated with widespread effects in regions with known roles in memory retrieval (e.g., hippocampus, inferior parietal lobule, dorsal medial and ventral lateral prefrontal cortex, anterior cingulate cortex, posterior cingulate cortex, late visual processing regions). In agreement with prior work (Dennis et al., 2012), we found that there were no regions that showed a false memory vividness effect that was greater than true memory vividness, which was also true when examined within each valence category. These findings suggest false memory vividness tends to emanate from many of the same regions involved in veridical memory vividness. However, that is not to say that the qualities that underlie true vivid

memories are not somehow different from those of false memories (Heaps and Nash, 2001). Below we discuss the principal findings in detail by regions of interest.

Regions that distinguished true from false memory vividness regardless of valence.

Regardless of valence, we found a main effect of accuracy in the hippocampus demonstrating a stronger link between vividness and activity for true memories, compared to false memories, consistent with other studies of true and false memory (Dennis et al., 2012). We also found a valence-invariant effect of accuracy in the retrosplenial cortex/precuneus, consistent with prior memory vividness work (Richter et al., 2016) that perhaps reflects a stronger link between visual imagery and re-experiencing of the original study images in the “mind’s-eye” during retrieval (Fletcher et al., 1995). We further found areas of ventral-parietal cortex correlated with true memory vividness, regardless of valence. This finding is consistent with previous work that has demonstrated a ventral-dorsal dissociation of activity in parietal cortex, with ventral and dorsal areas associated with bottom-up/recollection and top-down/familiarity responses, respectively (Cabeza et al., 2008; Wagner et al., 2005). Moreover, the link between ventral-parietal cortex and vividness was specific to true memories, perhaps reflecting a rapid, bottom-up signal from an actual memory trace as opposed to an effortful search or constructive process associated with familiarity signals or false memories.

Early visual cortex distinguishes true from false vividness for neutral memories.

In this study, the neutral stimuli served as a point of comparison for the valence conditions and also as a comparison condition to other studies of neutral true and false memory. In agreement with prior work (Richter et al., 2016; Slotnick and Schacter, 2004; Stark et al., 2010), we found an effect of true neutral memory vividness in early visual cortex (calcarine sulcus, V1) that was greater than false neutral memory vividness. We also found an interaction between patterns in early visual cortex and the left inferior temporal gyrus (BA20/37) for neutral memories: Early visual cortex distinguished true from false memory vividness but the left inferior temporal gyrus did not, further supporting the early-late distinction of visual region contributions to true-false memory. Interestingly, this distinction was significant only for neutral stimuli and did not extend to vividness for negative or positive stimuli. Future work is needed to clarify the role of the primary visual cortex in emotional memory vividness.

Valence-specific effect of negative memory vividness in occipito-temporal cortex

We demonstrated a valence-specific effect of negative memory vividness in a large swath of occipito-temporal cortex, including the left inferior temporal gyrus, and the left parahippocampal cortex. The occipito-temporal cortex region showed direct spatial overlap with two of our prior studies of negative memory recapitulation (Kark and Kensinger, 2015, in press), suggesting that this area is consistently involved in negative memory recapitulation processes and also contributes to a sense of strong negative memory vividness. Critically, the parameter estimates demonstrated a valence effect

(Negative > Neutral > Positive) in both regions and these findings were robust to controlling for item-level arousal ratings. These data suggest negative valence in particular is associated with enhanced memory processes in the ventral visual stream.

Parahippocampal cortex associated with true and false negative memory vividness

Given the behavioral overlap between true and false memories—particularly in negative memories—we specifically sought to demarcate regions of the brain where negative true and false memory vividness patterns were supported by the same brain regions and how those effects differed compared to emotionally positive memories. One of the principal findings of the current study is that the parahippocampal gyri supported negative memory vividness, regardless of accuracy, providing further evidence that overlapping neural processes support the retrieval of negative true memories as well as negative false memories. While we have previously shown that retrieval-related recapitulation of the parahippocampal cortex supports negative memory, compared to forgetting (Kark and Kensinger, 2015, in press), the current results suggest that increased activation in this region is linked with increased vividness regardless of memory accuracy. These data are also broadly consistent with prior work from Sharot, Delgado, and Phelps (2004) that showed the parahippocampal cortex predicted accurate memory for neutral items but not negative items, suggesting that visual activation might be less important for accurate endorsement of negative memories than neutral memories.

Recent work has shown that parahippocampal cortex activation can support both true and false memories (Karanian and Slotnick, 2014, 2017), contributing to an ongoing debate about the role of the parahippocampal cortex in memory. The parahippocampal

cortex has a well-accepted role in scene processing (often referred to as the parahippocampal place area, Epstein and Kanwisher, 1998) as well as episodic memory (Hayes et al., 2007) and envisioning the future (Schacter and Addis, 2009), with activity levels sometimes indistinguishable between memory and future thinking (Szpunar et al., 2007). Parahippocampal cortex activity has been associated with visual context memory (Hayes et al., 2007), is particularly responsive to scenes with strong contextual associations, and is subject to emotional modulation of retrieval processes (Chan et al., 2014; Smith et al., 2004). Even broader frameworks of the parahippocampal cortex in contextual processing have been proposed and include both spatial information and non-spatial information (Aminoff et al., 2007) as well as contexts more broadly construed, such as emotion (Aminoff et al., 2013). As the parahippocampal cortex is capable of supporting vivid mental representations of novel future visual-spatial contexts, it is possible that the negative line-drawing cues evoke strong emotional or visual contexts (possibly borrowed content from a similar studied item [e.g., snake, dog, plane crash] or content that is completely extralist) that drive a sense of negative false memory vividness.

Amygdala supports true memory vividness regardless of valence.

In the amygdala, there was an overall valence-invariant link between activity levels and true memory vividness. Somewhat surprisingly, there was no effect of valence on the link between the magnitude of amygdala engagement and subjective memory vividness, perhaps due to the use of relatively less-emotional line-drawing stimuli used during retrieval. The line-drawings were chosen strategically to elicit more false alarms for

fMRI analysis, but they are relatively less emotional than the full colorful IAPS images, which could have limited our amygdala findings for false emotional memory vividness. Future work with emotionally-laden stimuli—perhaps presented rapidly or alongside perceptually similar lures to induce sufficient false alarm trials for fMRI analysis—could further test for a link between amygdala activation and a false sense of memory vividness.

Temporal-parietal-occipital junction activity associated with emotional vividness regardless of accuracy.

Unexpectedly, both negative and positive valence showed a positive parametric effect of vividness regardless of accuracy in areas spanning the junction of the temporal, parietal, and occipital lobes (also referred to as the 'TPO' junction; see De Benedictis et al., 2014; Karnath, 2001), including the middle temporal gyrus, superior occipital gyrus, and angular gyrus. The TPO junction is a highly complex area involved in myriad of functions, including multimodal integration and visual-spatial recognition (De Benedictis et al., 2014). Future work is needed to understand the role of this area in subjective vividness for emotional stimuli that is not necessarily tethered to a veridical memory trace.

Functional connectivity profiles distinguish true from false negative memory vividness.

Finally, the results of the exploratory analysis further highlight the utility and potential for functional connectivity analyses to reveal network profile differences that distinguish true from false memory vividness emanating from a common locus of activation, as suggested by Dennis, Bowman, and Vandekar (2012). Here we found greater parahippocampal cortex and anterior cingulate cortex functional connectivity with increasing vividness for true negative memories, compared to false negative memory vividness. These findings suggest that while the magnitude of activity in a region can similarly track with true and false memory vividness, the region may be more strongly incorporated with other memory processes—including monitoring and verification processes in the frontal regions such as the anterior cingulate—when true memories are highly vivid.

Limitations and Future Directions.

While we can speculate, it is not possible to determine the content of memoranda driving the vividness responses and neural patterns for each valence. Based on the task instructions, participants were able to use a combination of memory for visual detail, thoughts, feelings, or reactions to the original IAPS images on the prior day in order to rate the vividness of their memory evoked by the line-drawing, such that the source of vividness could vary by memory and valence. Future work could use more objective measures for vividness and memory for visual features (Cooper et al., in press) to

decipher if negative true memory vividness is rooted in more objective accuracy or precision of visual details, compared to false memory vividness. The findings of the present study could be related to *perceptual recombination* in false memory, when fragmented perceptual features from an encoding episode are erroneously recombined and drive false recollection (for a review see Doss et al., 2016). Or in some trials, perceptually similar line-drawings could have prompted true recollections of studied pictures or *misidentification-related false recognitions* (Vannucci et al., 2012). Another interesting way to localize emotional enhancements of false memory vividness in the brain would be to utilize different stimulus modalities (e.g., true memories in visual domain, false memories in the auditory domain, as in Stark, Okado, and Loftus, 2010) or leverage cortical representation areas (e.g., fusiform face area or parahippocampal place area). Future work is needed to further understand the nature of the distortions that give rise to negative false memory vividness.

It is also possible that spurious activity in regions such as the parahippocampal cortex could drive a false sense of negative memory vividness, in which case negative false memories would not be due to monitoring processes gone awry or the aforementioned memory distortions. However, we examined false memory vividness in a subset of participants with a sufficient number of false alarm trials for parametric modulation analysis, such that even if spurious activations drove some trials for some individuals, it would not likely drive the valence differences observed here. Although we were able to elicit strong false recognitions in each valence category and we emphasized the effects that were robust to sampling in the false memory analysis to reduce the chance

of Type 1 error, the null effects for false memories in this study could be due to lower power and Type 2 error. It is entirely possible that there are effects that uniquely support false memory vividness that we were not able to capture in the current paradigm. Future work using an even longer study-test delay could elicit even more false alarms for analysis, as emotional false memories tend to increase over delay periods (Knott and Shah, 2018), particularly those that include sleep (McKeon et al, 2012).

Another important avenue for future research is to examine the effects of emotion on true and false memory in aging. Healthy aging has been associated with increases in the incidence of false memories (Vannucci et al., 2012), particularly emotional ones (Gallo et. al., 2009), a reduction in the neural differentiation between true and false memories (Duarte et al., 2010), and impaired emotional pattern separation and negative false recognition due to faulty overgeneralization and aberrations in the amygdala-hippocampal network in low-performing older adults (Leal et al., 2017). Future work is needed to understand how healthy and pathological aging could influence the neural correlates of emotional true and false memory vividness.

Conclusions

The current findings demonstrate valence-specific processes in the ventral visual stream for negative true and false memory vividness. These late visual processing regions appear to drive subjective vividness for negative memories compared to positive memories, but regardless of accuracy. We can speculate that these findings could map on to the behavioral finding that highly vivid negative false memories, although less frequent, can

occur and appear indistinguishable from a highly vivid true negative memory.

Investigating the neural profiles of memory distortions like false memories not only accelerates the understanding of veridical memory processes, but also carries important implications for real-world consequences of false memories in legal settings.

3.6 REFERENCES

- Aminoff, E., Gronau, N., Bar, M., 2007. The parahippocampal cortex mediates spatial and nonspatial associations. *Cereb Cortex* 17, 1493-1503.
- Aminoff, E.M., Kveraga, K., Bar, M., 2013. The role of the parahippocampal cortex in cognition. *Trends Cogn Sci* 17, 379-390.
- Barth, M., Breuer, F., Koopmans, P.J., Norris, D.G., Poser, B.A., 2016. Simultaneous multislice (SMS) imaging techniques. *Magn Reson Med* 75, 63-81.
- Bookbinder, S.H., Brainerd, C.J., 2016. Emotion and false memory: The context-content paradox. *Psychol Bull* 142, 1315-1351.
- Bowen, H.J., Kark, S.M., Kensinger, E.A., 2018. NEVER forget: negative emotional valence enhances recapitulation. *Psychon Bull Rev* 25, 870-891.
- Bowen, H.J., Kensinger, E.A., 2017. Recapitulation of emotional source context during memory retrieval. *Cortex* 91, 142-156.
- Buchsbaum, B.R., Lemire-Rodger, S., Fang, C., Abdi, H., 2012. The neural basis of vivid memory is patterned on perception. *J Cogn Neurosci* 24, 1867-1883.
- Cabeza, R., Ciaramelli, E., Olson, I.R., Moscovitch, M., 2008. The parietal cortex and episodic memory: an attentional account. *Nat Rev Neurosci* 9, 613-625.
- Cabeza, R., Rao, S.M., Wagner, A.D., Mayer, A.R., Schacter, D.L., 2001. Can medial temporal lobe regions distinguish true from false? An event-related functional MRI study of veridical and illusory recognition memory. *Proc Natl Acad Sci U S A* 98, 4805-4810.

- Cabeza, R., St Jacques, P., 2007. Functional neuroimaging of autobiographical memory. *Trends Cogn Sci* 11, 219-227.
- Chan, E., Baumann, O., Bellgrove, M.A., Mattingley, J.B., 2014. Negative emotional experiences during navigation enhance parahippocampal activity during recall of place information. *J Cogn Neurosci* 26, 154-164.
- Cooper, R.A., Kensinger, E.A., Ritchey, M., in press. Memories fade: The relationship between memory vividness and remembered visual salience. *Psychol Sci*.
- De Benedictis, A., Duffau, H., Paradiso, B., Grandi, E., Balbi, S., Granieri, E., Colarusso, E., Chioffi, F., Marras, C.E., Sarubbo, S., 2014. Anatomico-functional study of the temporo-parieto-occipital region: dissection, tractographic and brain mapping evidence from a neurosurgical perspective. *J Anat* 225, 132-151.
- Deese, J., 1959. On the prediction of occurrence of particular verbal intrusions in immediate recall. *J Exp Psychol* 58, 17-22.
- Dennis, N.A., Bowman, C.R., Turney, I.C., 2015. Functional Neuroimaging of False Memories. In: Addis, D.R., Barense, M., Duarte, A. (Eds.), *The Wiley Handbook on The Cognitive Neuroscience of Memory*. John Wiley & Sons, Ltd., Chichester, UK.
- Dennis, N.A., Bowman, C.R., Vandekar, S.N., 2012. True and phantom recollection: an fMRI investigation of similar and distinct neural correlates and connectivity. *Neuroimage* 59, 2982-2993.
- Dodson, C.S., Bawa, S., Slotnick, S.D., 2007. Aging, source memory, and misrecollections. *J Exp Psychol Learn Mem Cogn* 33, 169-181.

- Doss, M.K., Bluestone, M.R., Gallo, D.A., 2016. Two mechanisms of constructive recollection: Perceptual recombination and conceptual fluency. *J Exp Psychol Learn Mem Cogn* 42, 1747-1758.
- Duarte, A., Graham, K.S., Henson, R.N., 2010. Age-related changes in neural activity associated with familiarity, recollection and false recognition. *Neurobiol Aging* 31, 1814-1830.
- Epstein, R., Kanwisher, N., 1998. A cortical representation of the local visual environment. *Nature* 392, 598-601.
- Feinberg, D.A., Moeller, S., Smith, S.M., Auerbach, E., Ramanna, S., Gunther, M., Glasser, M.F., Miller, K.L., Ugurbil, K., Yacoub, E., 2010. Multiplexed echo planar imaging for sub-second whole brain fMRI and fast diffusion imaging. *PLoS One* 5, e15710.
- Fletcher, P.C., Frith, C.D., Baker, S.C., Shallice, T., Frackowiak, R.S., Dolan, R.J., 1995. The mind's eye--precuneus activation in memory-related imagery. *Neuroimage* 2, 195-200.
- Forgas, J., Laham, S., Vargas, P., 2005. Mood effects on eyewitness memory: Affective influences on susceptibility to misinformation. *Journal of Experimental Social Psychology* 41, 574-588.
- Gallo, D.A., Foster, K.T., Johnson, E.L., 2009. Elevated False Recollection of Emotional Pictures in Younger and Older Adults. *Psychol Aging* 24, 981-988.
- Garoff-Eaton, R.J., Slotnick, S.D., Schacter, D.L., 2006. Not all false memories are created equal: the neural basis of false recognition. *Cereb Cortex* 16, 1645-1652.

- Geraci, L., McCabe, D.P., 2006. Examining the basis for illusory recollection: the role of remember/know instructions. *Psychon Bull Rev* 13, 466-473.
- Hammers, A., Allom, R., Koepp, M., Free, S., Myers, R., Lemieux, L., Mitchell, T., Brooks, D., Duncan, J., 2003. Three-dimensional maximum probability atlas of the human brain, with particular reference to the temporal lobe. *Hum Brain Mapp* 19, 224-247.
- Hayes, S.M., Nadel, L., Ryan, L., 2007. The effect of scene context on episodic object recognition: parahippocampal cortex mediates memory encoding and retrieval success. *Hippocampus* 17, 873-889.
- Heaps, C., Nash, M., 2001. Comparing Recollective Experience in True and False Autobiographical Memories. *Journal of Experimental Psychology* 27, 920-930.
- Iidaka, T., Harada, T., Kawaguchi, J., Sadato, N., 2012. Neuroanatomical substrates involved in true and false memories for face. *Neuroimage* 62, 167-176.
- Johnson, M.K., Raye, C.L., 1981. Reality monitoring. *Psychological Review* 88, 67-85.
- Kahn, I., Davachi, L., Wagner, A.D., 2004. Functional-neuroanatomic correlates of recollection: implications for models of recognition memory. *J Neurosci* 24, 4172-4180.
- Kaplan, R., Van Damme, I., Levine, L., Loftus, E.F., 2016. Emotion and False Memory. *Emot Rev* 8, 8-13.
- Karanian, J.M., Slotnick, S.D., 2014. False memory for context activates the parahippocampal cortex. *Cogn Neurosci* 5, 186-192.

- Karanian, J.M., Slotnick, S.D., 2017. False memory for context and true memory for context similarly activate the parahippocampal cortex. *Cortex* 91, 79-88.
- Kark, S.M., Kensinger, E.A., 2015. Effect of emotional valence on retrieval-related recapitulation of encoding activity in the ventral visual stream. *Neuropsychologia* 78, 221-230.
- Kark, S.M., Kensinger, E.A., in press. Post-encoding Amygdala-Visuosensory Coupling Is Associated with Negative Memory Bias in Healthy Young Adults. *J Neurosci*.
- Karnath, H.O., 2001. New insights into the functions of the superior temporal cortex. *Nat Rev Neurosci* 2, 568-576.
- Kensinger, E.A., Kark, S.M., 2018. Emotion and Memory. In: Wagenmakers, E., Wixted, J. (Eds.), *Stevens' Handbook of Experimental Psychology and Cognitive Neuroscience*. Wiley, New York, pp. 1-26.
- Kensinger, E.A., Schacter, D.L., 2007. Remembering the specific visual details of presented objects: neuroimaging evidence for effects of emotion. *Neuropsychologia* 45, 2951-2962.
- Knott, L.M., Howe, M.L., Toffalini, E., Shah, D., Humphreys, L., 2018. The role of attention in immediate emotional false memory enhancement. *Emotion* 18, 1063-1077.
- Knott, L.M., Shah, D., 2018. The effect of limited attention and delay on negative arousing false memories. *Cogn Emot*, 1-9.
- Kurkela, K.A., Dennis, N.A., 2016. Event-related fMRI studies of false memory: An Activation Likelihood Estimation meta-analysis. *Neuropsychologia* 81, 149-167.

- Lacy, J.W., Stark, C.E.L., 2013. The neuroscience of memory: implications for the courtroom. *Nat Rev Neurosci* 14, 649-658.
- Lampinen, J.M., Meier, C.R., Arnal, J.D., Leding, J.K., 2005. Compelling untruths: content borrowing and vivid false memories. *J Exp Psychol Learn Mem Cogn* 31, 954-963.
- Laney, C., Loftus, E.F., 2008. Emotional content of true and false memories. *Memory* 16, 500-516.
- Lang, P.J., Bradley, M.M., Cuthbert, B.N., 2008. International affective picture system (IAPS): Affective ratings of pictures and instruction manual. Technical Report A-6. University of Florida, Gainesville, FL.
- Leal, S.L., Noche, J.A., Murray, E.A., Yassa, M.A., 2017. Age-related individual variability in memory performance is associated with amygdala-hippocampal circuit function and emotional pattern separation. *Neurobiol Aging* 49, 9-19.
- Loftus, E.F., 1979. *Eyewitness testimony*. Harvard University Press, Cambridge, MA.
- Loftus, E.F., Pickrell, J.E., 1995. The formation of false memories. *Psychiatr. Ann.* 25, 720-725.
- Loos, E., Egli, T., Coynel, D., Fastenrath, M., Freytag, V., Papassotiropoulos, A., de Quervain, D.J., Milnik, A., 2019. Predicting emotional arousal and emotional memory performance from an identical brain network. *Neuroimage* 189, 459-467.
- Maddock, R.J., 1999. The retrosplenial cortex and emotion: new insights from functional neuroimaging of the human brain. *Trends Neurosci* 22, 310-316.

- McLaren, D.G., Ries, M.L., Xu, G., Johnson, S.C., 2012. A generalized form of context-dependent psychophysiological interactions (gPPI): a comparison to standard approaches. *Neuroimage* 61, 1277-1286.
- McNally, R.J., Lasko, N.B., Clancy, S.A., Macklin, M.L., Pitman, R.K., Orr, S.P., 2004. Psychophysiological responding during script-driven imagery in people reporting abduction by space aliens. *Psychol Sci* 15, 493-497.
- Mickley, K.R., Kensinger, E.A., 2008. Emotional valence influences the neural correlates associated with remembering and knowing. *Cogn Affect Behav Neurosci* 8, 143-152.
- Mickley Steinmetz, K.R., Addis, D.R., Kensinger, E.A., 2010. The effect of arousal on the emotional memory network depends on valence. *Neuroimage* 53, 318-324.
- Mirandola, C., Toffalini, E., 2016. Arousal-But Not Valence-Reduces False Memories at Retrieval. *PLoS One* 11, e0148716.
- Moeller, S., Yacoub, E., Olman, C.A., Auerbach, E., Strupp, J., Harel, N., Ugurbil, K., 2010. Multiband multislice GE-EPI at 7 tesla, with 16-fold acceleration using partial parallel imaging with application to high spatial and temporal whole-brain fMRI. *Magn Reson Med* 63, 1144-1153.
- Neisser, U., Harsch, N., 1992. Phantom flashbulbs: False recollections of hearing the news about Challenger. In: Winograd, E., Neisser, U. (Eds.), *Affect and Accuracy in Recall: Studies of 'Flashbulb' Memories*. Cambridge University Press, New York, NY, US.

- Norman, K.A., Schacter, D.L., 1997. False recognition in younger and older adults: exploring the characteristics of illusory memories. *Mem Cognit* 25, 838-848.
- Otgaar, H., Muris, P., Howe, M.L., Merckelbach, H., 2017. What Drives False Memories in Psychopathology? A Case for Associative Activation. *Clin Psychol Sci* 5, 1048-1069.
- Palombo, D.J., McKinnon, M.C., McIntosh, A.R., Anderson, A.K., Todd, R.M., Levine, B., 2016. The neural correlates of memory for a life-threatening event: An fMRI study of passengers from flight AT236. *Clin Psychol Sci* 4, 312-319.
- Phelps, E.A., Sharot, T., 2008. How (and Why) Emotion Enhances the Subjective Sense of Recollection. *Curr Dir Psychol Sci* 17, 147-152.
- Porter, S., Spencer, L., Birt, A., 2003. Blinded by emotion? Effect of the emotionality of a scene on susceptibility to false memories. *Canadian Journal of Behavioural Science* 35, 165-175.
- Power, J.D., Barnes, K.A., Snyder, A.Z., Schlaggar, B.L., Petersen, S.E., 2012. Spurious but systematic correlations in functional connectivity MRI networks arise from subject motion. *Neuroimage* 59, 2142-2154.
- Richter, F.R., Cooper, R.A., Bays, P.M., Simons, J.S., 2016. Distinct neural mechanisms underlie the success, precision, and vividness of episodic memory. *Elife* 5.
- Roediger, H.L., McDermott, K.B., 1995. Creating false memories-remembering words not presented in lists. *Journal of Experimental Psychology: Learning, Memory, and Cognition* 21, 803-814.

- Schacter, D.L., 1999. The seven sins of memory. Insights from psychology and cognitive neuroscience. *Am Psychol* 54, 182-203.
- Schacter, D.L., Addis, D.R., 2009. On the nature of medial temporal lobe contributions to the constructive simulation of future events. *Philos Trans R Soc Lond B Biol Sci* 364, 1245-1253.
- Semmler, C., Brewer, N., Wells, G.L., 2004. Effects of postidentification feedback on eyewitness identification and nonidentification confidence. *J Appl Psychol* 89, 334-346.
- Sharot, T., Delgado, M.R., Phelps, E.A., 2004. How emotion enhances the feeling of remembering. *Nat Neurosci* 7, 1376-1380.
- Shaw, J., Porter, S., 2015. Constructing rich false memories of committing crime. *Psychol Sci* 26, 291-301.
- Slotnick, S.D., 2017. Resting-state fMRI data reflects default network activity rather than null data: A defense of commonly employed methods to correct for multiple comparisons. *Cogn Neurosci* 8.
- Slotnick, S.D., Schacter, D.L., 2004. A sensory signature that distinguishes true from false memories. *Nat Neurosci* 7, 664-672.
- Smith, A.P., Henson, R.N., Dolan, R.J., Rugg, M.D., 2004. fMRI correlates of the episodic retrieval of emotional contexts. *Neuroimage* 22, 868-878.
- St-Laurent, M., Abdi, H., Buchsbaum, B.R., 2015. Distributed Patterns of Reactivation Predict Vividness of Recollection. *J Cogn Neurosci* 27, 2000-2018.

- Stark, C.E., Okado, Y., Loftus, E.F., 2010. Imaging the reconstruction of true and false memories using sensory reactivation and the misinformation paradigms. *Learn Mem* 17, 485-488.
- Szpunar, K.K., Watson, J.M., McDermott, K.B., 2007. Neural substrates of envisioning the future. *Proc Natl Acad Sci U S A* 104, 642-647.
- Todd, R.M., Schmitz, T.W., Susskind, J., Anderson, A.K., 2013. Shared neural substrates of emotionally enhanced perceptual and mnemonic vividness. *Front Behav Neurosci* 7, 40.
- Turney, I.C., Dennis, N.A., 2017. Elucidating the neural correlates of related false memories using a systematic measure of perceptual relatedness. *Neuroimage* 146, 940-950.
- Vannucci, M., Mazzoni, G., Marchetti, I., Lavezzini, F., 2012. "It's a hair-dryer...No, it's a drill": misidentification-related false recognitions in younger and older adults. *Arch Gerontol Geriatr* 54, 310-316.
- Wagner, A.D., Shannon, B.J., Kahn, I., Buckner, R.L., 2005. Parietal lobe contributions to episodic memory retrieval. *Trends Cogn Sci* 9, 445-453.
- Wells, G.L., Olson, E.A., 2003. Eyewitness testimony. *Annu Rev Psychol* 54, 277-295.
- Xu, J., Moeller, S., Auerbach, E.J., Strupp, J., Smith, S.M., Feinberg, D.A., Yacoub, E., Ugurbil, K., 2013. Evaluation of slice accelerations using multiband echo planar imaging at 3 T. *Neuroimage* 83, 991-1001.
- Ye, Z., Zhu, B., Zhuang, L., Lu, Z., Chen, C., Xue, G., 2016. Neural Global Pattern Similarity Underlies True and False Memories. *J Neurosci* 36, 6792-6802.

Zhang, W., Gross, J., Hayne, H., 2018. Mood impedes monitoring of emotional false memories: evidence for the associative theories. *Memory*, 1-11.

Zheng, Z., Lang, M., Wang, W., Xiao, F., Li, J., 2018. Electrophysiological evidence for the effects of emotional content on false recognition memory. *Cognition* 179, 298-310.

4.0 EMOTIONAL VALENCE AND SUBJECTIVE RE-EXPERIENCING: AN RTMS STUDY

Manuscript In-Preparation for Submission:

Kark, S.M., Kensinger, E. A., in preparation. Emotional valence and subjective re-experiencing: An rTMS study.

4.1 ABSTRACT

While arousal-based frameworks of emotional memory account for enhancements of negative and positive memories, compared to neutral memories, valence-based accounts highlight the behavioral and neural differences between negative and positive memories. Negative memories tend to be associated with greater memory for the visual detail, compared to positive memories. Recent fMRI work suggests negative valence enhances memory-related activation of the occipito-temporal cortex (OTC). Yet it is unclear if this consistently-observed valence-specific enhancement of OTC is functionally necessary for retrieval or re-experiencing of negative memories. Here, Study 1 examined the effects of valence on subjective re-experiencing of perceptual details (i.e., visual re-experiencing), compared to thoughts and feelings (i.e., internal re-experiencing). In Study 1, participants (n=31) incidentally encoded line-drawings of emotional and neutral photos, followed by the complete photo. The next day, participants completed a surprise recognition memory test in which they were presented with old and new line-drawings. For each line-drawing, participants made an Old/New judgement followed by visual and internal re-experiencing ratings for “Old” responses. In a within-subjects design, Study 2 (n=21) utilized repetitive transcranial magnetic stimulation (rTMS) to test the effects of left OTC inhibition on negative memory re-experiencing, compared to stimulation of the vertex stimulation. Contrary to the hypotheses, negative and positive valence similarly enhanced subjective visual re-experiencing levels, compared to neutral stimuli (Study 1), and inhibitory rTMS applied to the left OTC did not influence retrieval or visual re-experiencing of negative memories (Study 2). The behavioral findings are consistent with

the enhancing effects of arousal on memory re-experiencing, but the rTMS findings suggest that while OTC activity is enhanced for negative memories, it might not be necessary. Future work is needed to understand the nature of the role of enhanced ventral visual stream activation in negative memory.

4.2 INTRODUCTION

A sense of ‘mental time travel’ is a hallmark feature of episodic memory (Tulving, 2002). Yet not all memories are accompanied by an equal sense of re-experiencing. Although many factors can influence the likelihood that an event is re-experienced, emotional valence has been demonstrated to be one key factor that can enhance the sense of re-experiencing (Phelps and Sharot, 2008). Further, valence might differentially influence how we re-experience different aspects of the prior event, such as re-experiencing of our external world (i.e., perceptual or visual details) compared to re-experiencing of our inner world (i.e., thoughts, feelings, reactions). Negative memories in particular have been associated with enhanced visual re-experiencing (Bowen et al., 2018) and enhanced negative memory-related reactivation in visual processing regions, but it is not known if there a *causal* link between visual brain activation and an accompanying sense of visual re-experiencing. Alternatively, retrieval-related activation in visual processing regions aides in—but is not necessary for—negative memory retrieval.

While basic science has historically focused on the contributions of the amygdala and other medial temporal lobe regions to emotionally enhanced memory, a series of functional magnetic resonance imaging (fMRI) studies have reported a consistent activation of the occipito-temporal cortex during successful encoding, early consolidation, and retrieval (Kark and Kensinger, 2015, in press; Kark et al., submitted; Loos et al., 2019; Murty et al., 2011). One particular area of left occipito-temporal cortex (LOTc)—corresponding to the posterior inferior temporal gyrus ($MNI_{xyz}=-50,-56,-10$)—has consistently shown retrieval-related reactivation of encoding processes, a valence-specific link with negative memory recollection, as well as a valence-specific correlation with subjective memory vividness 24 hours after study (Kark and Kensinger, 2015, in press; Kark et al., submitted; Mickley and Kensinger, 2008). However, in our recent study linking LOTc activation with valence-specific negative memory vividness (Kark et al., submitted), external and internal details were collapsed into one set of vividness rating instructions (i.e., use visual details and thoughts, feeling, reactions to rate overall vividness). Thus, it is not possible from those results to decipher if LOTc activity specifically supports visual aspects of memory. Prior work has also demonstrated a positive correlation between retrieval activity in visuocortical areas and the number of episodic details (visual and internal collapsed together) for highly emotional events and life-threatening traumas (e.g., a near plane crash, Palombo et al., 2016). Thus, enhanced activation in visual processing regions is relevant to re-experiencing both laboratory-based and real-life negative memories, but it is not known whether LOTc activity is *causally* linked to the ability to re-experience of the visual aspects of the memoranda.

Transcranial magnetic stimulation (TMS) has proven to be a safe, non-invasive, and effective method for assessing causal links between brain activity and behavior. Using neuro-navigation techniques, TMS can be applied to focal cortical regions of interest (ROI) with high levels of precision, with some level of spatial spreading of the induced electric field depending on the individual's brain anatomy and gyrification (Saturnino et al., 2018). Fifteen minutes of low-frequency (1-Hz) repetitive TMS (rTMS) can inhibit visual cortex for at least ten minutes (Boroogerdi et al., 2000). Previous work has shown that TMS applied to the lateral occipital cortex can disrupt memory for neutral stimuli (Slotnick and Thakral, 2011), including targeted reductions in recollection compared to familiarity (Waldhauser et al., 2016). These findings suggest visual processing regions are in some cases necessary for successful memory retrieval or memory strength. Here, we applied the first use of rTMS in an emotional memory study to examine the necessity of the LOTC in negative memory retrieval and subjective re-experiencing.

The current study utilized a within-subjects design to test the effects of inhibitory effects of low-frequency Hz repetitive (rTMS) applied to the LOTC on the ability to retrieve and re-experiencing negative memories. We used two re-experiencing ratings (visual and internal) to further parse valence and neural effects due to sensory and affective aspects of memory. We modified the line-drawing emotional recognition memory task used in our prior fMRI work and tested the behavioral effects alone in Study 1. In Study 2, we examined the effects of inhibitory rTMS on emotional memory performance re-experiencing to test for *causal* links between brain and behavior.

4.3 METHODS: STUDY 1

The behavioral-only study (Study 1) was conducted at Boston College. The Institutional Review Board of Boston College approved all study procedures and written informed consent was obtained from all participants. Participants were compensated \$10/hour or were awarded course credit for participation in Study 1.

Procedures. The task was a modified version of the line-drawing task previously reported (**Parts I-III**), but with fewer stimuli and additional recognition memory judgements. During encoding, participants viewed line-drawings of negative, positive and neutral photos (1.5 s each) followed by the full colorful photo (3 s, 25 photos of each valence) and indicated if they would “Approach” or “Back Away” from each of the scenes depicted in the images. Participants returned to the laboratory 24-hours later to complete a surprise recognition memory test in which they were shown all of the old line-drawings and an equal number of new line drawings. For each line-drawing (shown for 3 s), participants were asked to indicate if the line-drawing was “Old” by pressing 1 (studied on the previous day) or “New” by pressing 0 (not previously studied on the previous day). For all “New” responses, the program advanced to the next test line-drawing. For all “Old” responses, participants then separately rated Visual Re-experiencing (memory for visual or perceptual details of the original photo) and Internal Re-experiencing (memory for original thoughts, feelings or reactions to the original photo) on a 1-4 scale (1: “None”, 2: “Weak”, 3: “Moderate”, 4: “Strong”). Participants were given up to 3 s to make each of the re-experiencing ratings. The rating order (visual, internal) was alternated across participants. The inter-stimulus interval randomly varied

between 500-6000ms during encoding and 500-2000ms during retrieval. To ensure participants understood the task, they were given a practice version of the encoding and recognition task on Days 1 and 2, respectively.

Stimuli. In order to make meaningful valence comparisons, the subset of 75 stimuli (25 of each valence) selected for the current study were pre-matched using the International Affective Picture System normative data (Lang et al., 2008) such that negative and positive images were similar in absolute valence ($M_{\text{neg}}=2.03$, $SD_{\text{neg}}=0.83$; $M_{\text{pos}}=2.05$, $SD_{\text{pos}}=0.59$; $t(98) = 0.2$, $p=0.86$) and arousal ($M_{\text{neg}}=5.56$, $SD_{\text{neg}}=0.66$; $M_{\text{pos}}=5.48$, $SD_{\text{pos}}=0.59$; $t(98) = 0.68$, $p=0.5$). Negative stimuli were more arousing ($M_{\text{neut}}=3.19$, $SD_{\text{neut}}=0.57$; $t(98) = 16.83$ $p<0.001$) and of higher absolute valence ($M_{\text{neut}}=0.39$, $SD_{\text{neut}}=0.31$; $t(98) = 13.16$, $p<0.001$) than neutral stimuli and positive stimuli were more arousing ($t(98) = 16.88$, $p<0.001$) and of higher absolute valence ($t(98) = 17.75$, $p<0.001$) than neutral stimuli.

Participants. Of the thirty-four participants who completed the encoding task, three (1 female) did not return on the second day to complete the recognition memory task. Thirty-one participants completed the recognition memory study (aged 19-25, $M = 20.19$, $SD = 1.35$, 22 females). All participants were healthy, young adult native speakers of English without a history of neurological disorders, head injury, learning disorders, psychiatric problems, or current medications affecting the central nervous system. Participants reported normal or corrected-to-normal vision.

4.4 RESULTS: STUDY 1

The descriptive statistics for each memory measure are listed in Table 1.

Memory performance. Overall recognition memory performance (d') was higher ($M = 1.19$, $SD = 0.32$) than in the previous 24-hr delay fMRI version of the study ($M = 0.74$, $SD = 0.33$, in Kark and Kensinger, in press), likely due to halving the number of study stimuli. Negative memory performance was similar to positive ($t(30)=1.6$, $p=0.12$) and neutral ($t(30)=0.51$, $p=0.61$), but positive memory performance was significantly higher than neutral memory performance ($t(30)=2.23$, $p=0.03$). However, these findings are broadly consistent with the fMRI studies that have used this recognition memory task, which have found memory performance for positive to be numerically greater than negative and neutral memory performance (Kark and Kensinger, 2015, in press).

Re-experiencing ratings by accuracy. On average, participants false alarmed to 18.2% of the objectively New line-drawings, which left very few false alarm trials for analysis of false re-experiencing as a function of valence in the full sample of thirty-one participants (but see *False memory re-experiencing by valence*). Collapsed across valence, a 2x2 repeated-measured analysis of variance (rm-ANOVA) with factors of re-experiencing type (visual, internal) and memory accuracy (hits, false alarms) revealed a main effect of re-experiencing type (visual, internal), $F(1,30)=7.72$, $p=0.009$, $\eta^2=0.21$, indicating greater visual re-experiencing, compared to internal re-experiencing across true and false memories ($M_{\text{visual}} = 2.82$, $SE_{\text{visual}} = 0.08$; $M_{\text{internal}} = 2.54$, $SE_{\text{internal}} = 0.07$), and a main effect of memory accuracy ($F(1,26) = 114.3$, $p<0.001$, $\eta^2=0.79$), indicating greater re-experiencing for true memories, compared to false memories ($M_{\text{true}} = 2.96$,

$SE_{\text{true}} = 0.06$; $M_{\text{false}} = 2.39$, $SE_{\text{false}} = 0.06$). There was a trend toward an accuracy-by-re-experiencing type interaction ($F(1,30) = 4.06$, $p = 0.053$, $\eta^2 = 0.12$) associated with a greater boost in visual re-experiencing over internal re-experiencing for true memories ($M_{\text{visual-internal}} = 0.41$), compared to false memories ($M_{\text{visual-internal}} = 0.14$) and levels of visual and internal re-experiencing were not statistically different for false memories ($t(30) = 1.03$, $p = 0.31$). These findings are consistent with an fMRI study using a similar paradigm that found greater vividness for true memories, compared to false memories (Kark, Slotnick, and Kensinger, submitted), and further suggests that enhanced re-experiencing of perceptual details over internal details is unique to true memories.

Effect of valence on re-experiencing rating for remembered items. Next, we tested for valence-specific effects of re-experiencing type, with the prediction that negative memories would be associated with the greatest sense of visual re-experiencing, compared to neutral and positive memories. Average re-experiencing ratings for hits for each participant were entered into a 2x3 rm-ANOVA with factors of re-experiencing type (visual, internal) and valence (negative, positive, neutral). Results revealed a main effect of re-experiencing type ($F(1,30) = 20.68$, $p < 0.001$, $\eta^2 = 0.41$), a main effect of valence ($F(2,60) = 13.48$, $p < 0.001$, $\eta^2 = 0.31$), and a re-experiencing type-by-valence interaction ($F(2,60) = 8.25$, $p = 0.001$, $\eta^2 = 0.22$) (average and individual values are shown in Figure 1). As in the previous section, the main effect of re-experiencing type again demonstrated that visual re-experiencing was stronger than internal re-experiencing ($M_{\text{visual}} = 3.23$, $SE_{\text{visual}} = 0.07$; $M_{\text{internal}} = 2.91$, $SE_{\text{internal}} = 0.08$; $t(30) = 4.5$, $p < 0.001$) across valence categories. The main effect of valence demonstrated similar levels of

enhanced re-experiencing of negative and positive memories, compared to neutral memories ($M_{\text{neg}} = 3.13$, $SE_{\text{neg}} = 0.08$; $M_{\text{neut}} = 2.75$, $SE_{\text{neut}} = 0.07$; $M_{\text{pos}} = 3.01$, $SE_{\text{pos}} = 0.07$; Negative compared to Neutral: $t(30) = 4.96$, $p < 0.001$; Positive compared to Neutral: $t(30) = 4.4$, $p < 0.001$; Negative compared to Positive: $t(30) = 1.4$, $p = 0.18$). The interaction was driven by bigger differences between visual and internal re-experiencing ratings for neutral and positive memories, compared to negative memories (i.e., Visual-Internal differences: Neutral>Positive>Negative). Thus, an accompanying sense of internal re-experiencing drops off precipitously for neutral stimuli and to a lesser extent for positive stimuli, compared to negative stimuli. Contrary to the predicted effect, visual re-experiencing was similarly enhanced for negative and positive stimuli, compared to neutral stimuli (Negative compared to Neutral: $t(30) = 3.2$, $p = 0.003$; Positive compared to Neutral: $t(30) = 3.0$, $p = 0.006$; Negative compared to Positive: $t(30) = 0.3$, $p = 0.77$). As similar pattern was observed for internal re-experiencing (Negative compared to Neutral: $t(30) = 5.01$, $p < 0.001$; Positive compared to Neutral: $t(30) = 4.6$, $p < 0.001$; Negative compared to Positive: $t(30) = 1.8$, $p = 0.08$). Together, these findings are consistent with emotionally enhanced memory and do not reveal valence-specific effects of subjective visual-reexperiencing.

Analysis of the reaction times to make the re-experiencing rating judgements returned no main effects of re-experiencing type ($F(1,30) = 1.17$, $p = 0.29$, $\eta^2 = 0.04$) or valence ($F(2,60) = 1.14$, $p = 0.33$, $\eta^2 = 0.04$) or an interaction ($F(2,60) = 0.94$, $p = 0.40$, $\eta^2 = 0.03$) (see Table 1). These data suggest that participants are similarly confident in

their re-experiencing judgments and there are no time-on-task confounds (i.e., no difference in duration it takes to make an internal vs. visual re-experiencing judgment).

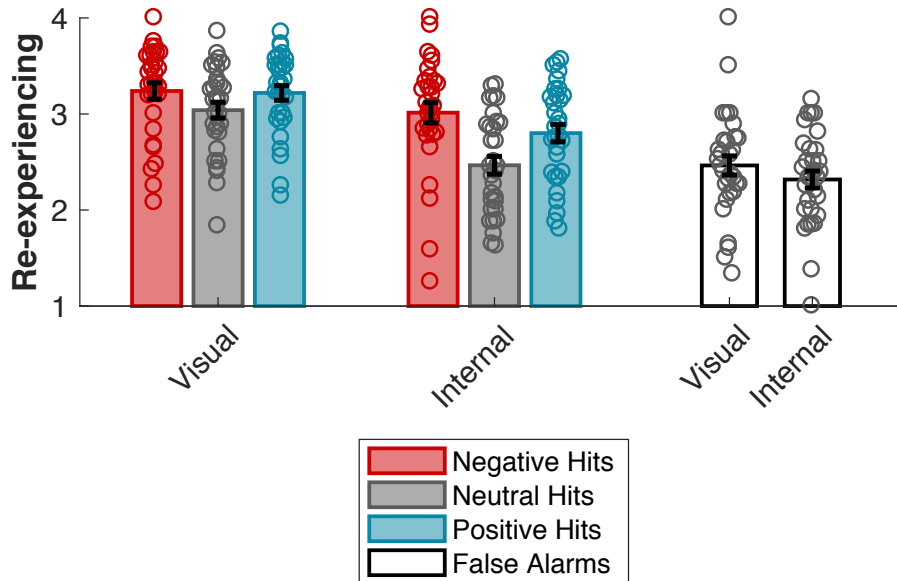


Figure 1. Study 1 visual and internal re-experiencing ratings for hits by valence and response type for the full sample (n=31). Re-experiencing ratings for false alarms collapsed across valence are shown in black and white. Error bars represent 1 standard error of the mean.

False memory re-experiencing by valence. A subset of twenty-two participants had at least two false alarms per valence category (Number of false alarms: $M_{\text{neg}} = 4.7$, $M_{\text{neut}} = 5.6$, $M_{\text{pos}} = 6.6$) for analysis of false memory re-experiencing ratings by valence and re-experiencing type. Re-experiencing ratings were entered into a 2x3 rm-ANOVA with factors of re-experiencing type (visual, internal) and valence (negative, positive, neutral). Results returned a was main effect of valence ($F(2,42) = 3.78$, $p = 0.03$, $\eta^2 = 0.15$)—with greater overall false re-experiencing of negative stimuli, compared to positive and neutral stimuli ($M_{\text{neg}} = 2.51$, $M_{\text{neut}} = 2.26$, $M_{\text{pos}} = 2.29$)—and a trend toward a re-experiencing type-by-valence-interaction ($F(2,42) = 3.04$, $p = 0.06$, $\eta^2 = 0.13$), driven

by reduced internal re-experiencing of neutral and positive stimuli, relative to negative internal re-experiencing (see Figure 2). Visual re-experiencing was similarly higher than internal re-experiencing across valences ($ps > 0.09$)¹, but negative false memories were also accompanied with a significantly greater sense of internal re-experiencing than neutral stimuli ($t(21) = 2.82, p = 0.01$) and a numerically greater sense of internal re-experiencing than positive stimuli ($t(21) = 2.01, p = 0.06$). These findings suggest visual re-experiencing similarly accompanies false memories, but that negative valence additionally enhances the false sense of re-experiencing thoughts or feelings.

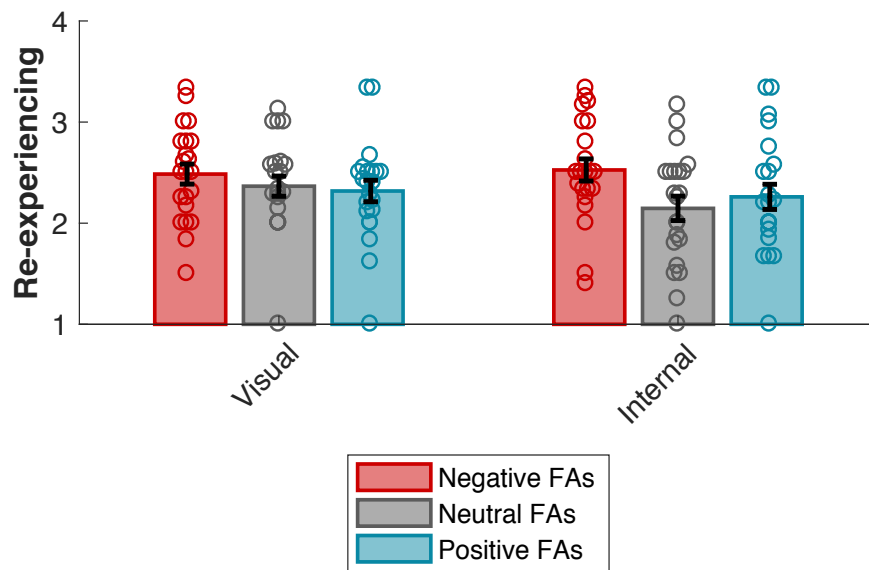


Figure 2. Study 1 visual and internal re-experiencing ratings for false alarms by valence and response type for a subset of participants (n=22). Error bars represent 1 standard error of the mean.

¹ However, analysis of visual re-experiencing ratings by accuracy (hits, false alarms) only showed a trend toward an accuracy-by-valence interaction ($F(1,21) = 2.93, p = 0.10, \eta^2 = 0.12$).

4.5 METHODS: STUDY 2

Participants. Twenty-nine participants were recruited to participate in the rTMS study. There was no overlap in the participant pool between Study 1 and Study 2. In addition to meeting the criteria outlined for Study 1 participants, Study 2 rTMS participants were additionally screened for contraindicators for the MRI environment and rTMS. Participants were administered the Transcranial Magnetic Stimulation Safety Screening Form (adapted from Keel et al., 2001; Rossi et al., 2011). Exclusion criteria were: Metal in the brain or body, potential for pregnancy, left-handedness, recent jetlag, or history of epilepsy or seizure (either personal or first-degree relative), migraines or frequent headaches, tinnitus, or fainting spells or syncope. Participants were additionally instructed to avoid alcohol consumption within 24 hours of their rTMS appointment and caffeine with 2 hours of rTMS appointment. Study 2 participants were compensated \$25/hour for their time.

Of the twenty-nine participants enrolled, data from four participants were removed from all analyses: One participant (22, male) did not return for the recognition task on Day 2, one participant (21, male) could not tolerate TMS and withdrew from the study, one (25, male) participant did not complete the memory task correctly (only gave “Old” responses), and one participant (23, female) was not considered in any between-subject analyses of the first retrieval block, as they did not tolerate the LOTC stimulation. Data from the remaining twenty-five participants were also considered for between-subject analyses of the first retrieval block (n=11 LOTC stimulation, n=14 Vertex stimulation). Four additional participants (2 females) included in the between-subject

analysis (Vertex stimulation first) were not entered into the within-subject analyses due to inaccuracies of LOTC stimulation (n=3) or technical failure of the second TMS session (1 female). In total, the principal within-subjects data analyses included data for twenty-one participants (7 males, 14 females; 11 Vertex first, 10 LOTC first).

Stimuli. The IAPS images and line-drawings were the same as those used in Study 1, except the removal of one image per valence category for the encoding stimuli (24 images/valence presented during encoding) and six line-drawings at retrieval such that each of the two retrieval blocks preceded by rTMS would have an even number of stimuli (72 stimuli per block: 12 Old and 12 New for each valence category).

MRI Acquisition and Processing. An anatomical MRI was required for neuro-navigated TMS and a resting-state fMRI was also acquired when time allowed. The MRI anatomical and resting state acquisition parameters have been described elsewhere (Kark and Kensinger, in press). For most participants, the MRI data were acquired on Day 1 either before or after the encoding task. Six of the twenty-five participants (4 females) already had a recent anatomical and resting state scan on file and did not undergo those procedures again. The anatomical images were registered to Montreal Neurological Institute (MNI) space using SPM8 (Wellcome Department of Cognitive Neurology, London, United Kingdom) implemented in MATLAB 2014a (The MathWorks, Natick, MA). The transformation matrix outputted from the MNI-registration process was used to back-transform the LOTC ROI (MNI_{xyz} = -50, -56, -10) into each participant's native space (see MNI space cluster Figure 3, left, and an example participant in Figure 3, right). In their native space, the ROI cluster was used to identify the LOTC posterior

inferior temporal gyrus ROI and the stimulation targeted the gyral crown. An additional subpeak (MNI_{xyz}=-52,-56,-18) with a larger cluster extent was also used to guide setting the target on the gyral crown.

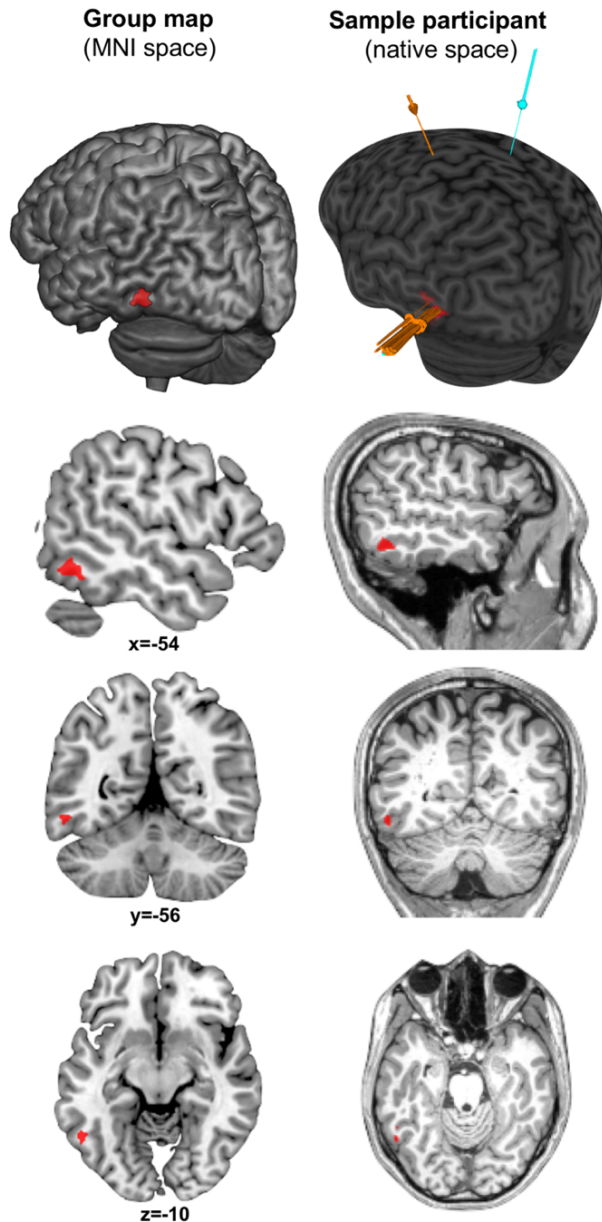


Figure 3. Visualization of the LOTC ROI in MNI space (left column) and in native space of a sample participant (right column), shown in red. The 3D full curvilinear reconstruction of a participant's brain in the top right corner also shows the TMS pulses (orange lines) applied to back-transformed ROI into their native space (shown in red). The cyan line depicts the vertex target position and other orange line points to the motor hotspot along the precentral gyrus.

Procedures. As in Study 1, participants completed the incidental encoding task approximately 24 hours before a surprise recognition memory session, this time held at Harvard CBS. On Day 1, participants completed consent and screening forms, the encoding practice and task, and underwent a brief 30-minute MRI scan (approximately a 1.5-hour time commitment). On Day 2, participants completed two rTMS sessions and the memory tasks (approximately a 4-hour time commitment). On Day 2, participants began with instructions and a practice version of the recognition memory task. After co-registration and motor thresholding (see *Neuronavigated rTMS*), participants completed the recognition memory task split between two sessions: One session preceded by rTMS to the Vertex (control region) and the other preceded by rTMS to the LOTC region. The stimulation order was alternated across participants. Immediately following each rTMS session, participants moved across the testing room from the rTMS chair to the testing computer to begin the recognition task. Before beginning the task, participants briefly rated the discomfort associated with the rTMS (1-no discomfort, 10-high discomfort; Koen et al., 2018) and their current level of sleepiness² (Stanford Sleepiness Scale [SSS]; Hoddes et al., 1972). On average, the retrieval task took approximately 4 minutes for participants to complete (range: 2-7 minutes, mode=5 minutes). After the recognition blocks, participants were given a 45-minute break in the waiting room to allow the effects

² The SSS rating scale was administered to n=20 and the discomfort rating scale to n=17. There were no significant differences in sleepiness after LOTC stimulation compared to Vertex stimulation ($M_{\text{LOTC}}=2.9$, $SD_{\text{LOTC}}=1.5$; $M_{\text{vertex}}=2.73$, $SD_{\text{vertex}}=1.0$; $t(14)=0.49$, $p=0.63$) or between the first and second sessions of the day ($M_{\text{first}}=2.93$; $M_{\text{second}}=2.67$; $p=0.33$). However, participants found LOTC stimulation to be significantly more uncomfortable than Vertex stimulation ($M_{\text{LOTC}}=5.4$, $SD_{\text{LOTC}}=2.66$; $M_{\text{vertex}}=3.53$, $SD_{\text{vertex}}=1.69$; $t(15)=2.84$, $p=0.01$). This was not surprising, given the majority of participants experienced twitching with each pulse in the facial and/or neck muscles. However, the degree of difference in Negative d' between the two stimulation sites was not linked differences in sleepiness or discomfort ($ps>0.6$).

of rTMS dissipate before the procedures were repeated for the second rTMS session. During the break periods, participants were instructed to not nap and were allowed to snack, read, work, or watch a TV series.

Perceptual matching control task. To ensure inhibitory rTMS of the LOTC did not interfere with *perception* of the line-drawing retrieval cues, participants completed twelve brief trials of a line-drawing matching task during both retrieval block³. In this control task, participants were presented with a line-drawing at the top of the computer display with two line-drawings of the same size displayed below (see example trials in Figure 4). Participants were instructed to decipher as quickly and accurately as possible if the line-drawing on the top matched one of the test line-drawings on the bottom (press “1” to indicate the match was on the left, “press 2” if the match is on the right). For 25% of trials, there was no match, in which case participants were instructed to press “0”. All of the line-drawings in the matching task were completely extraneous to the memory tasks. To make the task more challenging, line-drawings within a match trial were equated for edge density so that judgements could not be made based on the amount of visual detail available. Edge density was also matched across retrieval blocks, to ensure that one matching block was not more difficult than the other. Matching task performance was computed as the percent correct for each block and compared between retrieval

³For the majority of participants, these twelve trials occur consecutively at the beginning of each recognition block. However, the first six participants in the study completed these trials interleaved with memory trials throughout the retrieval blocks. The procedures were changed to limit the possibility of introducing a set-shifting burden that was not present in Study 1.

blocks (LOTC and vertex) to confirm that any memory-related effects were not due to differences in low-level visual processing effects of no interest.

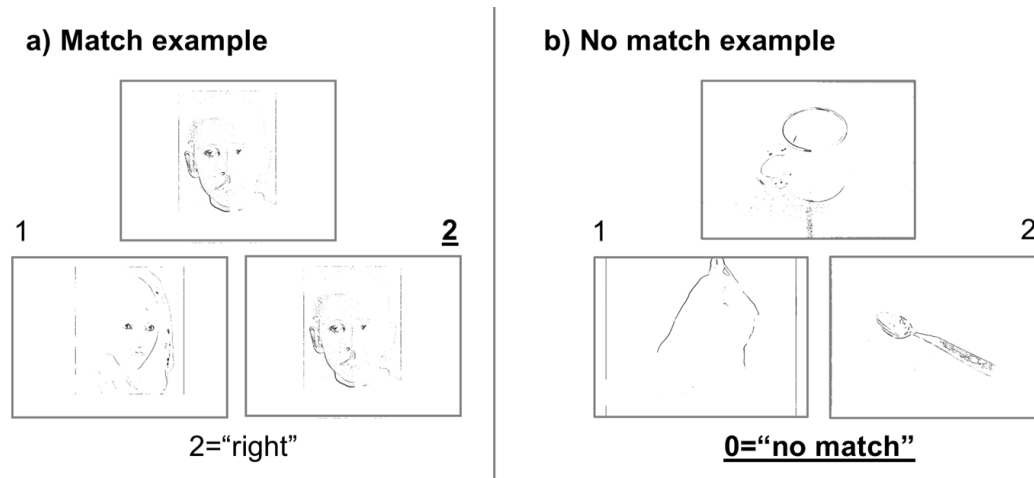


Figure 4. Perceptual matching control task. For each of the twelve trials that preceded the onset of the recognition memory tasks, participants were instructed to decide if the line-drawing shown central in the top row matched one of the two line-drawings displayed in the second row. **4A)** For example, if the matching line-drawing was on the right, participant's pressed "2". **4B)** If there was no matching line-drawings (25% of trials), participants pressed "0".

Neuronavigated rTMS.

Equipment and co-registration. Frameless stereotactic neuronavigation procedures were carried out at Harvard CBS using a MagPro X100 with MagOption Magnetic Stimulator (MagVenture Inc., Alpharetta, GA) in conjunction with theBrainsight 2 Neuronavigation System (Rogue, Montreal, Canada) and a Polaris infrared camera (Northern Digital Inc). Repetitive TMS was delivered using a MagVenture Cool-B65 A/P dynamic cooled butterfly coil, which is optimized for high repetition rates and long pulse trains. Motor threshold pulses were applied using a MagVenture C-B60 butterfly coil.

For co-registration, participants were fitted with a Velcro headband with three infrared position sensors. Using common co-registration reference points (i.e., tip of nose, nasion, intertragal notches), participants were co-registered to their individual anatomical image and 3D reconstructions of their brain and scalp using a tracked-pointer tool. Following the initial co-registration, additional points were added across the scalp to increase the accuracy of co-registration until it was within a target range of 2-3mm.

Motor threshold and stimulator intensity. Stimulator intensity was individualized using the motor threshold by measuring motor-evoked potentials (MEPs)—the minimum intensity that can induce motor evoked potentials 50% of the time—as defined by the International Committee of Clinical Neurophysiology (Rossini et al., 1994; Rossini et al., 2015). MEPs were recorded using an EMG amplifier in conjunction with PowerLab (ADInstruments). The mean motor threshold was 58% of maximum output ($SD = 12.4\%$, range: 41-79). For safety and comfort, stimulator intensity was capped at a maximum of 75% output, which was also the default stimulation intensity if no motor threshold was detected at 75% maximum output (as was the case for $n=6$ of the within-subject analysis participants). When necessary, the stimulator intensity was also adjusted if a participant experienced excessive discomfort related to facial twitching when a sample pulse was applied to LOTC before the onset of rTMS. On average, stimulation intensity for the within-subject sample was set to $M = 64.9\%$ ($SD = 9.2\%$, range: 48-75%), which on average corresponded to 119% of their individual motor thresholds ($SD = 3.4\%$, range: 110-120%).

Stimulation targets and protocol. The LOTC stimulation target was set such that the coil was approximately perpendicular to the skull and the coil handle was positioned posteriorly and upward approximately 45° above the horizontal, with minor adjustments ($\pm 15^\circ$) to ensure the TMS coil was not pressing on the participant's ear. The vertex was chosen as the control stimulation site—as it is assumed to not participate in memory processes (Koen et al., 2018; Thakral et al., 2017)—and was defined anatomically at the intersection of the central sulcus with the longitudinal fissure. For vertex stimulation, the coil was held approximately perpendicular to the scalp in the upright position (i.e., the coil handle toward the back of the head).

Each of the two separate stimulation sessions (LOTC and vertex control) consisted of 12-17 minutes of stimulation at a low frequency (1 Hz), which is common stimulation frequency that has shown to decrease cortical excitability in visual cortex (Boroojerdi et al., 2000). Given the length of the retrieval task (~5 minutes), participants were required to have at least 12 minutes⁴ of accurate stimulation (within 3mm of the target). On average, 98.5% ($SD = 3\%$) of pulses were delivered within 3 mm of the target locations on the scalp surface. Average distance from the target during stimulation was minimal (Vertex: $M = 0.64\text{mm}$, $SD = 0.26\text{mm}$; LOTC: $M = 0.87\text{mm}$, $SD = 0.31\text{mm}$) but was significantly lower for vertex stimulation, compared to LOTC stimulation ($p = 0.01$).

⁴ The aim was to stimulate for 17 minutes, but some participants could not tolerate the feeling of the TMS pulses longer than 12 minutes. Since the recognition task blocks took ~5 mins or less to complete, any participant with more than 12 minutes of useable TMS points were included in the analysis. Given that 15 minutes of 1 Hz TMS can inhibit visual cortex for up to 10 minutes (Boroojerdi et al., 2000), 12 minutes of rTMS should inhibit visual cortex for up to ~8 minutes.

Average angular and twist error were similar between the two stimulation sites ($ps > 0.14$)

Dependent variables.

The analyses focus on the dependent variables that address the *a priori* hypotheses that LOTC stimulation modulates the: 1) Likelihood of bringing a negative memory to mind (memory performance as calculated by $d'=[z(\text{HitRate})-z(\text{FalseAlarmRate})]$), 2) Strength of re-experiencing the visual details (average visual and internal re-experiencing ratings), and 3) Confidence in memory-related judgements (reaction times to make the Old/New and re-experiencing rating judgements).

4.6 RESULTS: STUDY 2

Contrary to our predictions, there were no effects of LOTC stimulation, compared to vertex, across any of the memory measures. The descriptive statistics for each measure and stimulation site are listed in Table 1.

Perceptual matching task. Study 2 included an additional perceptual matching task, to ensure LOTC inhibitory TMS did not influence the ability to make perceptual matching judgements of line-drawings that were completely extraneous to the recognition memory task. Seventeen out of twenty-one participants scored 100% on both blocks of the matching task (Vertex: $M = 98\%$, $SD = 5\%$; LOTC: $M = 99\%$, $SD = 3\%$) and there was no significant performance difference between the two stimulation sites ($p = .08$).

These findings suggest LOTC stimulation did not impair perceptual abilities, compared to vertex stimulation.

Memory performance. Results of a 2x3 rm-ANOVA with factors of stimulation site (LOTC, vertex) and valence (negative, neutral, positive) revealed no main effects of stimulation site ($F(1,20) = 0.68, p = 0.42, \eta^2 = 0.03$), valence ($F(2,40) = 0.76, p = 0.48, \eta^2 = 0.04$), or a stimulation site-by-valence interaction ($F(2,40) = 0.39, p = 0.68, \eta^2 = 0.02$) on memory performance. The results of nine paired sample *t*-tests also returned no significant effects of stimulation site or valence on memory performance (all $ps > 0.2$). A follow-up between-subjects analysis was conducted using behavioral data from each participant's first stimulation site of Day 2. Results of a mixed repeated-measures ANOVA with a between-subjects factor of first stimulation site (LOTC, vertex) and a within-subject factor of valence (negative, neutral, positive) also returned no effect of valence ($F(2,46) = 0.75, p = 0.48, \eta^2 = 0.03$) or a valence-by-stimulation site interaction ($F(2,46) = 0.63, p = 0.39, \eta^2 = 0.03$). Individual independent samples *t*-tests comparing participants based on first stimulation site (LOTC, vertex) also returned no differences in d' across the valences ($ps > 0.4$).

In Study 2, overall memory performance in the TMS environment at Harvard CBS ($M = 1.22, SD = 0.32$) was similar to the performance level observed in Study 1 in the laboratory at Boston College without TMS ($M = 1.12, SD = 0.32$). Although positive memory performance did not exceed that of neutral for either stimulation condition in Study 2 ($ps > 0.4$), a mixed rm-ANOVA with a between-subject factor of group (study 1, study 2) and a within-subjects factor of valence (negative, neutral, positive) returned no

evidence of a main effect of valence ($F(2,100) = 2.24, p = 0.11, \eta p^2 = 0.04$) or valence-by-group interaction ($F(2,100) = 0.74, p = 0.48, \eta p^2 = 0.02$). Taken together, these findings suggest similar levels of memory performance across Studies 1 and 2 and that inhibitory LOTC stimulation did not alter memory discriminability (d'), compared to Vertex stimulation⁵.

Despite a null effect of stimulation site, there was quite a bit of variability across participants (see individual data lines in Figure 5), with eleven participants showing a numerical reduction in Negative d' associated with LOTC stimulation, compared to Vertex⁶. This raises the intriguing possibility that other factors influence the effect of LOTC inhibition on emotional memory retrieval (e.g., individual differences in intrinsic connectivity of the stimulation site, trait emotional memory biases, or the spatial distribution of the induced electric field, see *Discussion*).

⁵ Follow-up repeated measures ANOVA also confirmed no effect of stimulation site on normalized criterion (c/d') ($ps > 0.2$), suggesting rTMS site does not modulate the willingness to indicate a stimulus is Old or New, although there was a pattern of a more conservative response bias for negative and neutral stimuli overall and a drop toward a more conservative value following LOTC stimulation.

⁶ Follow-up analyses suggest the degree of difference in Negative d' between the two stimulation sites ($\text{Negdprime}_{\text{vertex}} - \text{Negdprime}_{\text{LOTc}}$) was not linked with the intensity of the TMS stimulation ($r(21)=0.30, p=0.18$).

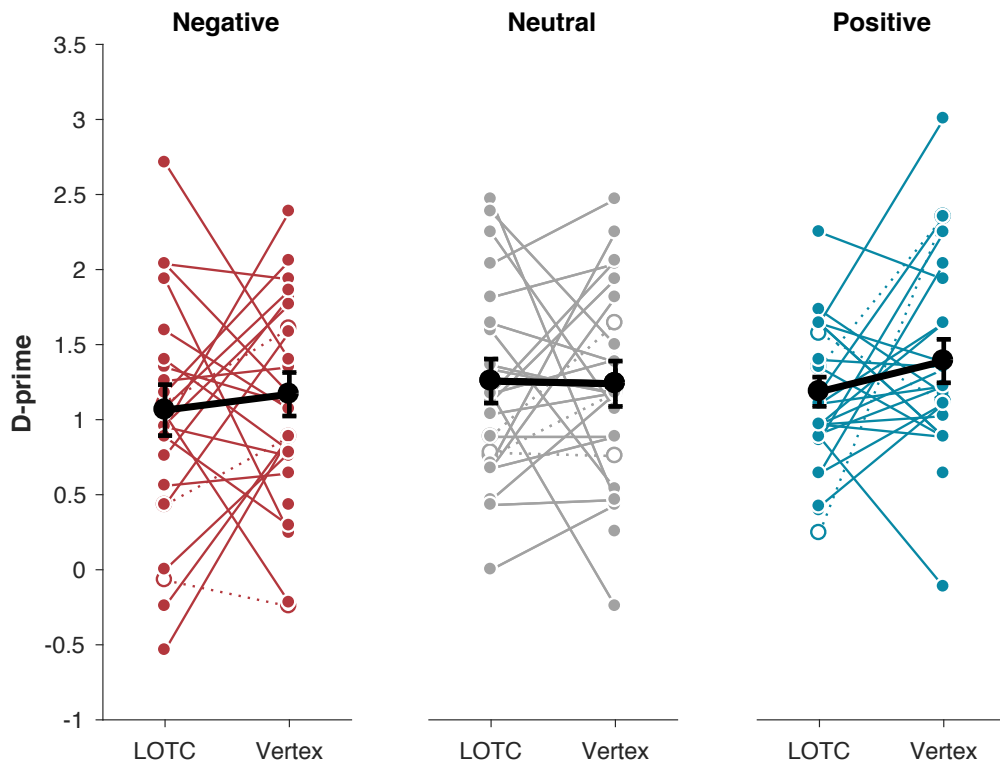


Figure 5. Average d-prime memory performance values by valence and rTMS stimulation site (plotted in black). Individual data points are shown behind the means. The three participants with a modified stimulation site (i.e., moved more superior or posterior of the ear and out of the LOTC) are indicated with open circles and dotted lines. Error bars represent 1 standard error of the mean.

Re-experiencing ratings by accuracy. As in Study 1, there was a main effect of accuracy ($p < 0.001$) in Study 2 reflecting greater re-experiencing of true memories, compared to false memories. There was also no accuracy-by-stimulation site interaction ($p = 0.51$), suggesting TMS did not influence the re-experiencing levels of false memories. There were not a sufficient number of false alarms to analyze false re-experiencing by re-experiencing type, stimulus site, and valence (i.e., only 8 participants had enough trials to conduct a repeated-measures ANOVA).

Effect of valence on re-experiencing rating for remembered items by stimulation site. Re-experiencing ratings for hits were entered in a 2x2x3 rm-ANOVA with factors of stimulation site (LOTc, vertex), re-experiencing rating type (visual, internal), and valence (negative, neutral, positive). Results returned a significant main effect of valence ($F(2,40) = 9.86, p < 0.001, \eta^2 = 0.33$) qualified by a valence-by-re-experiencing rating type interaction $F(2,40) = 7.21, p = 0.002, \eta^2 = 0.27$). Aside from a trend toward a stimulation site-by- re-experiencing rating type interaction ($F(1,20) = 4.1, p = 0.06, \eta^2 = 0.17$) (due to *increased* visual compared to internal re-experiencing with LOTc stimulation, $t(20) = 2.4, p=0.024$, but not with vertex stimulation, $t(20) = 0.4, p = 0.68$) there were no effects of stimulation site on the re-experiencing ratings (see average and individual data in Figure 6). A similar pattern was returned by a mixed ANOVA with a between-subjects factor of study group (study 1, study 2) and within-subjects' factors of valence, and re-experiencing type (visual, internal). However, a re-experiencing type by group interaction ($F(1,50) = 5.2, p = 0.03, \eta^2 = 0.09$) was driven by greater visual re-experiencing in Study 1 compared to Study 2 ($t(50) = 2.0, p = 0.048$, independent samples *t*-test) and greater visual compared to internal re-experiencing in Study 1 compared to Study 2 ($t(30) = 4.5, p < 0.001$, paired samples *t*-test). Unlike Study 1, visual and internal re-experiencing did not differ in Study 2 ($F(1,20) = 1.9, p = 0.18, \eta^2 = 0.09, t(20)=1.4, p=0.2$, paired samples *t*-test). These data suggest that either the TMS itself or the TMS environment was associated with reduced visual re-experiencing.

Previous work has shown that TMS of early visual cortex can drive memory confidence (Karanian and Slotnick, 2018). In the current study, there was interaction

between stimulation site and re-experiencing accuracy (hits, false alarms), $F(1,19) = 0.45$, $p = 0.51$, $\eta^2 = 0.02$, suggesting no effect of TMS site on overall greater re-experiencing for true compared to false memories. Average false memory visual and internal re-experiencing ratings were similar across Study 1 and Study 2 re-experiencing ($ps > 0.4$, independent samples t -tests) and between re-experiencing rating types ($ps > 0.15$, paired samples t -tests).

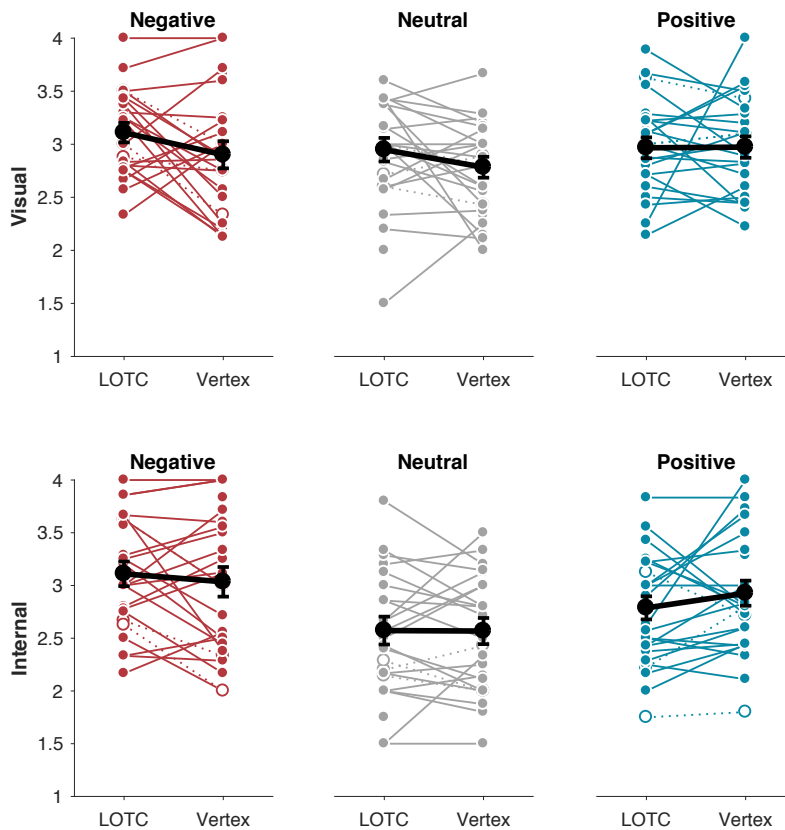


Figure 6. Average re-experiencing ratings by valence, re-experiencing type, and stimulation site (plotted in black). Individual data points are shown behind the means. The three participants with a modified stimulation site (i.e., moved more superior or posterior of the ear and out of the LOTC) are indicated with open circles and dotted lines. Error bars represent 1 standard error of the mean.

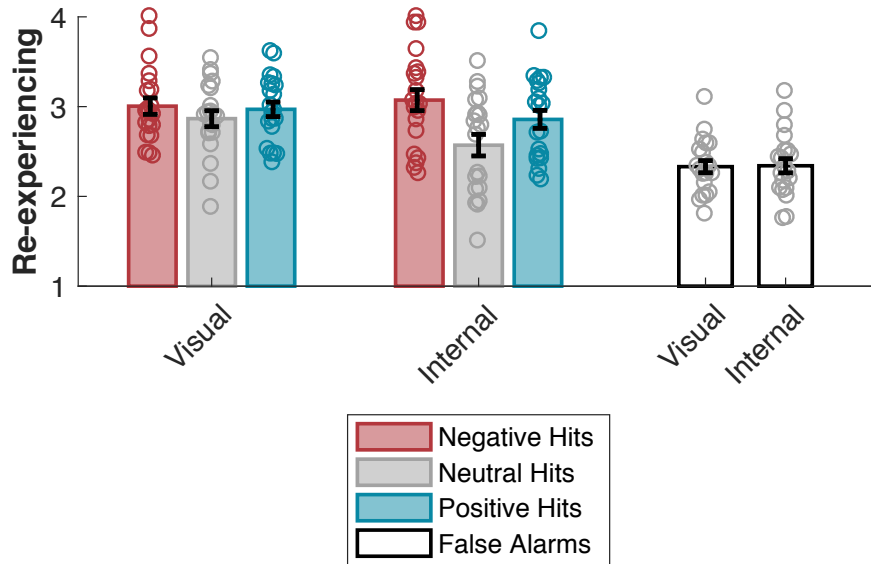


Figure 7. Study 2 average and individual re-experiencing ratings by valence and rating collapsed across stimulation site. Error bars represent 1 standard error of the mean.

Reaction times. There were no effects of stimulation site on reaction times to make the Old/New judgements ($ps > 0.21$) or re-experiencing ratings ($ps > 0.17$). A significant valence by re-experiencing type interaction ($F(2,40) = 8.83, p = 0.001, \eta^2 = 0.31$) reflected more rapid internal re-experiencing responses to negative stimuli than neutral ($t(20) = 3.5, p = 0.002$) and positive internal re-experiencing ($t(20) = 3.0, p = 0.007$), which were similar ($t(20) = 0.13, p = 0.90$). Emotional visual re-experiencing reaction times were equally slower than neutral re-experiencing ratings ($t(20) = 0.25, p = 0.02$).

Taken together, these results suggest no group effects of LOTC stimulation on negative memory performance, re-experiencing, or reaction times.

Table 1. Descriptive statistics of memory measures and reaction times for Study 1 and Study 2. Mean (SD) by study and stimulation site.

<i>Outcome measure</i>	<i>Valence</i>	Study 1	Study 2		
		n=31	n=21		
		no TMS	LOTIC	Vertex	
Memory Measures					
<i>D-prime</i>	Neg	1.15 (0.41)	1.06 (0.78)	1.17 (0.66)	
	Neut	1.10 (0.41)	1.26 (0.67)	1.24 (0.69)	
	Pos	1.32 (0.53)	1.19 (0.45)	1.39 (0.66)	
<i>Re-experiencing</i>	Visual	Neg	3.24 (0.09)~	3.11 (0.42)	2.90 (0.59)
		Neut	3.04 (0.08)	2.95 (0.51)	2.78 (0.45)
		Pos	3.22 (0.08)*	2.97 (0.45)	2.97 (0.46)
		False Alarms	2.45 (0.11)	2.37 (0.31)	2.30 (0.39)
	Internal	Neg	3.01 (0.59)	3.11 (0.54)	3.03 (0.64)
		Neut	2.47 (0.52)	2.57 (0.61)	2.57 (0.57)
		Pos	2.80 (0.51)	2.79 (0.50)	2.93 (0.55)
		False Alarms	2.48 (0.68)	2.31 (0.30)	2.39 (0.53)
Reaction Times					
<i>Re-experiencing</i>	Visual	Neg	772 (364)***	1067 (344)	1141 (442)
		Neut	806 (394)*	1021 (365)	1026 (349)
		Pos	752 (353)***	1077 (358)	1174 (425)
	Internal	Neg	827 (352)	1000 (381)	979 (452)
		Neut	872 (389)~	1064 (349)	1097 (471)
		Pos	866 (340)*	1089 (334)	1063 (477)

Independent samples comparison between Study 1 and the stimulation-site collapsed values from Study 2 ($p < 0.05$, *** $p < 0.01$).

4.7 DISCUSSION

The present two-part study examined 1) the effect of valence on the subjective sense of visual and internal re-experiencing and 2) utilized rTMS to examine the effects of occipito-temporal inhibition on retrieval and re-experiencing of negative memories. The aim of Study 1 was to test the effect of valence on visual and internal memory re-experiencing. Contrary to our predictions, negative and positive memories showed similar levels of enhanced subjective visual re-experiencing, compared to neutral memory visual re-experiencing. Next, we examined the effect rTMS to the posterior inferior temporal gyrus—an area of LOTC that has shown consistent valence-specific effects in a series of fMRI studies—compared to stimulation of the vertex. Contrary to the hypothesized effect, we found no evidence for a neuromodulatory effect of stimulation site on objective or subjective memory overall or as a function of valence. The current findings suggest that while the LOTC activation has consistently been *correlated* with negative memory formation and retrieval, it might not be *necessary* to bring negative memories to mind. Future work is needed to determine the importance of this particular LOTC ROI in negative memory retrieval.

Behaviorally, we also did not find evidence for valence-specific enhancement of negative visual re-experiencing. However, it is possible that subjective levels of re-experiencing can be similar but the *content* of the negative and positive memoranda might vary by valence. Objective measures of visual specificity or precision might be needed to reveal valence-specific effects of subjective visual re-experiencing that could also be modulated by LOTC-rTMS (see *General Discussion* of this dissertation).

The LOTC ROI was chosen from the overlap of several statistic maps from fMRI studies linking activation in this area with successful memory formation, retrieval, and a valence-specific correlation with vividness (Kark and Kensinger, 2015, in press; Kark et al., submitted). Given the number of free parameters in TMS experiments (e.g., stimulation type [repetitive, trial-level, theta burst, rhythmic], coil orientation) and spatial-extent of visuocortical areas associated with negative memory enhancement, we cannot strongly conclude from the current null results that activation in any of these regions during retrieval are not critical to negative memory. First, a right hemisphere OTC (ROTC) cluster has also appeared in these fMRI maps (Kark and Kensinger, 2015, in press), but did not appear to be linked with valence-specific vividness like the left hemisphere at the whole-brain level (Kark et al., submitted). Previous work has shown that unilateral lesions of the inferior temporal cortex cause deficits in visual discrimination and chromatic sensitivity in the contralateral field during perception (Merigan and Saunders, 2004). It is possible that the memory representations inhibited by rTMS to the LOTC can be compensated for by the ROTC, leaving behavioral output unaffected. To test this hypothesis, a double-coil TMS method could be used to apply bilateral OTC stimulation or the stimulus presentation paradigm could leverage visual field differences. Second, visual processing region interference might require stronger or online, trial-level or theta-burst stimulation to have effects on memory strength (Waldhauser et al., 2016). Third, it could be that this particular area of posterior inferior temporal gyrus is not necessary for *all* participants to remember and re-experience negative events—the effect could depend on the level negative or positive memory bias a

person typically exhibits. Recent work suggests that negative-biased retrieval activity in visuocortical areas is linked with negative memory biases across participants (Kark and Kensinger, in press), suggesting rTMS to more posterior visual regions could reduce the bias in participants who show a negative memory bias under vertex stimulation.

While there were no *group* effects of LOTC stimulation on memory performance or re-experiencing, future work is needed to understand the origins of the individual differences observed in the current study. Two sources of variability could stem from individual brain anatomy and function. Anatomically, while TMS is applied focally with great precision using neuronavigation techniques, the spatial distribution and propagation of the induced electric fields within the brain can vary by a person's individual anatomy (Saturnino et al., 2018). Future analysis of the induced magnetic field maps using software such as SimNIBS (<http://simnibs.de>) could provide insights into the effects of rTMS on memory and also aide in individualizing TMS targets and stimulation parameters. On a functional level, rTMS is known to not only affect activity in the local target regions, but also the inter-regional functional connectivity that can modulate memory (Halko et al., 2013; Siebner and Rothwell, 2003; Wang et al., 2014). Specifically, rTMS can exert a greater influence on the interconnectivity amongst brain regions that show greater coupling at baseline (Wang et al., 2014). These findings raise the intriguing possibility that individual differences in the susceptibility to rTMS on emotional memory retrieval are related to intrinsic connectivity of the LOTC stimulation site. For instance, LOTC-rTMS related memory disruptions might be strongest for those participants with the greatest intrinsic connectivity with other structures that have

consistently been associated with emotional memory (e.g., amygdala, hippocampus) or valence-specific negative memory retrieval (e.g., parahippocampal cortex or broader ventral visual stream). Future analysis of the resting-state scans collected for the majority of the participants in the current study will test the predication that the effect of LOTC stimulation on negative memory retrieval could depend on intrinsic LOTC connectivity strength with the amygdala and/or parahippocampal cortex. Further, rTMS during memory retrieval can influence subsequent retrieval attempts (for a review see Sandrini, Cohen, & Censor, 2015), which suggests that while LOTC stimulation might not have had an effect on retrieval immediately after stimulation, it is possible that retrieval under LOTC could influence later memory. Item-level analysis of repeat recognition test⁷ will test the effect of prior stimulation site on memory performance and re-experiencing.

Finally, it is also possible that the alternative hypothesis is true: Visual processing reactivation is not necessary for retrieval of negative memories. What then is the role of the observed valence-specific memory enhancements in visual processing regions? Prior work has shown that the subjective “flash” emotional vividness goes beyond perceptual vividness (Todd et al., 2013), suggesting low-level perceptual enhancements and reactivations are not necessary to *feel* a sense of re-experiencing. However future work is needed to test that possibly that activation in these areas are needed to accurately reconstruct the visual aspects of a visual memory.

⁷ When time allowed, participants were administered a repeat memory test at the very end of Day 2, at least 40 minutes after their second rTMS session. In the repeat memory test, all of the old line-drawings from Day 1 were presented intermixed with a new set of line-drawings not previously seen during any of the study or line-drawing matching tasks. The repeat recognition memory test had the same format (Old/New judgment following by visual and internal re-experiencing ratings for “Old” judgements) as the other memory task, except there was no line-drawing matching task. The repeat memory test was completed in one session lasting approximately 10 minutes.

It is well-documented that the amygdala is crucial for enhanced memory for negative events (Buchanan, 2007; Buchanan et al., 2005; Packard and Cahill, 2001). However, we did not find a link between amygdala activation and retrieval success or vividness. Instead, the group fMRI negative memory effects shown in Parts I-III were consistently accompanied by enhancements of ventro-lateral prefrontal (VLPFC) and parietal areas. In parietal cortex, the angular gyrus has been linked with objective memory precision (Richter et al., 2016) and TMS work has shown that the angular gyrus is necessary for retrieval of episodic details (Thakral et al., 2017), a region also associated with objective memory precision (Richter et al., 2016). On the other hand, the VLPFC has been linked with cognitive control of memory (Nyhus and Badre, 2015) and recent TMS work has suggested a causal link between VLPFC activation and emotional memory formation (Weintraub-Brevda and Chua, 2018). To that end, unpublished findings from the fMRI dataset used in Parts I-III suggest functional connectivity of the VLPFC with the LOTC, angular gyrus, and hippocampus, is related to successful retrieval of negative memories. Thus, activation in fronto-parietal regions might be necessary for successful search, reactivation, and monitoring of negative visual memory traces. These regions present potential alternative sites that could be causally linked to negative visual memory enhancements.

In conclusion, inhibitory rTMS to a focal, unilateral portion of the left occipito-temporal cortex did not influence memory performance or re-experiencing compared to the vertex control site overall or as a function of stimulus valence. However, the LOTC ROI targeted in the current study is one within a broader ventral visual network that has

been implicated in valence-specific negative memory retrieval. Future work is needed to understand the necessity of visuocortical activation in emotional memory retrieval and subjective, compared to objective, visual memory reconstruction and re-experiencing.

4.8 REFERENCES

- Boroojerdi, B., Prager, A., Muellbacher, W., Cohen, L.G., 2000. Reduction of human visual cortex excitability using 1-Hz transcranial magnetic stimulation. *Neurology* 54, 1529-1531.
- Bowen, H.J., Kark, S.M., Kensinger, E.A., 2018. NEVER forget: negative emotional valence enhances recapitulation. *Psychon Bull Rev* 25, 870-891.
- Buchanan, T.W., 2007. Retrieval of emotional memories. *Psychol Bull* 133, 761-779.
- Buchanan, T.W., Tranel, D., Adolphs, R., 2005. Emotional autobiographical memories in amnesic patients with medial temporal lobe damage. *J Neurosci* 25, 3151-3160.
- Halko, M.A., Eldaief, M.C., Pascual-Leone, A., 2013. Noninvasive brain stimulation in the study of the human visual system. *J Glaucoma* 22 Suppl 5, S39-41.
- Hoddes, E., Dement, W., Zarcone, V., 1972. The development and use of the Stanford sleepiness scale (SSS). *Psychophysiology*, 150.
- Karanian, J.M., Slotnick, S.D., 2018. Confident false memories for spatial location are mediated by V1. *Cogn Neurosci* 9, 139-150.
- Kark, S.M., Kensinger, E.A., 2015. Effect of emotional valence on retrieval-related recapitulation of encoding activity in the ventral visual stream. *Neuropsychologia* 78, 221-230.
- Kark, S.M., Kensinger, E.A., in press. Post-encoding Amygdala-Visuosensory Coupling Is Associated with Negative Memory Bias in Healthy Young Adults. *J Neurosci*.
- Kark, S.M., Slotnick, S.D., Kensinger, E.A., submitted. Effects of emotional valence on true and false memory vividness.

- Keel, J.C., Smith, M.J., Wassermann, E.M., 2001. A safety screening questionnaire for transcranial magnetic stimulation. *Clin Neurophysiol* 112, 720.
- Koen, J.D., Thakral, P.P., Rugg, M.D., 2018. Transcranial magnetic stimulation of the left angular gyrus during encoding does not impair associative memory performance. *Cogn Neurosci* 9, 127-138.
- Lang, P.J., Bradley, M.M., Cuthbert, B.N., 2008. International affective picture system (IAPS): Affective ratings of pictures and instruction manual. Technical Report A-6. University of Florida, Gainesville, FL.
- Loos, E., Egli, T., Coynel, D., Fastenrath, M., Freytag, V., Papassotiropoulos, A., de Quervain, D.J., Milnik, A., 2019. Predicting emotional arousal and emotional memory performance from an identical brain network. *Neuroimage* 189, 459-467.
- Merigan, W.H., Saunders, R.C., 2004. Unilateral deficits in visual perception and learning after unilateral inferotemporal cortex lesions in macaques. *Cereb Cortex* 14, 863-871.
- Mickley, K.R., Kensinger, E.A., 2008. Emotional valence influences the neural correlates associated with remembering and knowing. *Cogn Affect Behav Neurosci* 8, 143-152.
- Murty, V.P., Ritchey, M., Adcock, R.A., LaBar, K.S., 2011. Reprint of: fMRI studies of successful emotional memory encoding: a quantitative meta-analysis. *Neuropsychologia* 49, 695-705.
- Nyhus, E., Badre, D., 2015. Memory Retrieval and the Functional Organization of the Frontal Cortex In: Addis, D.R., Barense, M., Duarte, A. (Eds.), *The Wiley*

- Handbook on the Cognitive Neuroscience of Memory. John Wiley & Sons, Ltd., Hoboken, NJ.
- Packard, M.G., Cahill, L., 2001. Affective modulation of multiple memory systems. *Curr Opin Neurobiol* 11, 752-756.
- Palombo, D.J., McKinnon, M.C., McIntosh, A.R., Anderson, A.K., Todd, R.M., Levine, B., 2016. The neural correlates of memory for a life-threatening event: An fMRI study of passengers from flight AT236. *Clin Psychol Sci* 4, 312-319.
- Phelps, E.A., Sharot, T., 2008. How (and Why) Emotion Enhances the Subjective Sense of Recollection. *Curr Dir Psychol Sci* 17, 147-152.
- Richter, F.R., Cooper, R.A., Bays, P.M., Simons, J.S., 2016. Distinct neural mechanisms underlie the success, precision, and vividness of episodic memory. *Elife* 5.
- Rossi, S., Hallett, M., Rossini, P.M., Pascual-Leone, A., 2011. Screening questionnaire before TMS: an update. *Clin Neurophysiol* 122, 1686.
- Rossini, P.M., Barker, A.T., Berardelli, A., Caramia, M.D., Caruso, G., Cracco, R.Q., Dimitrijevic, M.R., Hallett, M., Katayama, Y., Lucking, C.H., et al., 1994. Non-invasive electrical and magnetic stimulation of the brain, spinal cord and roots: basic principles and procedures for routine clinical application. Report of an IFCN committee. *Electroencephalogr Clin Neurophysiol* 91, 79-92.
- Rossini, P.M., Burke, D., Chen, R., Cohen, L.G., Daskalakis, Z., Di Iorio, R., Di Lazzaro, V., Ferreri, F., Fitzgerald, P.B., George, M.S., Hallett, M., Lefaucheur, J.P., Langguth, B., Matsumoto, H., Miniussi, C., Nitsche, M.A., Pascual-Leone, A., Paulus, W., Rossi, S., Rothwell, J.C., Siebner, H.R., Ugawa, Y., Walsh, V.,

- Ziemann, U., 2015. Non-invasive electrical and magnetic stimulation of the brain, spinal cord, roots and peripheral nerves: Basic principles and procedures for routine clinical and research application. An updated report from an I.F.C.N. Committee. *Clin Neurophysiol* 126, 1071-1107.
- Saturnino, G.B., Puonti, O., Nielsen, J.D., Antonenko, D., Madsen, K.H.H., Thielscher, A., 2018. SimNIBS 2.1: A Comprehensive Pipeline for Individualized Electric Field Modelling for Transcranial Brain Stimulation. *bioRxiv*, 500314.
- Siebner, H.R., Rothwell, J., 2003. Transcranial magnetic stimulation: new insights into representational cortical plasticity. *Exp Brain Res* 148, 1-16.
- Slotnick, S.D., Thakral, P.P., 2011. Memory for motion and spatial location is mediated by contralateral and ipsilateral motion processing cortex. *Neuroimage* 55, 794-800.
- Thakral, P.P., Madore, K.P., Schacter, D.L., 2017. A Role for the Left Angular Gyrus in Episodic Simulation and Memory. *J Neurosci* 37, 8142-8149.
- Todd, R.M., Schmitz, T.W., Susskind, J., Anderson, A.K., 2013. Shared neural substrates of emotionally enhanced perceptual and mnemonic vividness. *Front Behav Neurosci* 7, 40.
- Tulving, E., 2002. Episodic memory: from mind to brain. *Annu Rev Psychol* 53, 1-25.
- Waldhauser, G.T., Braun, V., Hanslmayr, S., 2016. Episodic Memory Retrieval Functionally Relies on Very Rapid Reactivation of Sensory Information. *J Neurosci* 36, 251-260.

- Wang, J.X., Rogers, L.M., Gross, E.Z., Ryals, A.J., Dokucu, M.E., Brandstatt, K.L., Hermiller, M.S., Voss, J.L., 2014. Targeted enhancement of cortical-hippocampal brain networks and associative memory. *Science* 345, 1054-1057.
- Weintraub-Brevda, R.R., Chua, E.F., 2018. The role of the ventrolateral prefrontal cortex in emotional enhancement of memory: A TMS study. *Cogn Neurosci* 9, 116-126.

GENERAL DISCUSSION

The present research investigated valence-specific neural processes that support the successful formation and retrieval of negative memories. This four-part series of research tested multiple predictions of the valence-based ‘NEVER’ model of emotional memory (Bowen et al., 2018). The fMRI findings of **Parts I-III** provide evidence of valence-specific enhancements in activation and functional connectivity of the ventral visual stream across multiple phases of memory: Beginning with perception during encoding, persisting into post-encoding rest periods, and evident in patterns of successful and vivid negative memory retrieval.

The current set of experiments went beyond the controls of prior work to ensure negative and positive stimuli were matched on the basis of arousal, that low-level visual statistics were controlled at the item-level in fMRI models in order to minimize stimulus-bound effects of no interest, and follow-up analyses controlling for arousal at the item- and participant-level were utilized to demarcate the neural effects that were truly valence-specific. The valence-specific patterns (i.e., Negative > Neutral > Positive) observed here cannot be sufficiently explained by an exclusively arousal-based account of emotional memory, as the positive stimuli were more arousing and of greater emotional valence than the neutral stimuli. The following discussion aims to 1) connect broad themes across Parts I-IV, 2) situate the work within prominent frameworks of emotional memory, 3) speculate on the underlying neurobiology and related phenomenology of the observed

patterns, and 4) outline the limitations and future directions in valence-based examinations of emotional memory.

Encoding-related amygdala-visuocortical coupling supports negative memories

Physiological influences of the parasympathetic nervous system

In **Part I**, Kark and Kensinger (submitted) directly tested the sensory-focused encoding tenant of the ‘NEVER’ model and demonstrated that arousal-related amygdala-V1 coupling during encoding enhances subsequent negative memory vividness, but not positive or neutral memory vividness. The observed PAI effect is consistent with valence-specific influences of arousal on memory (Mickley Steinmetz and Kensinger, 2009; Mickley Steinmetz et al., 2010) and the localization of the effects to early visual cortex further implies that negative valence influences perceptual processes during encoding that are relevant to later memory vividness. These findings are broadly consistent with psychophysical work that suggests HRD—a freezing-like behavior—is associated with enhanced visual sensitivity (Lojowska et al., 2018), and adds that these processes have long-term consequences on later memory for those percepts.

The novel aspect of the study in **Part I** was the use of trial-level HRD responses during concurrent fMRI, which enabled analysis of the neural correlates of parasympathetic influences as a function of valence and later memory vividness. Parasympathetic HRD responses result from cholinergic activation of central amygdala projections to the medullar nuclei and ventrolateral periaqueductal gray that, in turn,

activate the vagus nerve, releasing acetylcholine onto the sinus node of the heart, which slows the heart rate (Roelofs, 2017). Thus, HRD serves as a proxy of vagal regulation and possibly cholinergic activation (Porges, 2011). In addition to brain-stem influences on heart rate, activation of the amygdala can initiate release of acetylcholine throughout the cortex via the nucleus basalis, resulting in enhanced vigilance and ‘cortical attention’ to negative stimuli (Corbetta and Shulman, 2002; Demeter and Sarter, 2013; Phelps and LeDoux, 2005). Consistent with these findings, increasing magnitudes of HRD responses were associated with increasing levels of amygdala functional connectivity with the ventrolateral prefrontal cortex and the ventral parietal attention areas, regardless of valence. In V1, acetylcholine release has been linked with enhanced perception, including increases in signal-to-noise ratios, contrast sensitivity, and orientation tuning (Breitmeyer et al., 2018; Galvin et al., 2018; Kang et al., 2014; Soma et al., 2013). Recent work has also shown that emotion enhances precision of visual memory encoding (Cooper et al., in press). Thus, it is plausible that parasympathetic HRD responses enhance the perception of negative visual stimuli via cholinergic interactions between the amygdala and early visual cortex. This enhanced visual processing at encoding could influence the resolution or extent of content that is available to support later vivid retrieval of negative memories. These arousal-related interactions could also plausibly “tag” those visual memory traces for prioritized consolidation (Bennion et al., 2015).

Prior work has established a sympathetic nervous system framework of arousal-enhanced memory, which purports that salient stimuli activate the norepinephrine-locus

coeruleus system, enhancing selective attention and top-down prioritization of goal-relevant stimuli during encoding, which enhances subsequent memory representations (Clewett et al., 2018; Glutamate Amplifies Noradrenergic Effects (GANE) model: Mather et al., 2016; Arousal biased competition theory: Mather and Sutherland, 2011). Here, the PAI effect of amygdala-V1 coupling survived controlling for sympathetic influences, which raises the intriguing possibility of a complementary parasympathetic cholinergic mechanism that enhances visual sensitivity to negative stimuli, which has downstream effects on subjective vividness at retrieval. Previous work has shown that cholinergic activation of the amygdala can elicit long-term potentiation (Jiang et al., 2016) and enhance memory consolidation, but likely acts downstream from the influences of the norepinephrine system (reviewed in Roozendaal and McGaugh, 2011). Although parasympathetic influences on memory might be secondary to the effects of the sympathetic nervous system, the findings of **Part I** nevertheless suggest that a qualitatively different, valence-based pattern might exist for parasympathetic influences on emotional memory processes.

Post-encoding influences

Whereas **Part I** revealed valence-specific effects of arousal on amygdala-visuocortical connectivity *during* encoding, **Part II** demonstrated a link between behavioral negative memory bias and amygdala-visuocortical coupling during post-encoding rest. One criticism of the NEVER model is that valence-differences could be driven by stimulus-bound differences, but the absence of external stimuli during resting-

state fMRI circumvented this possibility. Further, the exploratory moderated mediation results provided support for a core prediction of the NEVER model: Sensory-focused encoding of negative stimuli guides recapitulation of sensory activation. The results of the mediation analysis suggests that sensory-focused post-encoding amygdala coupling might set-up the brain for a retrieval mode that is biased toward retrieval of negative visual memory traces and drives the degree of the behavioral negative memory bias across individuals. The complete moderated mediation connected the effects of valence across multiple memory phases and further stipulated that the post-encoding-to-retrieval effects in visuocortical areas were moderated by co-occurring increases in post-encoding hippocampal coupling, which is consistent with the known amygdala-hippocampal interactions in emotional memory (Phelps, 2004). Interestingly, while post-encoding amygdala-visuocortical coupling changes were not correlated with neutral memory performance, post-encoding decreases in amygdala-visuocortical connectivity were associated a positive memory bias, implying a shift *away* from affective-sensory processing in positive memory bias (see Part II, Figure 4).

However, the post-encoding results in **Part II** only capture approximately 7 minutes of post-encoding amygdala resting connectivity out of a 24-hour study-test delay. Future work is needed to confirm if sleep-related selective consolidation of negative visual memory traces (as observed in Bennion et al., 2016) also accounts for a significant source of variability in negative memory biases, which would be consistent with consolidation-related predictions of the NEVER model. Previous work has shown links between individual differences in stress and post-learning amygdala-hippocampal

interactions (de Voogd et al., 2016; de Voogd et al., 2017). Further work is also needed to test if stress enhances the moderating effect of hippocampal connectivity on the relationship between amygdala-visuocortical coupling and negative memory biases, which could explain individual differences of stress reactivity on emotional memory biases.

Encoding-related amygdala-medial frontal coupling supports positive memories

The primary hypotheses of the current work were centered around negative valence, but a secondary hypothesis across **Parts I-III** predicted a link between prefrontal enhancements and positive memory outcomes. First, although it was not reported in **Part I**, there was valence-specific effect of HRD-related amygdala-dorsal medial prefrontal cortex (DMPFC) connectivity for positive stimuli. While amygdala-DMPFC connectivity was not related to subsequent memory vividness for positive stimuli (i.e., null PAI effect), future work is needed to examine if arousal-related attentional or self-referential processes in the DMPFC (Gutchess and Kensinger, 2018) for pleasant information confers a later valence-specific memory benefit. Interestingly, cholinergic release in medial PFC has been associated with detection of appetitive cues (Demeter and Sarter, 2013), again raising the possibility of arousal-related cholinergic influences of the amygdala during perception of emotional stimuli. Second, in striking opposition to the link between post-encoding visuocortical effects and negative memory biases, Part II also demonstrated a link between positive memory bias and amygdala-dACC coupling. The

dACC has consistently been associated with cognitive control of emotion (Ochsner et al., 2002), positivity bias, emotional stability (Brassen et al., 2011), and trait optimism (Sharot et al., 2007). It is possible that 7 mins of post-encoding resting state scanning captures the participants' proclivity toward rethinking their feelings and engaging in reappraisal after viewing emotional pictures. If these individuals tend to re-appraise the negative stimuli, it might shift memory processes away from sensory areas.

Implementation of an easy visual distractor task during the resting state scans (e.g., arrow direction task) could help reduce the possibility of active rehearsal or visual rumination of the negative stimuli or reappraisal of positive stimuli and adjudicate between the rehearsal/re-appraisal compared to consolidation accounts of the results of Part II.

Retrieval-related enhancements of the ventral visual stream and negative memories

Ventral visual activation in negative memory vividness

Whereas Parts I and II focused on encoding and peri-encoding influences on negative memories, **Part III** examined the effect of valence on the neural correlates of true and false memory vividness during retrieval. True negative memory vividness was specifically associated with retrieval-related activity in the left occipito-temporal and parahippocampal cortices—clusters that importantly also showed negative memory recapitulation effects in Part II (Kark and Kensinger, in press) and in a previous version of the study with a short study-test delay (Kark and Kensinger, 2015). These findings suggest that activation in these regions is important for both negative memory success

and subjective re-experiencing. However, analysis of false alarm vividness ratings suggests these areas also contribute to a false sense of vividness for stimuli that were never studied. This effect was particularly robust in the parahippocampal cortex, which exhibited a whole-brain main effect of valence. Thus, while these regions support successful memory, signals from these areas might also endow an individual with a false sense of vividness for negative stimuli or reflect false recollections. The results of Part III are broadly consistent with behavioral and psychophysiological work that suggest emotional true and false memories can be largely indistinguishable and add that neural patterns can also look very similar.

Speculation as to the content of negative memoranda

The current results can only allow for speculation as to the nature of the visual content that is brought to mind to support negative memory retrieval and vividness. Speculation can be based on what is known about the content (e.g., color, texture, granularity, contrast) carried by the brain regions consistently implicated in this work and what is known about the timing of their effects. The majority of valence-specific effects were observed in the ventral visual stream (the slower, parvocellular “what” pathway), with some of the encoding effects extending up the dorsal visual stream (the faster, magnocellular “where” pathway) (Kauffmann et al., 2014). Previous work has shown that arousal increases visual sensitivity to coarse features (low-spatial frequencies) at the expense of fine-grained details (high spatial frequencies), consistent with amygdala-visual processing enhancements along the magnocellular pathway (Lee et al., 2014;

Lojowska et al., 2015). Recent work suggests HRD-related amygdala-V1 coupling likely emanates predominantly from magnocellular projections of the basolateral amygdala to early visual processing regions (Amaral et al., 2003; Lojowska et al., 2018). These assertions would first appear to run counter to enhanced memory for visual detail in negative memory. However, the “coarse-to-fine” hypothesis (Kauffmann et al., 2014) purports that low-spatial frequency information arrives rapidly along the magnocellular pathway—creating a quick and coarse ‘rough draft’ of the percept—that then guides more detailed analysis of the color, texture, orientations, edges, and shape information carried by the parvocellular pathway. Perhaps enhanced rapid magnocellular processing (observed in Part I PAI effects) guides enhanced activation of detailed analysis by the ventral pathway, which ends up being more consistently related to negative memory processes at the group level (observed in Parts I-III).

Recollection of color is one aspect of re-experiencing the circumstances that were present during the time of encoding. Interestingly, an exact area of right inferior occipital gyrus and a similar portion of lingual gyrus that were linked with negative memory biases in Part II have also been associated with retrieval-related reactivation of colorful shapes, compared to white shapes ($MNI_{xyz} = 34, -88, -16$; see Ueno et al., 2007). The inferior temporal gyrus cluster associated with valence-specific negative memory vividness (Part III) has also been implicated in color processing (Bramao et al., 2010; Conway, 2018). Perhaps color is one aspect that is enhanced in negative memories. Novel new paradigms using objective metrics of visual memory reconstruction have linked vividness with objective precision and remembered salience (using continuous color and luminance

response sliders) (Cooper et al., in press). These types of paradigms will open new avenues for understanding the relationship between subjective memory vividness and objective visual memory reconstruction. However, prior work has shown that emotional enhancement of perceptual vividness—or the “metaphorical vivid light surrounding emotional memories”—goes beyond effects of color (Todd et al., 2013) and the perceptual saliency of visual memories literally “fades” (Cooper et al., in press). Hence, it is unclear when and how these fine-grain details aid in negative memory retrieval and vividness.

In addition to enhancements in perception, emotion also modulates the scope of the visual field of view. Specifically, negative valence is associated with an amygdala-related narrowing of the perceptual field-of-view—consistent with the weapons-focus and emotional memory trade-off effects—whereas positive valence is associated with a frontally-mediated broadening of the perceptual field-of-view (Schmitz et al., 2009). However, the medial visual cortex PAI effects in V1 would suggest enhanced processing of the periphery (Kauffmann et al., 2014), which is consistent with a defensive mechanism under threat (i.e., to detect a predator) but would not explain enhanced memory for central objects observed in the weapons-focus effect. Further investigation employing eye-tracking and psychophysical techniques are needed examine the memory consequences of valence-specific effects on the scope of the visual field (broaden, narrow) and across visual field eccentricities (central, peripheral).

Future Directions

In addition to the future directions of visual re-experiencing of negative memories, additional paths for future inquiry center around time: The effect of valence on memory for time as well as the temporal unfolding and oscillatory dynamics of emotional memory processes.

Effects of valence on temporal memory precision and episodic sequencing

William James once noted that ‘a certain emotional feeling accompanies the intervals of time’ (1890), and research on the effects of emotion on time perception have echoed this notion. Previous work has empirically tested the time-emotion paradox associated with the old adage that “time flies when you’re having fun.” Indeed, valence-specific effects of arousal have been found on time duration estimates: The time-emotion paradox asserts that positive arousal tends to speed the passage of time, while the duration of negative or fearful events tend to be over-estimated (Campbell and Bryant, 2007; Droit-Volet and Gil, 2009; Fayolle et al., 2015). Valence can also influence temporal perceptual acuity (Roberts et al., 2017): Positive valence results in the sense of speeded motion, decreased temporal sampling, and a subject sense of blurriness of a stimulus in motion, while negative valence is associated with slowing of motion, increased temporal sampling, and a sense of choppiness of a stimulus in motion. There is also some evidence that negative valence enhances memory for temporal information

(D'Argembeau and Van der Linden, 2005). These studies suggest valence-specific effects of time perception that could have consequences on later memory.

FMRI work has shown that the hippocampus is sensitive to time (Barnett et al., 2014; Hsieh et al., 2014; Thavabalasingam et al., 2018). Recent work from Montchal, Reagh, and Yassa (2019) utilized memory for events within an episode of the TV series *Curb Your Enthusiasm* to demonstrate that the lateral entorhinal cortex (LEC), perirhinal cortex, and hippocampal CA3 are involved in precise temporal memory judgements. The amygdala has been identified as a plausible modulator of emotional time distortions (Lake et al., 2016), and is well-positioned within the anterior temporal memory system alongside with the LEC and is heavily interconnected with the perirhinal cortex (Ranganath and Ritchey, 2012). Given the valence-specific effects of emotional arousal on time perception, how would emotional valence influence temporal memory precision and would amygdala modulation of LEC be responsible for those distortions or enhancements? Future work using dynamic emotional and neutral video stimuli could be used to reveal the neural underpinnings of time distortions in emotional memory. The findings of such work could be critical to understanding temporal memory precision in eyewitness testimony, when witnesses recount the durations and ordinal sequencing of often emotional information associated with a crime.

Valence influences on the timing and oscillatory mechanisms of recapitulation

While the current fMRI studies have revealed the spatial distribution of negative memory enhancements in the ventral visual stream, these findings cannot speak to the

temporal unfolding of neural effects. Rapid onset, low-frequency oscillations of the amygdala entrain hippocampal gamma during processing of emotionally salient information (Zheng et al., 2017). The amygdala also promotes gamma oscillations throughout the cortex, facilitating emotion memory formation (Headley and Pare, 2013). While there is some work examining oscillations and emotional memory, those studies typically compare negative to neutral stimuli. The parahippocampal cortex was implicated in negative memory enhancements across Parts I-III and given the role of the parahippocampal cortex in scene memory, this substrate could also represent an area that is necessary for retrieving vivid memories of negative scenes, or even falsely constructing negative memories. While intracranial recording studies of reinstatement have reported a greater role of parahippocampal cortex gamma in encoding, compared to retrieval (Johnson and Knight, 2015; Kucewicz et al., 2014), there are no studies examining the possibility that negative valence could enhance retrieval-related reinstatement of gamma during retrieval of negative scenes. Future work is needed to understand the timing of recapitulation processes and their oscillatory dynamics.

Conclusions

Together, these studies have laid a foundation for future work on the effect of emotional valence on perception and memory and highlight the need for valence-based accounts of emotional memory. Distressing and intrusive visual memory and imagery is common across a range of psychological disorders, from post-traumatic stress disorder and social anxiety to eating disorders and obsessive-compulsive disorder (Brewin et al.,

2010). The basic science understanding of valence differences in perception and memory are crucial for our understanding not only of how healthy individuals experience and re-experience their emotional worlds, but also how those processes go awry in psychopathology.

REFERENCES FOR GENERAL INTRODUCTION AND DISCUSSION

- Amaral, D.G., Behniea, H., Kelly, J.L., 2003. Topographic organization of projections from the amygdala to the visual cortex in the macaque monkey. *Neuroscience* 118, 1099-1120.
- Barnett, A.J., O'Neil, E.B., Watson, H.C., Lee, A.C., 2014. The human hippocampus is sensitive to the durations of events and intervals within a sequence. *Neuropsychologia* 64, 1-12.
- Balconi, M., Ferrari, C., 2013. Repeated transcranial magnetic stimulation on dorsolateral prefrontal cortex improves performance in emotional memory retrieval as a function of level of anxiety and stimulus valence. *Psychiatry Clin Neurosci* 67, 210-218.
- Bennion, K.A., Payne, J.D., Kensinger, E.A., 2015. Selective effects of sleep on emotional memory: What mechanisms are responsible? *Translational Issues in Psychological Science* 1, 79-88.
- Bennion, K.A., Payne, J.D., Kensinger, E.A., 2016. Residual effects of emotion are reflected in enhanced visual activity after sleep. *Cogn Affect Behav Neurosci* 17, 290-304.
- Bowen, H.J., Kark, S.M., Kensinger, E.A., 2018. NEVER forget: negative emotional valence enhances recapitulation. *Psychon Bull Rev* 25, 870-891.
- Bowen, H.J., Kensinger, E.A., 2017a. Memory-related functional connectivity in visual processing regions varies by prior emotional context. *Neuroreport* 28, 808-813.

- Bowen, H.J., Kensinger, E.A., 2017b. Recapitulation of emotional source context during memory retrieval. *Cortex* 91, 142-156.
- Bramao, I., Faisca, L., Forkstam, C., Reis, A., Petersson, K.M., 2010. Cortical brain regions associated with color processing: an fMRI study. *Open Neuroimag J* 4, 164-173.
- Brassen, S., Gamer, M., Buchel, C., 2011. Anterior cingulate activation is related to a positivity bias and emotional stability in successful aging. *Biol Psychiatry* 70, 131-137.
- Breitmeyer, B.G., Tripathy, S.P., Brown, J.M., 2018. Can Contrast-Response Functions Indicate Visual Processing Levels? *Vision* 2, 14.
- Brewin, C.R., Gregory, J.D., Lipton, M., Burgess, N., 2010. Intrusive images in psychological disorders: characteristics, neural mechanisms, and treatment implications. *Psychol Rev* 117, 210-232.
- Buchanan, T.W., 2007. Retrieval of emotional memories. *Psychol Bull* 133, 761-779.
- Campbell, L.A., Bryant, R.A., 2007. How time flies: a study of novice skydivers. *Behav Res Ther* 45, 1389-1392.
- Clewett, D.V., Huang, R., Velasco, R., Lee, T.H., Mather, M., 2018. Locus Coeruleus Activity Strengthens Prioritized Memories Under Arousal. *J Neurosci* 38, 1558-1574.
- Comblain, C., D'Argembeau, A., Van der Linden, M., Aldenhoff, L., 2004. The effect of ageing on the recollection of emotional and neutral pictures. *Memory* 12, 673-684.

- Conway, B.R., 2018. The Organization and Operation of Inferior Temporal Cortex. *Annu Rev Vis Sci* 4, 381-402.
- Cooper, R.A., Kensinger, E.A., Ritchey, M., in press. Memories fade: The relationship between memory vividness and remembered visual salience. *Psychol Sci*.
- Corbetta, M., Shulman, G.L., 2002. Control of goal-directed and stimulus-driven attention in the brain. *Nat Rev Neurosci* 3, 201-215.
- D'Argembeau, A., Van der Linden, M., 2005. Influence of emotion on memory for temporal information. *Emotion* 5, 503-507.
- de Voogd, L.D., Fernandez, G., Hermans, E.J., 2016. Awake reactivation of emotional memory traces through hippocampal-neocortical interactions. *Neuroimage* 134, 563-572.
- de Voogd, L.D., Klumpers, F., Fernandez, G., Hermans, E.J., 2017. Intrinsic functional connectivity between amygdala and hippocampus during rest predicts enhanced memory under stress. *Psychoneuroendocrinology* 75, 192-202.
- Demeter, E., Sarter, M., 2013. Leveraging the cortical cholinergic system to enhance attention. *Neuropharmacology* 64, 294-304.
- Droit-Volet, S., Gil, S., 2009. The time-emotion paradox. *Philos Trans R Soc Lond B Biol Sci* 364, 1943-1953.
- Fayolle, S., Gil, S., Droit-Volet, S., 2015. Fear and time: Fear speeds up the internal clock. *Behav Processes* 120, 135-140.

- Galvin, V.C., Arnsten, A.F.T., Wang, M., 2018. Evolution in Neuromodulation—The Differential Roles of Acetylcholine in Higher Order Association vs. Primary Visual Cortices. *Frontiers in Neural Circuits* 12.
- Gutchess, A., Kensinger, E.A., 2018. Shared Mechanisms May Support Mnemonic Benefits from Self-Referencing and Emotion. *Trends Cogn Sci* 22, 712-724.
- Headley, D.B., Pare, D., 2013. In sync: gamma oscillations and emotional memory. *Front Behav Neurosci* 7, 170.
- Hsieh, L.T., Gruber, M.J., Jenkins, L.J., Ranganath, C., 2014. Hippocampal activity patterns carry information about objects in temporal context. *Neuron* 81, 1165-1178.
- Jiang, L., Kundu, S., Lederman, J.D., Lopez-Hernandez, G.Y., Ballinger, E.C., Wang, S., Talmage, D.A., Role, L.W., 2016. Cholinergic Signaling Controls Conditioned Fear Behaviors and Enhances Plasticity of Cortical-Amygdala Circuits. *Neuron* 90, 1057-1070.
- Johansson, M., Mecklinger, A., Treese, A.C., 2004. Recognition memory for emotional and neutral faces: an event-related potential study. *J Cogn Neurosci* 16, 1840-1853.
- Johnson, E.L., Knight, R.T., 2015. Intracranial recordings and human memory. *Curr Opin Neurobiol* 31, 18-25.
- Kang, J.I., Huppe-Gourgues, F., Vaucher, E., 2014. Boosting visual cortex function and plasticity with acetylcholine to enhance visual perception. *Front Syst Neurosci* 8, 172.

- Kark, S.M., Kensinger, E.A., 2015. Effect of emotional valence on retrieval-related recapitulation of encoding activity in the ventral visual stream. *Neuropsychologia* 78, 221-230.
- Kark, S.M., Kensinger, E.A., in press. Post-encoding Amygdala-Visuosensory Coupling Is Associated with Negative Memory Bias in Healthy Young Adults. *J Neurosci*.
- Kauffmann, L., Ramanoel, S., Peyrin, C., 2014. The neural bases of spatial frequency processing during scene perception. *Front Integr Neurosci* 8, 37.
- Kensinger, E.A., Choi, E.S., 2009. When side matters: hemispheric processing and the visual specificity of emotional memories. *J Exp Psychol Learn Mem Cogn* 35, 247-253.
- Klein, S.B., Nichols, S., 2012. Memory and the Sense of Personal Identity. *Mind* 121, 677-702.
- Kucewicz, M.T., Cimbalnik, J., Matsumoto, J.Y., Brinkmann, B.H., Bower, M.R., Vasoli, V., Sulc, V., Meyer, F., Marsh, W.R., Stead, S.M., Worrell, G.A., 2014. High frequency oscillations are associated with cognitive processing in human recognition memory. *Brain* 137, 2231-2244.
- Lake, J.I., LaBar, K.S., Meck, W.H., 2016. Emotional modulation of interval timing and time perception. *Neurosci Biobehav Rev* 64, 403-420.
- Lee, T.H., Baek, J., Lu, Z.L., Mather, M., 2014. How arousal modulates the visual contrast sensitivity function. *Emotion* 14, 978-984.
- Lojowska, M., Gladwin, T.E., Hermans, E.J., Roelofs, K., 2015. Freezing promotes perception of coarse visual features. *J Exp Psychol Gen* 144, 1080-1088.

- Lojowska, M., Ling, S., Roelofs, K., Hermans, E.J., 2018. Visuocortical changes during a freezing-like state in humans. *Neuroimage* 179, 313-325.
- Markowitsch, H.J., Vandekerckhove, M.M., Lanfermann, H., Russ, M.O., 2003. Engagement of lateral and medial prefrontal areas in the ephory of sad and happy autobiographical memories. *Cortex* 39, 643-665.
- Mather, M., Clewett, D., Sakaki, M., Harley, C.W., 2016. Norepinephrine ignites local hotspots of neuronal excitation: How arousal amplifies selectivity in perception and memory. *Behav Brain Sci* 39, e200.
- Mather, M., Sutherland, M.R., 2011. Arousal-Biased Competition in Perception and Memory. *Perspect Psychol Sci* 6, 114-133.
- Mickley, K.R., Kensinger, E.A., 2008. Emotional valence influences the neural correlates associated with remembering and knowing. *Cogn Affect Behav Neurosci* 8, 143-152.
- Mickley Steinmetz, K.R., Addis, D.R., Kensinger, E.A., 2010. The effect of arousal on the emotional memory network depends on valence. *Neuroimage* 53, 318-324.
- Mickley Steinmetz, K.R., Kensinger, E.A., 2009. The effects of valence and arousal on the neural activity leading to subsequent memory. *Psychophysiology* 46, 1190-1199.
- Montchal, M.E., Reagh, Z.M., Yassa, M.A., 2019. Precise temporal memories are supported by the lateral entorhinal cortex in humans. *Nat Neurosci* 22, 284-288.

- Murty, V.P., Ritchey, M., Adcock, R.A., LaBar, K.S., 2011. Reprint of: fMRI studies of successful emotional memory encoding: a quantitative meta-analysis. *Neuropsychologia* 49, 695-705.
- Nyhus, E., Badre, D., 2015. Memory Retrieval and the Functional Organization of the Frontal Cortex In: Addis, D.R., Barense, M., Duarte, A. (Eds.), *The Wiley Handbook on the Cognitive Neuroscience of Memory*. John Wiley & Sons, Ltd., Hoboken, NJ.
- Ochsner, K.N., 2000. Are affective events richly recollected or simply familiar? The experience and process of recognizing feelings past. *J Exp Psychol Gen* 129, 242-261.
- Ochsner, K.N., Bunge, S.A., Gross, J.J., Gabrieli, J.D., 2002. Rethinking feelings: an FMRI study of the cognitive regulation of emotion. *J Cogn Neurosci* 14, 1215-1229.
- Phelps, E.A., 2004. Human emotion and memory: interactions of the amygdala and hippocampal complex. *Curr Opin Neurobiol* 14, 198-202.
- Phelps, E.A., LeDoux, J.E., 2005. Contributions of the amygdala to emotion processing: from animal models to human behavior. *Neuron* 48, 175-187.
- Phelps, E.A., Sharot, T., 2008. How (and Why) Emotion Enhances the Subjective Sense of Recollection. *Curr Dir Psychol Sci* 17, 147-152.
- Porges, S., 2011. *The Polyvagal Theory: Neurophysiological Foundations of Emotions, Attachment, Communication Self-Regulation*. W. W. Norton & Company, New York, NY.

- Porter, S., Spencer, L., Birt, A., 2003. Blinded by emotion? Effect of the emotionality of a scene on susceptibility to false memories. *Canadian Journal of Behavioural Science* 35, 165-175.
- Ranganath, C., Ritchey, M., 2012. Two cortical systems for memory-guided behaviour. *Nat Rev Neurosci* 13, 713-726.
- Richter, F.R., Cooper, R.A., Bays, P.M., Simons, J.S., 2016. Distinct neural mechanisms underlie the success, precision, and vividness of episodic memory. *Elife* 5.
- Reid, T., 1785. *Memory. Essays on the Intellectual Powers of Man.*
- Roberts, K.H., Truong, G., Kingstone, A., Todd, R.M., 2017. The Blur of Pleasure: Appetitively Appealing Stimuli Decrease Subjective Temporal Perceptual Acuity. *Psychol Sci* 28, 1563-1582.
- Roelofs, K., 2017. Freeze for action: neurobiological mechanisms in animal and human freezing. *Philos Trans R Soc Lond B Biol Sci* 372.
- Roosendaal, B., McGaugh, J.L., 2011. Memory modulation. *Behav Neurosci* 125, 797-824.
- Schmitz, T.W., De Rosa, E., Anderson, A.K., 2009. Opposing influences of affective state valence on visual cortical encoding. *J Neurosci* 29, 7199-7207.
- Sharot, T., Riccardi, A.M., Raio, C.M., Phelps, E.A., 2007. Neural mechanisms mediating optimism bias. *Nature* 450, 102-105.
- Soma, S., Shimegi, S., Suematsu, N., Sato, H., 2013. Cholinergic modulation of response gain in the rat primary visual cortex. *Sci Rep* 3, 1138.

- Thakral, P.P., Madore, K.P., Schacter, D.L., 2017. A Role for the Left Angular Gyrus in Episodic Simulation and Memory. *J Neurosci* 37, 8142-8149.
- Thavabalasingam, S., O'Neil, E.B., Lee, A.C.H., 2018. Multivoxel pattern similarity suggests the integration of temporal duration in hippocampal event sequence representations. *Neuroimage* 178, 136-146.
- Todd, R.M., Schmitz, T.W., Susskind, J., Anderson, A.K., 2013. Shared neural substrates of emotionally enhanced perceptual and mnemonic vividness. *Front Behav Neurosci* 7, 40.
- Tulving, E., 2002. Episodic memory: from mind to brain. *Annu Rev Psychol* 53, 1-25.
- Tulving, E., Thomson, D., 1973. Encoding specificity and retrieval processes in episodic memory. *Psychological Review* 80, 352-373.
- Ueno, A., Abe, N., Suzuki, M., Hirayama, K., Mori, E., Tashiro, M., Itoh, M., Fujii, T., 2007. Reactivation of medial temporal lobe and occipital lobe during the retrieval of color information: A positron emission tomography study. *Neuroimage* 34, 1292-1298.
- Weintraub-Brevda, R.R., Chua, E.F., 2018. The role of the ventrolateral prefrontal cortex in emotional enhancement of memory: A TMS study. *Cogn Neurosci* 9, 116-126.
- Wheeler, M.A., Stuss, D.T., Tulving, E., 1997. Toward a theory of episodic memory: the frontal lobes and autonoetic consciousness. *Psychol Bull* 121, 331-354.
- Zheng, J., Anderson, K.L., Leal, S.L., Shestyuk, A., Gulsen, G., Mnatsakanyan, L., Vadera, S., Hsu, F.P., Yassa, M.A., Knight, R.T., Lin, J.J., 2017. Amygdala-

hippocampal dynamics during salient information processing. Nat Commun 8,
14413.